

รายงานวิจัยฉบับสมบูรณ์

โครงการ

การเพิ่มประสิทธิภาพของแอฟฟินิตีใบโอเซนเซอร์ แบบไม่ติดฉลากโดยใช้วัสดุนาโน

Enhancement of Label–free Affinity Biosensor Performance Using Nanomaterials

โดย ปณต ถาวรังกูร และคณะ

มีนาคม 2556

รายงานวิจัยฉบับสมบูรณ์

โครงการ การเพิ่มประสิทธิภาพของแอฟฟินิตีไบโอเซนเซอร์แบบไม่ติด

ฉลากโดยใช้วัสดุนาโน

8. จงดี ธรรมเขต

9. ชิตนนท์ บูรณชัย

Enhancement of Label-free Affinity Biosensor

Performance Using Nanomaterials

คณะผู้วิจัย

ปณต ถาวรังกูร
 ภาควิชาฟิสิกส์ คณะวิทยาศาสตร์
 เพริศพิชญ์ คณาธารณา
 ภาควิชาเคมี คณะวิทยาศาสตร์
 บุญเจริญ วงศ์กิตติศึกษา
 ภาควิชาวิศวกรรมไฟฟ้า คณะวิศวกรรมศาสตร์
 วรากร ลิ่มบุตร
 ภาควิชาวิทยาศาสตร์ประยุกต์ คณะวิทยาศาสตร์
 พรรณี อัศวตรีรัตนกุล
 ภาควิชาชีวเคมี คณะวิทยาศาสตร์
 อาภรณ์ นุ่มน่วม
 ภาควิชาวิศวกรรมไฟฟ้า คณะวิศวกรรมศาสตร์
 ชูศักดิ์ ลิ่มสกุล

มหาวิทยาลัยสงขลานครินทร์

ภาควิชาเคมี คณะวิทยาศาสตร์

ภาควิชาฟิสิกส์ คณะวิทยาศาสตร์

สนับสนุนโดยสำนักงานกองทุนสนับสนุนการวิจัย (ความเห็นในรายงานนี้เป็นของผู้วิจัย สกว. ไม่จำเป็นต้องเห็นด้วยเสมอไป)

กิตติกรรมประกาศ

โครงการนี้ได้รับทุนอุดหนุนการวิจัยจากสำนักงานกองทุนสนับสนุนการวิจัย (สกว.) ทุนองค์ความรู้ใหม่ที่เป็นพื้นฐานต่อการพัฒนา สัญญาเลขที่ BRG5280014 ตั้งแต่วันที่ 15 เดือนกรกฎาคม พ.ศ. 2552 ถึงวันที่ 31 เดือนมีนาคม พ.ศ. 2556

ขอขอบคุณการสนับสนุนนักศึกษาจากโครงการปริญญาเอกกาญจนาภิเษก (คปก.) ศูนย์ความเป็นเลิศด้านนวัตกรรมทางเคมี (PERCH-CIC) และ สถานวิจัยการวิเคราะห์สาร ปริมาณน้อยและไบโอเซนเซอร์ (TAB-RC) มหาวิทยาลัยสงขลานครินทร์

ปณต ถาวรังกูร
เพริศพิชญ์ คณาธารณา
บุญเจริญ วงศ์กิตติศึกษา
วรากร ลิ่มบุตร
พรรณี อัศวตรีรัตนกุล
อาภรณ์ นุ่มน่วม
ชูศักดิ์ ลิมสกุล
จงดี ธรรมเขต
ชิตนนท์ บูรณชัย

บทคัดย่อ

โครงการนี้ศึกษาการเพิ่มสัญญาณของระบบแอฟฟินิตีแบบไม่ติดฉลากที่วัดตามเวลาจริงโดยใช้ วัสดุนาโน และวัดสัญญาณของค่าความจุไฟฟ้าและอิมพีแดนซ์ในระบบโฟลว์อินเจกชันเพื่อให้สามารถ วิเคราะห์ได้อย่างต่อเนื่อง วัสดุนาโนบนผิวของตัวตรวจวัดช่วยเพิ่มพื้นที่สำหรับการตรึงวัสดุชีวภาพ ทำให้ปริมาณของวัสดุชีวภาพบนตัวตรวจวัดเพิ่มขึ้น สามารถจับกับสารที่ต้องการวิเคราะห์ได้มากขึ้น และได้สัญญาณเพิ่มขึ้น งานวิจัยนี้ศึกษาวิธีต่างๆ สี่วิธีในการจัดการให้วัสดุนาโนอยู่บนตัวตรวจวัด วิธี แรก ทำให้อนุภาคนาโนเงินเกาะติดบนผิวของอิเล็กโทรดทองผ่านชั้นเซลฟ์แอสเซิมเบิลโมโนเลเยอร์ของ สารกลุ่มไธออล หลังจากนั้นจึงตรึงแอนติบอดีบนอนุภาคนาโน ในวิธีที่สอง หลังจากตรึงอนุภาคนาโน เช่นเดียวกับวิธีแรก ก่อนที่จะตรึงแอนติบอดีจะเติมชั้นของสารกลุ่มไธออลที่มีหมู่ฟังก์ชันอิสระสองหมู่ที่ สามารถจับกับแอนติบอดีบนชั้นของอนุภาคนาโน ทำให้แอนติบอดีถูกตรึงได้มากขึ้น วิธีที่สาม เพิ่ม พื้นที่ผิวของตัวตรวจวัดโดยการตรึงอนุภาคนาโนแบบชั้นต่อชั้น และวิธีสุดท้าย เพิ่มพื้นที่โดยทำให้ผิว อิเล็กโทรดทองเกิดรูพรุน ในทุกวิธีได้ทดสอบระบบที่พัฒนาขึ้นโดยเปรียบเทียบสัญญาณระหว่างอิเล็ก โทรดที่มีและไม่มีวัสดุนาโน พบว่าระบบที่มีวัสดุนาโนให้สัญญาณที่มีความไววิเคราะห์สูงกว่ามากและ ให้ขีดจำกัดการตรวจวัดที่ต่ำมาก ในช่วง 1×10⁻¹⁴ – 1×10⁻¹⁹ โมลต่อลิตร ในทุกๆ ระบบสามารถ วิเคราะห์ตัวอย่างจริง เช่น ซีรั่ม ปัสสาวะ หรือสารละลายที่ใช้สกัดสารปนเปื้อนจากเนื้อกุ้งได้อย่างมี นอกจากนี้ได้ศึกษาการเพิ่มพื้นที่ผิวของอิเล็กโทรดโดยพัฒนาเทคนิคใหม่ในการเตรียม แท่งนาโนทองแบบตั้งตรงที่มีผิวเป็นรูพรุน และได้ใช้ในการตรวจวัดปริมาณสารผ่านเทคนิคทางเคมี วิธีต่างๆ ที่ได้ศึกษานี้สามารถนำไปประยุกต์ใช้วัดสารอื่นๆ และใช้ในการศึกษาอันตรกิริยา ระหว่างโมเลกุล

คำสำคัญ อนุภาคนาโน ทองที่มีรูพรุน แท่งนาโนทองแบบตั้งตรงที่มีผิวเป็นรูพรุน ไม่ติดฉลาก ไบโอเซนเซอร์ ความจุไฟฟ้า อิมพีแดนซ์ เทคนิคทางเคมีไฟฟ้า การเพิ่มความไว วิเคราะห์

Abstract

This report focused on the study of the enhancement of label-free real-time affinity detectors using capacitive and impedimetric measurements by incorporating nanomaterials. A flow injection system was applied to obtain continuous analysis. To increase the response signal, the main idea is to increase the surface area of the electrode with nanomaterials, thus, more surface area for the biorecognition elements to be immobilized. This in turn provides higher number of binding sites for the analytes. The studies were based on the use of various protocols to incorporate nanomaterials on a gold electrode surface. Four different approaches have been studied. The first procedure was to incorporate silver nanoparticles on a gold electrode surface via a self-assembled monolayer of a thiol compound and then immobilized the antibody onto the nanoparticles. The second approach was to add another layer of a thiol compound, with two free functional groups that can bind to and immobilized the antibody, on This would further increase the amount of the immobilized top of the nanoparticles. antibodies. The third procedure was to study the effect of additional layers of nanoparticles in a layer-by-layer technique. The final approach was to increase the immobilized surface area using a porous structure. These systems were used to detect the specific binding between the sensing antibodies and the analytes of interest. When compared to a bare gold electrode all of the studied protocols provided much higher sensitivities and extremely low detection limits, 1×10⁻¹⁴ - 1×10⁻¹⁹ mol L⁻¹. All of these techniques have been successfully applied for real sample analysis, such as serum, urine and solution mixture from homogenized shrimp. In addition a novel method to fabricate nanoporous wire arrays that can increase the surface area of the sensing electrode was also developed and successfully applied for an electrochemical detection. All of these strategies would be potential useful for the sensitive detection of various analytes and for the sensitive studies of binding interactions between molecules.

Keywords: Nanoparticles; Porous gold; Porous Nanowire arrays; Label-free; Biosensor; Capacitance; Impedance; Electrochemical detection; Sensitivity enhancement.

Table of Contents

Executive Summary	1
1. Introduction	3
2. Objective	5
3. Comparative study of enhancement of label-free affinity biosensor by gold ar	nd silver
nanoparticles	6
3.1 Introduction	6
3.2 Experimental	6
3.2.1 Antibody immobilization	6
3.2.2 Capacitance measurement	6
3.2.3 Real sample analysis	7
3.3 Results	7
3.3.1 Effect of amount of nanoparticles	7
3.3.2 Analytical performance	7
3.3.3 Performance of gold and silver nanoparticles	8
3.3.4 Effect of the size of analytes	8
3.3.5 Determination of HSA in urine samples	8
3.4 Conclusions	8
4. Enhancement of label-free affinity biosensor by nanoparticles with additional	l layer 9
4.1 Introduction	9
4.2 Experimental	9
4.2.1 Modified electrodes	9
4.2.2 Impedimetric measurement	10
4.2.3 Real sample analysis	10
4.3 Results	10
4.3.1 Performances of the system	10
4.3.3 Real sample analysis	11
4.4 Conclusions	11
5. Capacitive immunosensor signal enhancement using layer-by-layer gold	
nanoparticles	12
5.1 Introduction	12
5.2 Experimental	12
5.2.1 Fabrication of the layer by layer gold nanoparticles electrode	12
5.2.3 Surface characterization	13
5.3 Results	13
5.3.1 Characterization of the electrode	13
5.3.2 Capacitive immunosensor	14
5.3.3 Determination of HSA in real samples	14
5.4 Conclusions	14

6. Porous Gold Electrode for Electrochemical Impedance Spectroscopy Immunose	nsor
Detection	15
6.1 Introduction	15
6.2 Experimental	15
6.2.1 Immobilization of anti-HSA on porous gold	15
6.2.2 Impedance measurement	15
6.2.3 Determination of HSA in serum and urine samples	16
6.3 Results	16
6.3.1 Characterization of porous electrode modification	16
6.3.2 Impedimetric measurement	16
6.3.3 Effect of blocking solution	17
6.3.4 Determination of HSA in serum and urine samples	17
6.4 Conclusions	17
7. Novel template-assisted fabrication of porous gold nanowire arrays	18
7.1 Introduction	18
7.2 Experimental	18
7.2.1 Preparation of NPG-NWAs electrode	18
7.2.2 Detection principle and analytical performances	18
7.2.3 Real sample analysis	19
7.3 Results	19
7.3.1 Nanowire arrays	19
7.3.2 Performances of the NPG-NWAs electrode for detecting glutathione	19
7.3.3 Real sample analysis	20
7.4 Conclusions	20
8. Concluding remarks	21
References	22
Output	24
Publications	24
Other related activities	25
Conference reports	25
Invited speaker	25

Executive Summary

The main objective of this project is the development of real-time label-free affinity biosensors with enhanced sensitivity and detection limit by incorporating nanomaterials to be used in continuous analysis. The investigation involved the development and evaluation of the performances of real-time label-free affinity biosensor systems for the quantitative analysis of trace amounts of molecules, and to validate the results with conventional methods. This involves the development of different protocols for the immobilization of bioaffinitiy element incorporated with nanomaterials. Four approaches were studied.

The first approach was to modify gold electrodes with silver nanoparticles (AgNPs) via a self-assembled monolayer of thiourea. Appropriate antibodies were used to detect analytes of different sizes using real-time capacitive detection. It was found that there was an optimal amount of nanoparticles that provided the highest immobilization yield and response. Comparing to the use of gold nanoparticles (AuNPs) the lower cost AgNPs provided the same performance to the one prepared with AuNPs. The incorporation of AgNPs can improve the detection sensitivity and detection limit for both large and small molecules.

To further improve the analytical performances of the label-free affinity biosensor, a layer of mercaptosuccinic acid (MSA) was added on top of the AuNPs before immobilizing the antibody. This MSA has two free functional groups that can bind to the antibody, hence increase the amount of the immobilized antibody. The real-time impedance change due to the binding between chloramphenicol, a small molecule, and its antibody was measured. Under optimal conditions this modified electrode was compared to the bare gold and the one modified with only AuNPs. The one with AuNPs and MSA provided the highest sensitivity, and the lowest determination limit of 1.0×10^{-16} M. This very low limit makes it very suitable for residue detection.

The third procedure was based on layer-by-layer (LBL) self-assembled AuNPs. The additional layer can effectively enhance the sensitivity of a label-free capacitive immunosensor due to the increase of the amount of AuNPs that results in an increase of the effective surface area for the immobilized sensing elements. It was found that there was an optimal concentration (71 nmol L⁻¹) and a number of layer (2 layers) of the AuNPs that provided the highest sensitivity. This work presented for the first time the effect of the direction of AuNPs deposition. The face-down deposition direction of the electrode into AuNPs solution, provided a better sensitivity, lower detection limit (10⁻¹⁹ mol L⁻¹ human serum albumin) and a wider linear range than the face-up, into the AuNPs, deposition direction. The extremely low detection limit demonstrated that the system could easily determine the analyte at ultra trace level.

The final approach was to enhance the modified electrode surface area by a porous gold structure. The porous electrode with a much larger surface area than the flat electrode (19 ± 1 times) could be simply prepared in a one-step electro-process. The enhanced label-free immunosensor detection was based on electrochemical impedance spectroscopy (EIS). Due to the porous structure, antibody immobilized via a self-assembled monolayer (SAM) of a relatively long thiol compound provided a better analytical performance than the one modified with a shorter compound or a polymer. This is most likely because SAMs can cover

more surface area than the polymer and the longer chain SAM can extend further into the solution making it more accessible by the antibody during immobilization and also by the analyte during analysis. The modified porous electrode, blocked with BSA, greatly enhanced the sensitivity and provided a much lower detection limit than the sensitivity of the flat electrode (1×10^{-14} mol L⁻¹ or 0.68 ng L⁻¹), by 2 orders of magnitude. Besides immunosensors, this method would also be a useful tool to improve the study of biological molecules interactions.

In addition another porous structure, i.e., porous nanowires, was also investigated. The novelty of this work is the direct growing of the nanoporous gold nanowire arrays (NPG-NWAs) onto the surface of a disposable gold electrode through the pores of a conductivelayer-free membrane placed on top of a working electrode set inside a costom-made batch cell. The NPG-NWAs electrode was then directly applied as the working electrode for the detection of analyte within the same batch cell. The porosity of the NPG-NWAs increased the surface area of the electrode, about 160 times compared to a bare gold electrode. Initially the fabricated NPG-NWAs electrode was intended for a label-free affinity biosensor. However, the results from the previous work indicated that it might be difficult for the sensing molecules to get access to the pores along the length of the nanowires to be immobilized. Therefore, the advantage of the large surface area of the porous nanowire structure was investigated by applying the NPG-NWAs electrode for the electrochemical detection of an analyte and glutathione was used as the model. The increase surface area of the electrode improved the sensor sensitivity and the limit of detection. This technique can be easily applied for other type of NWAs using different plating solutions or electrode substrates for many fields of applications.

The various investigated strategies to incorporate nanomaterials into label-free affinity clearly enhanced the analytical performances of detection systems. The improved sensitivities and limit of detections make them suitable for ultra trace analysis. In addition all of the modified surfaces provided good reproducibility. One preparation of each of the modified systems could be reused at least 40 analysis cycles and this helps to reduce the cost of analysis. When they were applied for real samples analysis, no significant differences were observed between the results obtained by the developed systems and the conventional methods. These strategies can easily be applied for the sensitive detection of other analytes.

1. Introduction

Development of systems for trace level analysis of environmental, food, biomedical or pharmaceutical samples is a challenge because this requires specific and sensitive techniques. An interesting approach is the development of affinity biosensors. Affinity biosensors are analytical devices composed of a biological recognition element such as an antibody, receptor protein, biomimetic material, or DNA interfaced to a signal transducer (Rogers, 2000). Detection principle of reported transducers includes, for examples, electrochemical (Grieshaber et al., 2008; Ronkainen et al., 2010), optical (Borisov & Wolfbeis, 2008; Scarano et al., 2010) and piezoelectric (Ermolaeva & Kalmykova, 2006; Lucarelli et al., 2008). Among these, electrochemical biosensors provide an attractive mean to analyze the content of a sample due to the direct conversion of a biological event to an electronic signal (Grieshaber et al., 2008; Ronkainen et al., 2010). Detection of affinity binding can also be classified as labeled (indirect) or label-free (direct) (Bilitewski, 2006). For indirect assay, the detection of analyte and bioaffinity molecule relied on the determination of a label molecule, however, this type of affinity biosensor requires several steps, is time-consuming and makes real-time measurement impossible (Berggren, 2001). Therefore, it would be more advantageous to develop affinity biosensors capable of direct assay of target analytes.

For label-free affinity biosensor, when the analyte binds to its bioaffinity molecule the response is determined from the change in physical properties of the surface during the affinity complex formation. This physical change has been detected using optical (surface plasmon resonance, SPR) (Homola, 2008; Guo, 2012), piezoelectric (Ermolaeva & Kalmykova, 2006; Lucarelli *et al.*, 2008) and electrochemical methods (Berggren, 2001; Daniels & Pourmand, 2007). Among the electrochemical principles capacitive and impedimetric techniques have proven to be very sensitive, with the lower detection limits in the pico molar range or lower (Berggren, 2001; Dijksma et al., 2001; Bart et al., 2005).

At the Trace Analysis and Biosensor Research Center (TAB-RC), Prince of Songkla University, we have investigated and evaluated the label-free detection technique for several affinity binding pairs based on electrochemical detection principles such as capacitive detection of alpha-fetoprotein and anti-alpha-fetoprotein (Limbut et al., 2006a), carcinoembryonic antigen and anti-carcinoembryonic antigen (Limbut et al., 2006b) and impedimetric detection of penicillin G and anti-penicillin G (Thavarungkul et al., 2007). These systems are highly selective, sensitive, can detect analyte with accuracy within a short analysis time. The detection limit of the system is generally very low, in the range of pico to femto molar. These devices can be applied for the quantitative analysis of trace amounts of analytes.

Although these methods can provide very low detection limit, for some substances that are not approved by the authorities guideline values are normally set at or about the analytical limit of determination (Hamilton et al., 2003). Therefore, the control of diseases, food quality and safety, and quality of our environment would be much better if the performance of the analysis method can be enhanced to obtain better sensitivity and the lowest possible detection limit. This will enable the detection at the lowest possible concentration especially when the molecule of the detecting analyte is small (resulting in a small physical change when forming

affinity complex) and are with the presence of interfering substances. If a detection limit is very low the interfering effect could easily be overcome by diluting the samples. In view of these, the enhancement of system sensitivity is needed.

One way of improving the efficiency of label-free affinity detection is to incorporate nanoparticles during the immobilization procedure. This has shown to help increase the response in label-free affinity detection, for examples, when using optical (Liu et al., 2006; Lai et al., 2007; Wang et al., 2008) and some electrochemical detections (Hu et al., 2003; Wu et al., 2005; Pingarrón et al., 2008). Although some of these techniques could produce real-time response (Liu et al., 2006; Lai et al., 2007; Wang et al., 2008) the analysis still has to be done in discrete manner where the sensing surface has to be incubated with the analyte before detection could take place (Hu et al., 2003; Wu et al., 2005; Liu et al., 2006; Lai et al., 2007; Wang et al., 2008). Therefore, there is a vast area that still needed to be explored, especially in the real-time and continuous schemes.

The work in this project focuses on the study of the enhancement of label-free real-time affinity detection using electrochemical measurements by incorporating nanomaterials. A flow injection system was applied to obtain continuous analysis. To increase the response signal, the main idea is to increase the surface area of the electrode with nanomaterials, thus, more surface area for biorecognition element to be immobilized. This in turn provides higher number of binding site for the analytes. In this project, different approaches to incorporate nanomaterials to achieve even higher performances were studied. The aim is to obtain higher sensitivity and the lowest possible detection limit. The systems were used to detect the specific binding between the sensing element and the analyte of interest.

2. Objective

The objective of this research is to develop real-time label-free affinity biosensors with enhanced sensitivity and detection limit by incorporating nanomaterials to be used in continuous analysis.

The investigation involved the development and evaluation of the performances of real-time label-free affinity biosensor systems for the quantitative analysis of trace amounts of molecules, and to validate the results with conventional methods. This involves the development of different protocols for the immobilization of bioaffinitiv element incorporated with nanomaterials. Four approaches were investigated. The first study was to modify electrodes with silver nanoparticles (AgNPs), via a self-assembled monolayer of thiourea. Appropriate antibodies were used to detect analytes of different sizes using capacitive detection. The second approach was to add a layer of mercaptosuccinic acid (MSA) on top of the nanoparticles before immobilizing the antibody. The impedance change due to the binding between chloramphenicol, a small molecule, and its antibody was measured. The third procedure was based on layer-by-layer (LBL) self-assembled gold nanoparticles (AuNPs). The additional layer can effectively enhance the sensitivity of a label-free capacitive immunosensor. The final approach was to fabricated a porous gold structure. A porous gold surface was achieved by a simple one-step electro-process. The enhanced label-free immunosensor detection was based on electrochemical impedance spectroscopy (EIS).

3. Comparative study of enhancement of label-free affinity biosensor by gold and silver nanoparticles

3.1 Introduction

One way to enhance the performance of a label-free affinity biosensor is by using nanoparticles to increase the effective surface area for the immobilized sensing molecules. Such previously developed methods have mostly used gold nanoparticles (AuNPs) (Li et al., 2005; Wu et al., 2005; Yang et al., 2009) with only a few applications of silver nanoparticles (AgNPs) have been studied (Loyprasert et al., 2008; Wu et al., 2010). Since silver is cheaper than gold and the preparation of its nanoparticles is also simple it is possible that AgNPs can effectively enhance the sensitivity and detection limit of a capacitive immunosensor system, comparable to the system with AuNPs. First the optimum amount of AgNPs required to increase the sensing molecule immobilization area was investigated. Then electrodes with a suitable concentration of nanoparticles incorporated were tested for their activities in the capacitive system. To investigate how this might enhance the detection of both large and small molecules, three antibody-antigen pairs were tested: (i) anti-human serum albumin (anti-HSA) and human serum albumin (HSA) (MW 68000 g mol⁻¹), (ii) antimicrocystin-LR (anti-MCLR) and microcystin-LR (MCLR) (MW 995.17 g mol-1) and (iii) anti-penicillin G (anti-Pen G) and penicillin G (Pen G) (MW 356.37 g mol⁻¹). The system for the detection of HSA was also compared with one that had AuNPs incorporated. To test the application of this new electrode for real sample detection, the system was employed to analyse HSA in urine samples.

This work is published in *Analytica Chimica Acta* (Dawan *et al.*, 2011) (Journal Impact Factor 2011: 4.555) (Paper I). A short summary is presented.

3.2 Experimental

3.2.1 Antibody immobilization

Nanoparticles were added onto the modified electrode by adsorption on the self-assembled monolayer (SAM) of thiourea. Antibody was also simply adsorbed on the surface of nanoparticles. Three types of antibody, anti-HSA, anti-MCLR and anti-Pen G, were studied. Different amounts of nanoparticles per unit volume were tested to obtained the one that provided the highest effective surface area for the immobilization of the antibody. For the electrode without the nanoparticles, antibodies were immobilized on the electrode via the SAM of thiourea.

3.2.2 Capacitance measurement

Experiments were carried out using a flow injection capacitive system. The measurement was carried out using a three-electrode system consisted of a working electrode (modified electrode), an auxiliary electrode (Pt wire) and a reference electrode (Ag/AgCl) connected to a custom-built capacitive analyzer (Wongkittisuksa *et al.*, 2011). This

instrumentation automatically applies 50 mV potential pulses on the working electrode at 60-s intervals. The capacitance at the electrode/solution interface was determined by the computer program from the current response of each pulse. The obtained capacitance values were plotted with respect to time on the monitor and stored on the computer. When the solution containing analytes was injected into the system, the analytes bound to the immobilized antibody on the electrode causing the capacitance to decrease in proportion to the concentration of the analyte. The change in capacitance (Δ C) due to the binding was related to the concentration of the analyte. The surface of the electrode was then regenerated with a regeneration solution to remove the analytes from the immobilized antibody so a new analytical cycle could be performed.

3.2.3 Real sample analysis

The flow capacitive immunosensor system using electrodes modified with AgNPs was applied to detect HSA in urine samples obtained from Songklanagarind Hospital, Hat Yai, Thailand. The results were compared with those obtained by the hospital using an immunoturbidimetric assay.

3.3 Results

3.3.1 Effect of amount of nanoparticles

Four concentrations of AgNPs were investigated. The results indicated that there exist an optimal amount of AgNPs, 48 pmol (in 2 mL), that can provided the largest effective surface area. Beyond this amount the density of nanoparticles is too high and the particles cluster together and hence decrease the surface area. The amount of antibody that could be immobilized on the surface with different amount of AgNPS was also determined. The results were related to the effective surface area. At the optimal amount of AgNPs the highest immobilization yield (88%) was obtained due to the large surface area.

3.3.2 Analytical performance

The capacitance change caused by the binding between the antibody and the antigen (analyte) was plotted against the logarithm of the analyte concentration. Immunosensors for HSA prepared with different amount of AgNPs were tested. As expected the responses of the electrodes corresponded well to the amount of immoblized antibody. At the optimal amount of AgNPs the sensitivity of the capacitive system (slope of the linear region of the calibration plot) for HSA detection was the highest. This was 2.1 times higher than the electrode without the nanoparticles. The linear range was also wider, from 1.0×10^{-18} to 1.0×10^{-10} M compared to 1.0×10^{-16} to 1.0×10^{-10} M. In addition, the limit of detection of the electrode with nanoparticles was extremely low, i.e., 1.0×10^{-18} M, lower than the electrode without the nanoparticles by two orders of magnitude.

3.3.3 Performance of gold and silver nanoparticles

Electrodes were modified with AgNPs and AuNPs of approximately the same size (AgNPs = 10 ± 2 nm and AuNPs = 8 ± 2 nm) at the optimal concentration. Both electrodes provided the same linear range, 1.0×10^{-18} to 1.0×10^{-10} M and the same detection limit of 1.0×10^{-18} M with nearly the same sensitivity. These results indicated that both nanoparticles could provide the same high sensitivity and low detection limit.

3.3.4 Effect of the size of analytes

Capacitive immunosensors with incorporated AgNPs were investigated for their performances with different sizes of analytes, i.e. HSA (68,000 g mol⁻¹), MCLR (995.17 g mol⁻¹) and Pen G (365.37 g mol⁻¹). The electrodes modified with AgNPs enhanced the sensitivity by about 2.2, 2.8 and 2.7 times for HSA, MCLR and Pen G, respectively. The detection limit was also lowered by two orders of magnitude for HSA (macromolecule to 10⁻¹⁸ M) and one order of magnitude for small molecules, i.e., MCLR (to 10⁻¹⁴ M) and Pen G (to 10⁻¹⁵ M).

3.3.5 Determination of HSA in urine samples

The advantage of a very low detection limit of the capacitive immunosensor is that the effect of othe matrices in a real sample can be reduced by just simply diluting the sample. After the dilution the concentration of the analyte would be lower but was still detectable by the sensitive capacitive system. Seven urine samples were tested, each sample was diluted 10^6 times before analysis. The concentrations determined by the capacitive immunosensor system are in good agreement with the results obtained by the hospital (P>0.05).

3.4 Conclusions

Detection of ultra-trace amounts of antigens by label-free capacitive immunosensors was achieved using electrodes modified with silver nanoparticles (AgNPs) that allows for an increase in the amount of immobilized antibodies. There was an optimal amount of AgNPs that provided the highest immobilization yield and response. The performances of immunosensor electrodes for human serum albumin prepared with AgNPs provided the same performance to the one prepared with gold nanoparticles. That is, AgNPs that can be prepared with lower cost could be effectively applied. The incorporation of AgNPs provides better sensitivity and detection limit than without nanoparticles for both large and small molecules. The high sensitivity and very low detection limits are potentially useful for the analysis of toxins or residues present in samples at ultra-trace levels and this method could easily be applied to other affinity pairs.

4. Enhancement of label-free affinity biosensor by nanoparticles with additional layer

4.1 Introduction

In the previous section an enhancement of the biosensor performance was achieved by the direct adsorption of the bioaffinity element on nanoparticles. To further enhance the response, the amount of immobilized bioaffinity molecules could be increased through an additional layer with functional group(s) that can bind with bioaffinity molecules. It is expected that more bioaffinity molecules can be immobilized with stronger bond than the simple adsorption on nanoparticles, thus, increase the binding capacity with the analyte. For this system, impedance measurement, another highly sensitive label-free detection system (Dijksma *et al.*, 2001; Bart *et al.*, 2005; Thavarungkul *et al.*, 2007), was employed.

In this part of the project a layer of nanoparticles (on a self-assembled thiourea monolayer) was first attached on the electrode surface. Then a layer of mercaptosuccinic acid (MSA), a thiol compound, was formed on the nanoparticles layer. This MSA has two free functional carboxylic groups (Lewis & Hawley, 1993) that can be used to immobilize the antibody. The electrode modification steps were optimized to obtain the maximum amount of the immobilized antibody. Chloramphenicol (CAP) was chosen as a model analyte because it is a widely used antibiotic, with a low molecular weight (MW 323.13 g mol⁻¹). Also there is need to detect very small residual amounts of CAP in food samples to ensure there will be no possible dangers to human health. The proposed system was then applied to analyse CAP (analyte) in shrimp samples.

This part of the project is published in *Biosensors and Bioelectronics* (Chullasat *et al.*, 2011) (Journal Impact Factor 2011: 5.602) (Paper II). A short summary is presented as follows.

4.2 Experimental

4.2.1 Modified electrodes

A self-assembled monolayer of thiourea (SATUM) was first allowed to form on gold rod electrode (diameter = 3.0 mm). The AuNPs were then adsorbed on SATUM. The volume of AuNPs and incubation time were optimized. Next a layer of MSA was adsorbed on the AuNPs where the concentrations of MSA and incubation time were also optimized. The modified surface was then activated with EDC/NHS (EDC 1% (v/v), NHS 2.5% (v/v) in 50 mM phosphate buffer pH 5.00 with 50 mM KCl) after which anti-CAP was placed on the modified electrode and left for the binding reaction to occurred overnight at 4°C. This is the SATUM/AuNPs/MSA modified electrode.

For a SATUM modified electrode, after the SAM was formed as described above, anti-CAP was immobilized on this layer. For SATUM/AuNPs modified electrode, after the formation of SAM and adsorption of AuNPs, anti-CAP was allowed to adsorb on the AuNPs.

4.2.2 Impedimetric measurement

CAP was determined using a flow injection impedimetric immunosensor system using an Autolab PGSTAT30 electrochemical impedance analyzer and potentionstat/galvanostat (Metrohm Autolab, The Netherlands) connected to a computer. The modified electrode was used as the working electrode (WE) together with a custom-made Ag/AgCl electrode (RE) and a Pt wire auxiliary electrode (AE). Eco Chemie software, Frequency Response Analyzer (FRA 4.9.005), was used to monitor the impedance.

The CAP-anti-CAP interaction was monitored via the change of the imaginary part of impedance (Z'') as a function of time at a single frequency. The carrier buffer was passed through the system to obtain the baseline of Z''. When CAP (analyte) was injected, it bound to the immobilized anti-CAP (antibody) on the modified electrode and the impedance increased ($\Delta Z''$), corresponded with the concentration of CAP. After each analysis, the immobilized electrode was prepared for the next analysis by using regeneration solution to remove the bound antigen from the modified electrode surface.

4.2.3 Real sample analysis

Six shrimp samples were collected from six markets in Hat Yai, Songkhla, Thailand. Two gram of blended shrimp sample was mixed with 10.0 mL of carrier buffer, and then homogenized by ultrasonic homogenizer (Biologics, Inc. USA) for 15 min. The mixture was centrifuge at 10,000 rpm for 15 min, discarded the sediment and 200 μ L of the supernatant was then transferred to a desalt column (Bio-Rad Laboratories, USA). The desalted sample was then diluted 10,000 times by the carrier buffer and analyzed in the flow injection impedimetric immunosensors system.

4.3 Results

4.3.1 Performances of the system

Linear range and limit of determination

Using the optimal operating conditions the linear range for the SATUM/AuNPs/MSA modified electrode was the lowest detectable range, (0.50 - $10) \times 10^{-16}$ M. For the SATUM/AuNPs modified electrode, a linear range of (1.0 - $10) \times 10^{-15}$ M was obtained. The SATUM modified electrode gave a linear range of (1.0 - $10) \times 10^{-14}$ M. The determination limit of the SATUM/AuNPs/MSA modified electrode was also the lowest, 1.0×10^{-16} M, much better than the electrode modified with SATUM/AuNPs $(1.0 \times 10^{-15} \text{ M})$ and SATUM $(4.7 \times 10^{-14} \text{ M})$. This would be very useful for residue analysis.

Reproducibility

The reproducibility of the responses of two SATUM/AuNPs/MSA electrodes was evaluated at optimum conditions, by repeatedly injecting the same concentration of standard CAP (1.0×10^{-15} M). The regeneration solution was used to remove CAP analyte from the immobilized anti-CAP after each detection. The two electrodes showed similar results, i.e., the modified electrode can be reused about 45 times. A cyclic voltammogram of the electrode

after the loss of activity indicate that the modified electrode layer remained intact. The decrease of the percentage of residual activity was therefore probably due to the loss of activity of the immobilized antibody.

The reproducibility of six different electrodes modified with SATUM/AuNPs/MSA and anti-CAP prepared in the same batch was also tested by comparing the sensitivity (slope of the calibration plot). The values did not differ significantly (P>0.05) indicating that the performance of the different electrodes can be reproduced.

Selectivity

The immunosensor was tested for its selectivity to CAP. Antibiotics with similar structure to CAP, i.e. florfenicol, thiamphenicol and chloramphenicol base, and those which are frequency tested in shrimp i.e. tetracycline and oxolinic acid were tested at the same concentration range. All of these antibiotics provide very low impedance changes. The signals were the same value as blank response. Hence, this system showed very good selectivity for CAP.

4.3.3 Real sample analysis

The six samples were analyzed by the label-free impedimetric immunosensor under optimum conditions. The concentration of chloramphenical for all samples was not determinable because the obtained signals were much lower than the determination limit.

To validate the method, recovery was studied by spiking CAP to obtained a final concentration of 1.6, 4.0, 8.1 and 16.2 ppt of CAP in the shrimp samples. The recoveries of CAP in shrimp sample were in the range of 87% to 116% with a relative standard deviation between 1 and 14 %. These values were acceptable (Taverniers, 2004).

CAP (1.00 - 2.50 ppm) of the same six samples was also analyzed by a label-free impedimetric immunosensor and HPLC technique. Comparison between the two analysis techniques was done by the Wilcoxon signed rank test and there was no evidence for any systematic difference between the results obtained from the label-free impedimetric immunosensor and HPLC (P > 0.05).

4.4 Conclusions

A multilayer electrode modified with a self-assembled thiourea monolayer followed by gold nanoparticles, mercaptosuccinic acid and antibody was investigated for the detection of ultra trace amount of a small molecule (chloramphenicol) in an impedimetric system. The formation of the antibody–antigen complex at the electrode surface caused the impedance to increase. Under optimum conditions three modified electrodes were compared the SATUM/ AuNPs/MSA electrode provided a wide linear range $(0.50 - 10) \times 10^{-16}$ M, and a very low determination limit of 1.0×10^{-16} M, makes it very suitable for residue detection. The modified electrode provided good selectivity and can be reused up to 45 times and this helps to reduce analysis cost. When applied to determine chloramphenicol in shrimp samples, the results agreed well with those obtained by the high-performance liquid chromatography coupled with a photo diode array detector (P > 0.05). The developed system can be applied to detect other small molecules using appropriate affinity binding pairs.

5. Capacitive immunosensor signal enhancement using layer-by-layer gold nanoparticles

5.1 Introduction

In the previous two sections the electrode surface was modified with a layer of selfassembled monolayer (SAM) of thiourea before further modification with nanoparticles and antibodies was performed. Another strategy that may be appropriate for label-free affinity biosensing is to immobilize bioaffinity molecules via an electropolymerization layer of a nonconducting polymer, the one that can provide functional group to incorporate nanomaterials (Teeparuksapun et al., 2009; Loyprasert et al., 2010). It is expected that through the optimization of electropolymerized potential, scan rate and scan number a large number of binding site will be obtained. Further enhancement can also be done by added layer of nanomaterials before bioaffinity molecules was adsorbed directly on to these nanomaterials (Figure 5.1). This so called layer by layer (LBL) technique was investigated in this part of the project on a poly-tyramine (Pty) modified gold electrode. The layer by layer of gold nanoparticles (AuNPs) was formed using thiourea (TU) as a cross linker. Anti-human serum albumin (anti-HSA) and human serum albumin (HSA) were used as a model of the immunosensing. This work also investigated the electrochemical properties and the morphology of the electrode with different layers and different concentration of AuNPs. Finally, the performance of the capacitive immunosensor system such as its linear range, limit of detection and real sample analysis were studied.

This part of the project is published in *Electrochimica Acta* (Samanman *et al.*, 2012) (Journal Impact Factor 2011: 3.832) (Paper III). A short summary is presented as follows.

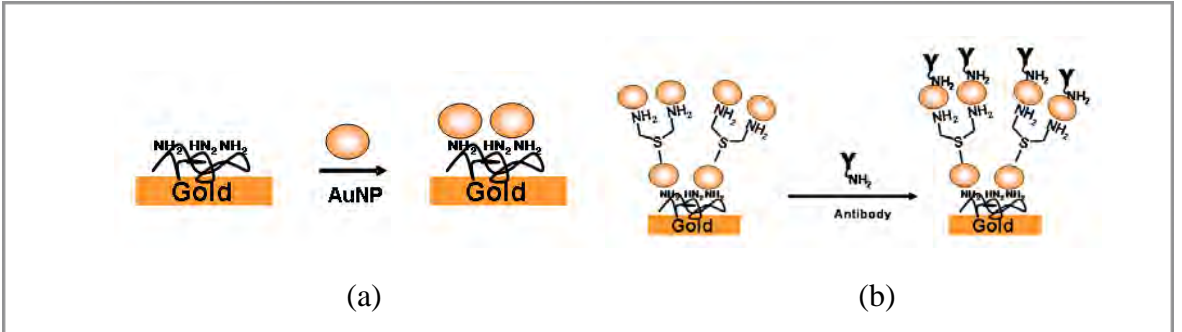


Figure 5.1 Polymer modified electrode with (a) one layer of nanomaterials and (b) layer-by-layer of nanomaterials via a self-assembled monolayer of thiourea.

5.2 Experimental

5.2.1 Fabrication of the layer by layer gold nanoparticles electrode

A gold rod electrode (diameter = 3.0 mm) was polished, cleaned by electrochemical etching, washed with distilled water and dried using nitrogen gas. Pty was then

electropolymerized onto the gold electrode using the potential from 0.0 to 0.8 V versus a Ag/AgCl reference electrode with a scan rate of 0.05 V s⁻¹ for 10 scans (Loyprasert *et al.*, 2010). The Pty modified electrode was then immersed in 1.0 ml of colloidal AuNPs for 4 h at 4 °C, then removed and rinsed with water. This will be referred to as the first layer of AuNPs (AuNPs₁). The AuNPs₁/Pty modified electrode was then immersed in TU, the cross linker, for 24 h at room temperature. This step will be referred to as the TU₁ step. These two steps were repeated to obtain a multilayered electrode (AuNPs_n/TU_{n-1}) where n is the number of layers (n = 1 - 5). The electrode with different numbers of layers and different concentrations of AuNPs were studied for the conditions that provided the largest surface area, good electron transfer, the largest immobilization yield and the highest detection sensitivity by the capacitive system. The electrodes with different layers of colloidal particles were immobilized with anti-HSA and left overnight at 4 °C and blocked with 1-dodecanethiol.

5.2.3 Surface characterization

The surface coverage of the electrode with different layers of AuNPs was determined by cyclic voltammetry. The surface morphology of the electrodes with different layers of AuNPs was observed by scanning electron microscopy (SEM). The resistance of the electron transfer between the solution and the electrode surface and the constant phase element were obtained by electrochemical impedance spectroscopy (EIS).

5.2.4 Capacitance measurement

A potentiostatic step method was used to measure the capacitance, the same method as in 3.2.2. The potential pulse was applied at a regular interval and the analog current responses from the potentiostat was sampled and recorded using the Powerlab data acquisition system system (ADInstrument, Australia). The current responses was analysed to obtain the capacitance. When the solution containing the analyte was injected, it bound to the immobilized sensing elements on the gold electrode causing the capacitance to decrease until it reached a stable value. The change in capacitance, due to the binding, is correlated with the analyte concentration.

5.2.5 Determination of HSA in a real sample

Urine samples were obtained from Songklanagarind Hospital, Hat Yai, Thailand. The samples were analyzed by the flow capacitive immunosensor system using the electrode with optimal layers of AuNPs. The results of the samples were compared with those obtained by the Hospital.

5.3 Results

5.3.1 Characterization of the electrode

The results showed that there exist an optimal amount of AuNPs and an optimal number of layer. An electrode with two layers of 71 nmol L⁻¹ of AuNPs provided the highest surface coverage (150 % compared to bare gold) and hence the immobilization yield (90 %). The decrease of the surface area after two layer is possibly because more and more particles

were adsorbed on the surface and they came into contact with each other. Therefore, the total surface area from the curvature surface of separated individual nanoparticles decreased. This hypothesis was confirmed by the SEM images where electrodes with more than two layers of AuNPs showed large clusters clearly indicated the closely packed particles.

5.3.2 Capacitive immunosensor

The electrode with two layers provided the highest sensitivities. The sensitivity is related to the surface coverage. The electrode with one layer of AuNPs provided a lower sensitivity than the two layers because of the reduced surface area due to the presence of fewer nanoparticles, hence, less antibody was immobilized. The electrodes with more than two layers also provided a lower sensitivity because of a lower surface area, however, in this case it was caused by too many nanoparticles became closely packed and, hence, there was a reduced surface enhancement caused by the reduction of the curvature from individual nanoparticles. The test for the immobilization yields of the anti-HSA on the electrode also confirmed the above reasoning. More antibody was immobilized on the surface with a larger surface area. That is, the immobilization yield was highest with two layers of AuNPs.

5.3.3 Determination of HSA in real samples

Six urine samples were obtained from Songklanagarind Hospital, Hat Yai, Thailand. The diluted urine samples were injected into the capacitive system. The responses were used to obtain the concentrations from the calibration plot. The results obtained from the capacitive immunosensor and the results from the hospital analysis were compared by the Wilcoxon signed rank test. There is no evidence for systematic differences between the results obtained from the two methods (P > 0.05). That is, the concentrations determined by the capacitive immunosensor system are in good agreement to the normal hospital analysis.

5.4 Conclusions

The sensitivity of a label-free capacitive immunosensor can be improved by the LBL technique due to the increase of the amount of assembled gold nanoparticles that results in an increase of the effective surface area for the immobilized sensing elements. The electrode with two layers of 71 nmol L^{-1} AuNPs provided the highest sensitivity and this was related to the highest surface coverage and hence the immobilization yield. The high sensitivity $(9.36\pm0.30, 9.78\pm0.30 \text{ -nF cm}^{-2} \log \text{mol } L^{-1})$ and extremely low detection limit $(10^{-19} \text{ mol } L^{-1})$ demonstrated that the system could easily determine the analyte at ultra trace level.

6. Porous Gold Electrode for Electrochemical Impedance Spectroscopy Immunosensor Detection

6.1 Introduction

To increase the electrode surface area another platform of interest is the one with a porous structure and the use of a porous gold electrode fabricated by a one-step electro-process for the improvement of a direct immunosensor detection was investigated. For the direct immunosensor detection, the pair of anti-human serum albumin (anti-HSA) and human serum albumin (HSA) was used as a model. The antibody was immobilized on the porous surface via a self assembled monolayer (SAM) compared to a polymer film (Loyprasert et al. 2010; Teeparuksapun et al. 2009). The system with the highest sensitivity and the lowest detection limit was then used to test the albumin concentration in urine and serum samples.

This part of the project is submitted to *Electrochimica Acta* (Dawan et al.) (Journal Impact Factor 2011: 3.832) (Paper IV). A short summary is presented as follows.

6.2 Experimental

6.2.1 Immobilization of anti-HSA on porous gold

A gold electrode (diameter 3 mm, 99.99% purity) was polished, cleaned, dried and placed in 5.0 ml of 2.0 mol L⁻¹ HCl and a potential of 1.50 V for 100 s was applied followed Deng's method (Deng *et al.*, 2008). Three different surface modifications of the flat gold and porous gold electrodes, used for antibody immobilization, were first investigated. Two were based on a self-assembled monolayer, i.e., 11- mercaptoundecanoic acid (11-MUA) and thiourea. The other was by a layer of electropolymerized polytyramine. The electrochemical characteristics of the modified electrodes were investigated using cyclic voltammetry. By comparing the performances of the three surface modifications, two of the better performed surfaces (11-MUA and polytyramine) were used to investigate the effect of two of the frequently used blocking molecules, 1% BSA and 1-dodecanethiol.

6.2.2 Impedance measurement

The electrochemical impedance spectroscopy (EIS) was performed at a frequency that ranged from 0.01 to 10,000 Hz at a +200 mV DC potential with an AC amplitude of 10 mV. The measurement was carried out in a stop-flow system. The flow cell (10 μ l) consisted of a working electrode (modified electrode), an auxiliary electrode (Pt wire) and a reference electrode (Ag/AgCl) connected to an Autolab PGSTAT30 electrochemical impedance analyzer and potentiostat/galvanostat (Metrohm Autolab B.V., The Netherlands). A Randles equivalent circuit consists of the solution resistance (R_s), the electron-transfer resistance (R_{et}), the Warburg impedance (Z_W) and a constant phase element (CPE), was used to fit the impedance curves. The fitting by the Autolab program provided the values of the circuit elements. The change in the R_{et} value was used to determine the binding between HSA and immobilized anti-HSA (Δ R_{et}). Then, the surface of the electrode was regenerated to remove the analytes from the immobilized antibody so a new analytical cycle could be performed.

6.2.3 Determination of HSA in serum and urine samples

Serum and urine samples were obtained from Songklanagarind Hospital, Hat Yai, Thailand and analyzed by the impedimetric immunosensor system. The results were compared with those obtained by the hospital using their photometric bromocresal green method (BCG) for serum sample and an immunoturbidimetric assay for the urine samples.

6.3 Results

6.3.1 Characterization of porous electrode modification

From an SEM image the thickness of porous gold was determined using a digital vernier caliper. The average thickness is 0.11 ± 0.04 mm. The area of the electrode was determined from the charge by integrating the gold oxide reduction peak in the cyclic voltammogram. From 20 electrodes, the area of the porous electrode was larger than the flat electrode by 19 ± 1 times.

The cyclic voltammograms at each modification steps via the SAM of 11-MUA and polytyramine on the porous gold electrode were investigated. The redox peaks were reduced after the formation of a self-assembled monolayer and the immobilization of antibody. When the surface was blocked with 1-dodecanethiol, the redox peaks disappeared. For the porous electrode modified with polytyramine, although every modification steps provided a reduction of the redox peaks, the last step, after the blocking solution, a background current could still be observed. This may be because the polymer can only covered the outer surface of the porous structure but could not reach the inner pores so the porous electrode modified with polymer was not totally insulated.

6.3.2 Impedimetric measurement

The affinity binding between the injected antigen and the immobilized antibody caused the R_{et} to increase. On the flat surface electrodes, the three modifications provided the same linear range and LOD but different sensitivities. The polymer layer provided the highest sensitivity due to the availability of a large number of free amino groups for the covalent attachment of the antibody. Between the two SAMs, their sensitivities were about the same.

When comparing the flat electrodes to the porous modified electrodes, all porous electrodes provided a wider linear range and a lower detection limit. The sensitivities were also higher. This is due to the higher surface area of the porous electrodes that helped to increase the amount of the immobilized antibody.

For the porous surface with different modifications, between the two SAMs, 11-MUA and thiourea, the longer chain 11-MUA provided a higher sensitivity, a wider linear range and a lower detection limit than the shorter chain thiourea. It is possible that the longer chain can extend further from the pores surface making it more accessible by the antibody, hence, more antibody can be immobilized. In addition, the longer chain of 11-MUA may also help the immobilized antibody to extend further into the sample solution enabling more binding with the analytes, thus, a higher response. When comparing the porous electrode modified with 11-MUA and polytyramine, they provided the same linear range and detection limit but the 11-MUA modified electrode gave a higher sensitivity. this is probably because not all the porous

surface was covered by the polymer layer, led to a reduced immobilization surface resulted in a lower immobilization yield and, hence, a lower sensitivity.

6.3.3 Effect of blocking solution

11-MUA was used to investigate the effect of blocking solution compared with the polymer modified electrode. The electrode blocked with 1% BSA provided higher sensitivity than the one blocked with 1-dodecanethiol. This is because the one blocked with BSA is more conductive and, thus, the electrode surface is more accessible to the redox species which is a more desirable condition for a faradaic sensor. This was confirmed by the cyclic voltammograms, the one of an electrode blocked with BSA was broader then the one blocked with 1-dodecanethiol indicated more background current, hence, less insulated. As a consequence when HSA bound to the immobilized antibody the effect of insulation caused by the binding was more pronounced on the electrode blocked with BSA, hence, a higher sensitivity. Therefore, the electrode blocked with 1%BSA was chosen to investigate the stability and test the real sample.

6.3.4 Determination of HSA in serum and urine samples

Seven urine and seven serum samples were diluted with buffer 10^6 times and 10^9 times, respectively. The results of the impedimetric immunosensor and the results from the hospital (immunoturbidimetric assay for urine samples and the bromocresal green method for the serum samples) were compared by the Wilcoxon signed rank test and indicated that there is no evidence for systematic differences between the results obtained from the two methods (P > 0.05). That is, the concentrations determined by the impedimetric immunosensor system are in good agreement to the immunoturbidimetric assay and bromocresal green method.

6.4 Conclusions

The porous electrode with a much larger surface area than the flat electrode could be simply prepared in a one-step electro-process. The advantage of this large surface area was demonstrated by applying it for a direct immunosensing based on EIS detection. The porous gold modified electrode provides a high sensitivity, low detection limit and good reproducibility. The porous electrode modified with SAM of 11-MUA, compared to the one modified with SAM of thiourea and polytyramine, gave the highest sensitivity and immobilization yield of antibody. This is most likely because SAMs can cover more surface area than the polymer and the longer chain SAM (11-MUA) can extend further into the solution making it more accessible by the antibody during immobilization and also by the analyte during analysis. The electrode blocked with BSA, due to the more conductive nature, provided a higher sensitivity than the one blocked with 1-dodecanethiol. This modified porous electrode greatly enhanced the sensitivity, to 8.7 times higher than the sensitivity of the flat electrode and a much lower detection limit (1×10⁻¹⁴ mol L⁻¹ or 0.68 ng L⁻¹), by 2 orders of magnitude. The improved performance by this porous gold electrode would be valuable for other faradaic measurements that targets higher sensitivities. Together with the EIS it would also be a useful tool to improve the study of biological molecules interactions such as surface loading, binding constants and rate constants.

7. Novel template-assisted fabrication of porous gold nanowire arrays

7.1 Introduction

Another investigated nanostructure was the porous nanowire. It is expected that the large surface area of the porous nanowire can help increase the performance of the sensors. The novelty of this work is the direct growing of the nanoporous gold nanowire arrays (NPG-NWAs) onto the surface of a disposable gold electrode through the pores of a conductivelayer-free anodic alumina oxide (AAO) membrane placed on top of a working electrode set inside a costom-made batch cell. The NPG-NWAs electrode was then directly applied as the working electrode for the detection of analyte within the same batch cell. fabricated NPG-NWAs electrode was intended for a label-free affinity biosensor. However, from the results of the nanoporous gold on a flat surface in chapter 6, a longer chain SAM (11-MUA) that can extend further into the solution is required for a better immobilization of the sensing elements and provided better interaction with the analytes. Therefore, for a porous nanowires with a three dimensional structure it would be more difficult for the sensing molecules to get access to the pores along the whole length and deep into all of the nanowires to be immobilized. In view of this the advantage of the large surface area of the porous nanowire structure was investigated by applying the NPG-NWAs electrode for the electrochemical detection of an analyte and glutathione was used as the model.

This part of the project is submitted to *Electrochimica Acta* (Samanman et al.) (Journal Impact Factor 2011: 3.832) (Paper V). A short summary is presented as follows.

7.2 Experimental

7.2.1 Preparation of NPG-NWAs electrode

The NPG-NWAs electrode was fabricated in a custom-made Teflon® batch cell. A short section of gold was first electrodeposited inside the bottom part of the pores of the AAO membrane and directly attached onto the disposable gold electrode surface. The purpose is to act as a support base for the upper porous structure section. This was followed by the coelectrodeposition of gold and silver. NaOH was then used to dissolve the AAO membrane template leaving only the NWAs to stand on the surface of the disposable gold electrode. The silver component was etched out of the alloy NWAs using HNO3 to obtain the NPG-NWAs.

7.2.2 Detection principle and analytical performances

Electrochemical detection of glutathione was carried out in the same batch cell used for fabrication of the NPG-NWAs using a three-electrode set-up consisting of a NPG-NWAs working electrode, a platinum counter electrode and an Ag/AgCl reference electrode. The indirect detection of glutathione is based on the measurement of a decrease of the peak current of copper in the presence of glutathione. The linear range and the limit of detection of the developed system were determined.

7.2.3 Real sample analysis

Three packs of glutathione dietary supplement product samples purchased from local pharmaceutical stores in Hat Yai, Thailand were analysed. The powder sample in each capsule was weighed and dissolved in buffer, filtered through a filter paper and then analysed. The obtained concentrations of glutathione in the samples analysed by the proposed method were then compared with those of the labeled values from the manufacturer.

7.3 Results

7.3.1 Nanowire arrays

The fabrication optimal conditions were: plating solution for the electrodeposition of gold and silver 20 mmol L⁻¹ KAu(CN)₂ and 100 mmol L⁻¹ KAg(CN)₂ in 0.25 mol L⁻¹ Na₂CO₃; deposited at -1.20 V for 0.2 C; membrane dissolving time 60 min; silver dealloying time 30 min. Figure 7.1 shows SEM images of the NPG-NWAs. The diameter of nanowire is approximately 200 nm, which is defined by the diameter of the AAO template.

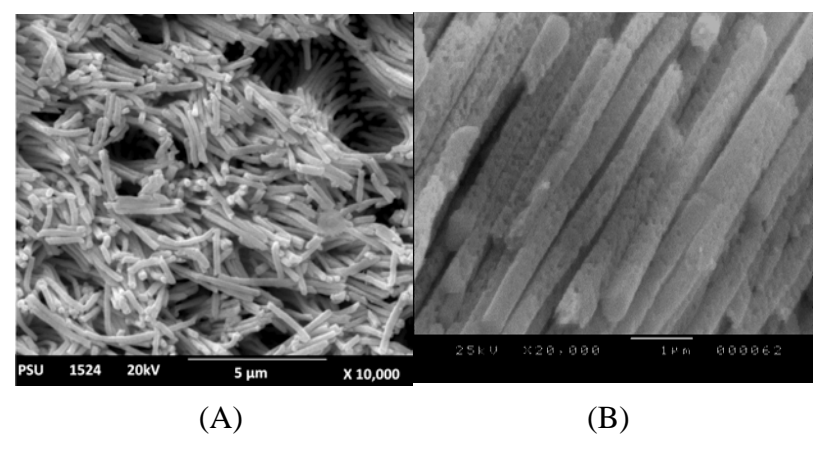


Figure 7.1 SEM images of NPG-NWAs (A) top view and (B) the porous region.

The NPG-NWAs electrode was characterized electrochemically in 1 M H₂SO₄ by cyclic voltametry. The charge accumulated by the reduction of a monolayer of gold oxide on the surface of the NPG-NWAs electrode was used for the estimation of the surface area of the porous AuNW array electrode. The surface area of the NPG-NWAs was 12 \pm 1 cm² (n=10 electrodes); this surface area was higher than those obtained from GNWAs (2.4 \pm 0.1 cm² , n = 3 electrodes) and the bare gold electrodes (0.072 \pm 0.002 cm² , n = 5 electrodes) by 5 and 167 times, respectively.

7.3.2 Performances of the NPG-NWAs electrode for detecting glutathione

This sensor provided two linear dynamic ranges: 1.0 to 10.0 nmol $L^{\text{-}1}$ with a sensitivity (slope of the calibration plot) of $1.13 \pm 0.04 \,\mu\text{A}$ (nmol $L^{\text{-}1}$)⁻¹ and 10 to 100 nmol $L^{\text{-}1}$ with a sensitivity of $0.16 \pm 0.01 \,\mu\text{A}$ (nmol $L^{\text{-}1}$)⁻¹. The limit of detection was 0.88 ± 0.08 nmol $L^{\text{-}1}$ (3σ /slope).

A disposable gold electrode and a GNWAs electrode was also tested. However, only very small responses, very much smaller than the NPG-NWAs, were observed in the high concentration range (≥ 10 nmol L⁻¹).

The reusability of the NPG-NWAs electrode was determined from the percentage response of the copper current determined at the beginning of each analysis cycle. The NPG-NWAs electrode could be used up to 60 times with an average response of 98 ± 1 %. The electrode-to-electrode reproducibility of the fabrication procedure was also investigated from the surface area of five electrodes which was found to be 11 ± 1 cm²(RSD = 9%) indicating good reproducibility.

7.3.3 Real sample analysis

Results of the analysis of glutathione dietary supplement product, 6 capsules/ pack \times 3 packs (24 samples) showed no significant difference between the glutathione concentration obtained from the developed electrochemical sensor and those from the labeled values provided by the manufacturer after a statistical testing with a Wilcoxon Signed Rank at a 95% confident limit. Thus it can be concluded that the proposed method was reliable.

7.4 Conclusions

A novel fabrication technique for NPG-NWAs based on the use of a conductive-layer-free AAO membrane using an electrochemical batch cell has been developed. The technique is simple, rapid and very cost effective. After fabrication, the NPG-NWAs electrode can be directly applied for the analysis of analytes within the same electrochemical cell. The porosity of the NPG-NWAs increased the surface area of the electrode and hence improved the sensor sensitivity and the limit of detection. This technique can be easily applied for other type of NWAs using different plating solutions or electrode substrates for many fields of applications.

8. Concluding remarks

This work showed that it is possible to enhance the performances of label-free affinity biosensors by modifying the sensing surface with nanomaterials. For nanoparticles, there exist an optimal amount that provides the largest surface area for the immobilization of the sensing elements (Paper I, II and III). This leads to a system with the highest sensitivity and lowest detection limit. Similarly, in the layer-by-layer technique there is also an optimal number of layers that provides the best performance (Paper III). For the detection systems, both capacitive and impedimetric systems have proven to be very sensitive for the real-time label-free detection. Between the two systems, the potentiostatic step capacitive detector is less expensive and the principle is relatively simple. Nonetheless, the impedimetric system provides more flexibility. The response can be obtained in the form of impedance (Paper II) or as resistance (Paper IV) (or capacitance). In the case of porous structure, the surface area is greatly amplified and provides a very large platform for the immobilized sensing elements (Paper IV) or for other electrochemical reaction (Paper V). In effect, this helps to increase the However, it seems that the 2- and 3-dimensional porous performances tremendously. structures may limit the accessibility of the molecules to the surface deep inside the structure, thus, reduces the effectiveness of the very large surface area. Further study on the optimal thickness and/or pore size of the porous surface as well as the optimal length of the porous nanowire arrays would be useful.

References

- Bart M, Stigter ECA, Stapert HR, de Jong GJ & van Bennekom WP. (2005). On the response of a label-free interferon-[gamma] immunosensor utilizing electrochemical impedance spectroscopy. *Biosensors and Bioelectronics* **21**, 49-59.
- Berggren C, Bjarnason, B. and Johansson, G. (2001). Review; Capacitive Biosensors. *Electroanalysis* **13**, 173-180.
- Bilitewski U. (2006). Protein-sensing assay formats and devices. *Analytica Chimica Acta* **568**, 232-247.
- Borisov SM & Wolfbeis OS. (2008). Optical biosensors. Chemical Reviews 108, 423-461.
- Chullasat K, Kanatharana P, Limbut W, Numnuam A & Thavarungkul P. (2011). Ultra trace analysis of small molecule by label-free impedimetric immunosensor using multilayer modified electrode. *Biosensors and Bioelectronics* **26**, 4571-4578.
- Dawan S, Kanatharana P, Wongkittisuksa B, Limbut W, Numnuam A, Limsakul C & Thavarungkul P. (2011). Label-free capacitive immunosensors for ultra-trace detection based on the increase of immobilized antibodies on silver nanoparticles. *Analytica Chimica Acta* **699**, 232-241.
- Dawan S, Wannapob R, Kanatharana P, Limbut W, Numnuam A & Thavarungkul P. One-step porous gold fabricated electrode for electrochemical impedance spectroscopy immunosensor detection. Submitted to *Electrochimica Acta*.
- Deng Y, Huang W, Chen X & Li Z. (2008). Facile fabrication of nanoporous gold film electrodes. *Electrochemistry Communications* **10**, 810-813.
- Dijksma M, Kamp B, Hoogvliet JC & van Bennekom WP. (2001). Development of an Electrochemical Immunosensor for Direct Detection of Interferon-gat the Attomolar Level. *Analytical Chemistry* **73**, 901-907.
- Ermolaeva TN & Kalmykova EN. (2006). Piezoelectric immunosensors: Analytical potentials and outlooks. *Russian Chemical Reviews* **75**, 397-409.
- Grieshaber D, MacKenzie R, Vörös J & Reimhult E. (2008). Electrochemical biosensors Sensor principles and architectures. *Sensors* **8**, 1400-1458.
- Guo X. (2012). Surface plasmon resonance based biosensor technique: A review. *Journal of Biophotonics* **5**, 483-501.
- Homola J. (2008). Surface Plasmon Resonance Sensors for Detection of Chemical and Biological Species. *Chem Rev* **108**, 462-493.
- Lewis RJ & Hawley GG. (1993). *Hawley's Condensed Chemical Dictionary*. Van Nostrand Reinhold, New York.
- Li J, Wu Z, Wang H, Shen G & Yu R. (2005). A reusable capacitive immunosensor with a novel immobilization procedure based on 1,6-hexanedithiol and nano-Au self-assembled layers. *Sensors and Actuators B: Chemical* **110,** 327-334.
- Loyprasert S, Hedström M, Thavarungkul P, Kanatharana P & Mattiasson B. (2010). Subattomolar detection of cholera toxin using a label-free capacitive immunosensor. *Biosensors and Bioelectronics* **25**, 1977-1983.
- Loyprasert S, Thavarungkul P, Asawatreratanakul P, Wongkittisuksa B, Limsakul C & Kanatharana P. (2008). Label-free capacitive immunosensor for microcystin-LR using self-assembled thiourea monolayer incorporated with Ag nanoparticles on gold electrode. *Biosensors and Bioelectronics* **24**, 78-86.

- Lucarelli F, Tombelli S, Minunni M, Marrazza G & Mascini M. (2008). Electrochemical and piezoelectric DNA biosensors for hybridisation detection. *Analytica Chimica Acta* **609**, 139-159.
- Ronkainen NJ, Halsall HB & Heineman WR. (2010). Electrochemical biosensors. *Chemical Society Reviews* **39**, 1747-1763.
- Samanman S, Kanatharana P, Asawatreratanakul P & Thavarungkul P. (2012). Characterization and application of self-assembled layer by layer gold nanoparticles for highly sensitive label-free capacitive immunosensing. *Electrochimica Acta* **80**, 202-212.
- Samanman S, Thammakhet C, Kanatharana P, Buranachai C & Thavarungkul P. Novel template-assisted fabrication of porous gold nanowire arrays using a conductive-layer-free anodic alumina oxide membrane. Submitted to *Electrochimica Acta*.
- Scarano S, Mascini M, Turner APF & Minunni M. (2010). Surface plasmon resonance imaging for affinity-based biosensors. *Biosensors and Bioelectronics* **25**, 957-966.
- Taverniers I, Loose, M. D. and Bockstaele, E. V. (2004). Trends in Quality in the Analytical Laboratory. II. Analytical Method Validation and Quality Assurance. . *Trends in Analytical Chemistry* **23**, 535-552.
- Teeparuksapun K, Kanatharana P, Limbut W, Thammakhet C, Asawatreratanakul P, Mattiasson B, Wongkittisuksa B, Limsakul C & Thavarungkul P. (2009). Disposable Electrodes for Capacitive Immunosensor. *Electroanalysis* **21**, 1066-1074.
- Thavarungkul P, Dawan S, Kanatharana P & Asawatreratanakul P. (2007). Detecting penicillin G in milk with impedimetric label-free immunosensor. *Biosensors and Bioelectronics* **23**, 688-694.
- Wongkittisuksa B, Limsakul C, Kanatharana P, Limbut W, Asawatreratanakul P, Dawan S, Loyprasert S & Thavarungkul P. (2011). Development and application of a real-time capacitive sensor. *Biosensors and Bioelectronics* **26**, 2466-2472.
- Wu W, Yi P, He P, Jing T, Liao K, Yang K & Wang H. (2010). Nanosilver-doped DNA polyion complex membrane for electrochemical immunoassay of carcinoembryonic antigen using nanogold-labeled secondary antibodies. *Analytica Chimica Acta* **673**, 126-132.
- Wu Z-S, Li J-S, Luo M-H, Shen G-L & Yu R-Q. (2005). A novel capacitive immunosensor based on gold colloid monolayers associated with a sol-gel matrix. *Analytica Chimica Acta* **528**, 235-242.
- Yang G-J, Huang J-L, Meng W-J, Shen M & Jiao X-A. (2009). A reusable capacitive immunosensor for detection of Salmonella spp. based on grafted ethylene diamine and self-assembled gold nanoparticle monolayers. *Analytica Chimica Acta* **647**, 159-166.

Output

Publications

- Paper I: Dawan S, Kanatharana P, Wongkittisuksa B, Limbut W, Numnuam A, Limsakul C & Thavarungkul P. (2011). Label-free capacitive immunosensors for ultra-trace detection based on the increase of immobilized antibodies on silver nanoparticles. *Analytica Chimica Acta* **699**, 232-241. (Journal Impact Factor 2011: 4.555)
- Paper II: Chullasat K, Kanatharana P, Limbut W, Numnuam A & Thavarungkul P. (2011). Ultra trace analysis of small molecule by label-free impedimetric immunosensor using multilayer modified electrode. *Biosensors and Bioelectronics* **26**, 4571-4578. (Journal Impact Factor 2011: 5.602)
- Paper III: Samanman S, Kanatharana P, Asawatreratanakul P & Thavarungkul P. (2012). Characterization and application of self-assembled layer by layer gold nanoparticles for highly sensitive label-free capacitive immunosensing. *Electrochimica Acta* **80**, 202-212. (Journal Impact Factor 2011: 3.832)
- Paper IV: Dawan S, Wannapob R, Kanatharana P, Limbut W, Numnuam A & Thavarungkul P. One-step porous gold fabricated electrode for electrochemical impedance spectroscopy immunosensor detection. Submitted to *Electrochimica Acta*. (Journal Impact Factor 2011: 3.832)
- Paper V: Samanman S, Thammakhet C, Kanatharana P, Buranachai C & Thavarungkul P. Novel template-assisted fabrication of porous gold nanowire arrays using a conductive- layer-free anodic alumina oxide membrane. Submitted to *Electrochimica Acta*. (Journal Impact Factor 2011: 3.832)

Other related activities

Conference reports

Oral presentation

- Samanman S, Kanatharana P & Thavarungkul P. (2011). Highly Sensitive Label-free Capacitive Immunosensor Based on Layer-by-Layer Self-assembled Gold Nanoparticles. In *The 14th Asian Chemical Congress (14ACC)*. 5-8 September 2011, Queen Sirikit Convention Center in Bangkok, Thailand.
- <u>Thavarungkul P</u>, Chullasat K, Dawan S, Samanman S, Kanatharana P, Limbut W, Numnuam A, Wongkittisuksa B & Limsakul C. (2012). Strategies to Incorporate Nanoparticles into Label-free Immunosensor for Ultra Trace Detection. In การประชุมนักวิจัยรุ่นใหม่ พบ เมธีวิจัย อาวุโส สกว ครั้งที่ 12. 10-12 ตุลาคม 2555 โรงแรมฮอลิเดย์อินน์ รีสอร์ท รีเจนท์ บีซ ซะอำ จังหวัดเพชรบุรี.

Poster presentation

- Chullasat K, Kanatharana P, Limbut W, Numnuam A, Asawatreratanakul P & Thavarungkul P. (2011). Multilayer modified electrode for label-free impedimetric immunosensing for small molecule. In *PERCH-CIC Congress VII*. 4-7 May 2011, Jomtien Palm Beach Hotel & Resort Pattaya, Chonburi, Thailand.
- Thavarangkul P, Dawan S, Kanatharana P, Limbut W, Numnuam A, Wongkittisuksa B, Asawatreratanakul P, Thammakhet C, Buranachai C & Limsakul C. (2010). Sensitivity Enhancement of Label-free Capacitive Immunosensor Based on the Increase of Antibody Immobilization Yield on Silver Nanoparticles. In การประชุมนักวิจัยรุ่นใหม่ พบ เมธิ์ วิจัยอาวุโส สกว ครั้งที่ 10. 14-16 ตุลาคม 2553 โรงแรมฮอลิเดย์อินน์ รีสอร์ท รีเจนท์ ปีช ชะอำ จังหวัด เพชรบุรี.

Invited speaker

- <u>Thavarungkul P</u>, Kanatharana P, Asawatreratanakul P, Wongkittisuksa B, Limsakul C, Limbut W, Numnuam A, Dawan S, Jantra J, Chullasat K & Wannapob R. (2011). Biosensors based on Direct Detection of Affinity Binding. In *The 14th Asian Chemical Congress* (14ACC). 5-8 September 2011, Queen Sirikit Convention Center, Bangkok, Thailand
- Thavarungkul P, Kanatharana P, Asawatreratanakul P, Wongkittisuksa B, Limsakul C, Limbut W, Numnuam A, Loyprasert S, Suwansa-ard S, Teeparauksapun K & Wannapob R. (2010). Highly Sensitive Capacitive Label-free Affinity Detection and a Move Towards Real-time Analysis. In *Pure and Applied Chemistry International Conference 2010 (PACCON 2010)*. January 21-23, 2010, Sunee Grand Hotel and Convention Center, Ubonratchathani, Thailand.

ELSEVIER

Contents lists available at ScienceDirect

Analytica Chimica Acta

journal homepage: www.elsevier.com/locate/aca



Label-free capacitive immunosensors for ultra-trace detection based on the increase of immobilized antibodies on silver nanoparticles

Supaporn Dawan^{a,b,c}, Proespichaya Kanatharana^{a,b,c}, Booncharoen Wongkittisuksa^{a,d}, Warakorn Limbut^{a,b,e}, Apon Numnuam^{a,b,c}, Chusak Limsakul^{a,d}, Panote Thavarungkul^{a,b,f,*}

- ^a Trace Analysis and Biosensor Research Center, Prince of Songkla University, Hat Yai, Songkhla 90112, Thailand
- b Center of Excellence for Innovation in Chemistry, Faculty of Science, Prince of Songkla University, Hat Yai, Songkhla 90112, Thailand
- ^c Department of Chemistry, Faculty of Science, Prince of Songkla University, Hat Yai, Songkhla 90112, Thailand
- d Department of Electrical Engineering, Faculty of Engineering, Prince of Songkla University, Hat Yai, Songkhla 90112, Thailand
- e Department of Applied Science, Faculty of Science, Prince of Songkla University, Hat Yai, Songkhla 90112, Thailand
- f Department of Physics, Faculty of Science, Prince of Songkla University, Hat Yai, Songkhla 90112, Thailand

ARTICLE INFO

Article history: Received 15 February 2011 Received in revised form 17 May 2011 Accepted 24 May 2011 Available online 1 June 2011

Keywords: Capacitance Label-free biosensor Small molecule Macromolecule Nano material High sensitivity

ABSTRACT

Detection of ultra-trace amounts of antigens by label-free capacitive immunosensors was investigated using electrodes modified with silver nanoparticles (AgNPs) that allows for an increase in the amount of immobilized antibodies. The optimal amount of AgNPs that provided the highest immobilization yield was 48 pmol (in 2.0 mL). The performances of immunosensor electrodes for human serum albumin prepared with AgNPs, were compared to electrodes prepared with gold nanoparticles. The two systems provided the same linear range $(1.0 \times 10^{-18} \text{ to } 1.0 \times 10^{-10} \text{ M})$ and detection limit $(1.0 \times 10^{-18} \text{ M})$. The system with AgNPs was used to analyze albumin in urine samples and the results agreed well with the immunoturbidimetric assay (P > 0.05). Electrodes modified with AgNPs and appropriate antibodies were tested for their performances to detect analytes of different sizes. For a macromolecule (human serum albumin) the incorporation of AgNPs improved the detection limit from 100 to 1 aM. For small molecules, microcystin-LR and penicillin G, the detection limits were lowered from 100 and 10 fM to 10 and 0.7 fM, respectively. The high sensitivity and very low detection limits are potentially useful for the analysis of toxins or residues present in samples at ultra-trace levels and this method could easily be applied to other affinity pairs.

© 2011 Elsevier B.V. All rights reserved.

1. Introduction

A capacitive label-free immunosensor using the potentiostatic step method is a highly sensitive system that can directly detect antigen–antibody interactions. The principle is based on the measurement of the change in capacitance caused by the change of dielectric properties on the electrode surface due to binding of the antigen to the antibody [1,2]. Several immunosensors using this technique have provided very low detection limits in the order of nanograms or even femtograms per milliliter [2–8]. However, it would still be useful to further stretch the limit of detection to the lowest possible level, especially for samples with complex matrices. In that case with such low limits of detection it will be possible to simply dilute samples so that any matrix effects will not interfere

E-mail address: panote.t@psu.ac.th (P. Thavarungkul).

with any measurement. This would also be beneficial for the detection of toxins or trace residues where the lower the detection limit the better. The low detection limit is easier to obtain when the analyte is large since it is generally expected that the response will be more pronounced if the target is substantially larger than the probe [9]. Small analyte could also be detected with low detection limit if the probe property is altered, such as the use of a protein whose conformation changed upon binding with small heavy metal ions [10]. However, in general when the analyte molecule is present in such small sizes and only the binding interaction occur this might produce only a small change leading to a poor detection limit.

One way to attempt to improve the detection limit is by using nanoparticles to increase the effective surface area for the immobilized sensing molecules. Such previously developed methods have mostly used gold nanoparticles (AuNPs) [11–13] with only a few applications of silver nanoparticles (AgNPs) have been studied [14,15]. Since silver is cheaper than gold and the preparation of its nanoparticles is also simple we would like to show that AgNPs can effectively enhance the sensitivity and detection limit of a capacitive immunosensor system, comparable to the sys-

^{*} Corresponding author at: Department of Physics, Faculty of Science, Prince of Songkla University, Hat Yai, Songkhla 90112, Thailand. Tel.: +66 74 288753; fax: +66 74 558849.

tem with AuNPs. First we investigated the optimum amount of AgNPs required to increase the sensing molecule immobilization area. Then electrodes with a suitable concentration of nanoparticles incorporated were tested for their activities in the capacitive system. To investigate how this might enhance the detection of both large and small molecules, three antibody–antigen pairs were tested: (i) anti-human serum albumin (anti-HSA) and human serum albumin (HSA) (MW 68,000 g mol⁻¹), (ii) anti-microcystin-LR (anti-MCLR) and microcystin-LR (MCLR) (MW 995.17 g mol⁻¹) and (iii) anti-penicillin G (anti-Pen G) and penicillin G (Pen G) (MW 356.37 g mol⁻¹). The system for the detection of HSA was also compared with one that had AuNPs incorporated. To test the application of this new electrode for real sample detection, the system was employed to analyze HSA in urine samples and the result compared with the standard assay method.

2. Materials and methods

2.1. Materials

Polyclonal anti-human serum albumin (anti-HSA) (IgG) and human serum albumin (HSA) were from Dako (Denmark), monoclonal anti-penicillin G (anti-Pen G) (IgG1) and penicillin G sodium salt (Pen G) were from US Biological (MA, USA), monoclonal antibodies against microcystin-LR (anti-MCLR) (MC10E7) (IgG1) and microcystin-LR (MCLR) were obtained from Alexis Biochemicals (Lausen, Switzerland). Thiourea and silver nitrate were from BDH laboratory reagents (Poole, England), 1-dodecanethiol and chloroauric acid trihydrate were from Aldrich (Milwaukee, USA) and sodium borohydride was from Fluka Chemie AG (Buchs, Switzerland). All other chemicals were of analytical grade. Buffers were prepared with deionized water. Before use, buffers were filtered through a Millipore filter, pore size 0.22 µm, with subsequent degassing.

2.2. Preparation of silver (AgNPs) and gold nanoparticles (AuNPs)

All glasswares were immersed in 10% HNO $_3$ overnight, and then thoroughly rinsed with distilled water. AgNPs were prepared from 100 mL of 1.0 mM AgNO $_3$ and 300 mL of 2.0 mM NaBH $_4$ prepared in ultrapure water at room temperature. AgNO $_3$ solution was rapidly added to the NaBH $_4$ solution, stirred at 1300 rpm (Framo 8 -Gerätetechnik M21/1, Germany) for a few minutes [14,16] and then kept in the dark at 4 °C until used. AuNPs were prepared from 200 mL of aqueous solution containing 0.25 mM of HAuCl $_4$ and 0.375 mM of trisodium citrate by rapidly adding 2.0 mL of 125 mM NaBH $_4$ under continuous stirring (1300 rpm). The solution was stirred overnight. Solutions containing the nanoparticles were then kept in the dark at 4 °C.

2.3. Immobilization of antibody

Gold electrodes (diameter 3 mm, 99.99% purity) were polished (Gripo® 2 V, Metkon Instruments Ltd., Turkey) using alumina slurries with particle diameters of 5, 1, and 0.30 μ m, respectively. Each electrode was cleaned by sonication in distilled water for 15 min, followed by electrochemical etching in 0.5 M H_2SO_4 using a cycling electrode potential of between 0 and 1.5 V versus an Ag/AgCl reference electrode with a scan rate of 0.1 V s $^{-1}$ for 25 scans. The electrode was then dried using pure nitrogen gas.

The cleaned electrodes were immersed in 250 mM thiourea solution at room temperature for 24 h [17] (Fig. 1A(a)), thoroughly rinsed with distilled water and dried with pure nitrogen gas. Electrodes modified without nanoparticles were treated with 5% (v/v) glutaraldehyde in 10 mM sodium phosphate buffer pH 7.00 at room temperature for 20 min to produce reactive aldehyde

groups (Fig. 1A(b)). Twenty microliters of each type of antibody $(500 \, \mu g \, mL^{-1} \, of \, anti-HSA \, [18], 250 \, \mu g \, mL^{-1} \, of \, anti-Pen \, G \, [19]$ and $20 \, \mu g \, mL^{-1}$ of anti-MCLR [14]) was placed on the surface and left to incubate overnight at $4 \, ^{\circ} C \, (Fig. \, 1A(c))$. The concentrations of the three antibodies followed those employed by existing reports so the results obtained from these experiments could be later compared. They were then immersed in an 0.1 M ethanolamine pH 8.50 solution for 20 min, this step was to occupy all the non reacted aldehyde groups. Finally, remaining pinholes on the electrode surface were blocked with a 10 mM 1-dodecanethiol ethanolic solution for 20 min.

For electrodes with nanoparticles, after being modified with a self-assembled monolayer (SAM) of thiourea (Fig. 1A(a)), the electrodes were immersed in 2.0 mL of a nanoparticle solution in a 10 mL beaker at 4 °C for 4 h in the dark (Fig. 1A(d)) [20], then rinsed with deionized water and dried with pure nitrogen gas. This was followed by the attachment of antibodies (Fig. 1A(e)) and the blocking of pinholes as described above. The insulation of the electrode surface during the various immobilization steps were investigated by cyclic voltammetry in 0.005 M potassium ferricyanide solution using a potentiostat (Microautolab type III, Metrohm Autolab B.V., The Netherlands) coupled to an electrochemical cell containing the modified working electrode, an Ag/AgCl reference electrode and a platinum rod auxiliary electrode.

2.4. Immobilization yield

Immobilization yield of the antibody was determined as the difference between the amount of the antibody in the solution before and after immobilization by using a silver binding method [21,22]. Five microliters of antibody was first diluted to 50 μL with distilled water containing 0.2% of sodium dodecyl sulfate (SDS) and 0.4% of Tween 20. Then 950 μL of distilled water and 20 μL of 2.5% glutaraldehyde were added to each sample and mixed with 200 μL of ammoniacal silver. After 20 min the reaction was stopped by adding 40 μL of 30 mg mL $^{-1}$ sodium thiosulfate solution. Absorbance was measured at 420 nm and this was used to calculate the concentration from the calibration curve of the standard antibody.

2.5. Capacitive measurement

Experiments were carried out using a flow injection system. The flow cell ($10\,\mu L$) consisted of a working electrode (modified electrode), an auxiliary electrode (Pt wire; diameter 0.5 mm) and a reference electrode (Ag/AgCl) connected to a custom-built capacitive analyzer [23]. This instrumentation automatically applies 50 mV potential pulses (from 0 mV to 50 mV, pulse width 75 ms) on the working electrode at 60-s intervals. The current response evoked by the potential pulse followed the equation.

$$i(t) = \frac{u}{R_s} \exp\left(-\frac{t}{R_s C_{total}}\right) \tag{1}$$

where i(t) is the current response as a function of time, u is the applied pulse potential, R_s is the electrical resistance of elements serially connected to the layer and C_{total} is the total capacitance at the electrode/solution interface. The capacitance was determined by the computer program from the current response of each pulse by taking the logarithm of Eq. (1) to obtain Eq. (2).

$$\ln i(t) = \ln \frac{u}{R_s} - \frac{t}{R_s C_{total}}$$
 (2)

Then, C_{total} and R_s were obtained from the slope and intercept of the linear least squares fitting of $\ln i(t)$ versus t [1,2,5]. The obtained capacitance values were plotted with respect to time on the monitor and stored on the computer. When the solution containing analytes was injected into the system, the analytes bound to the

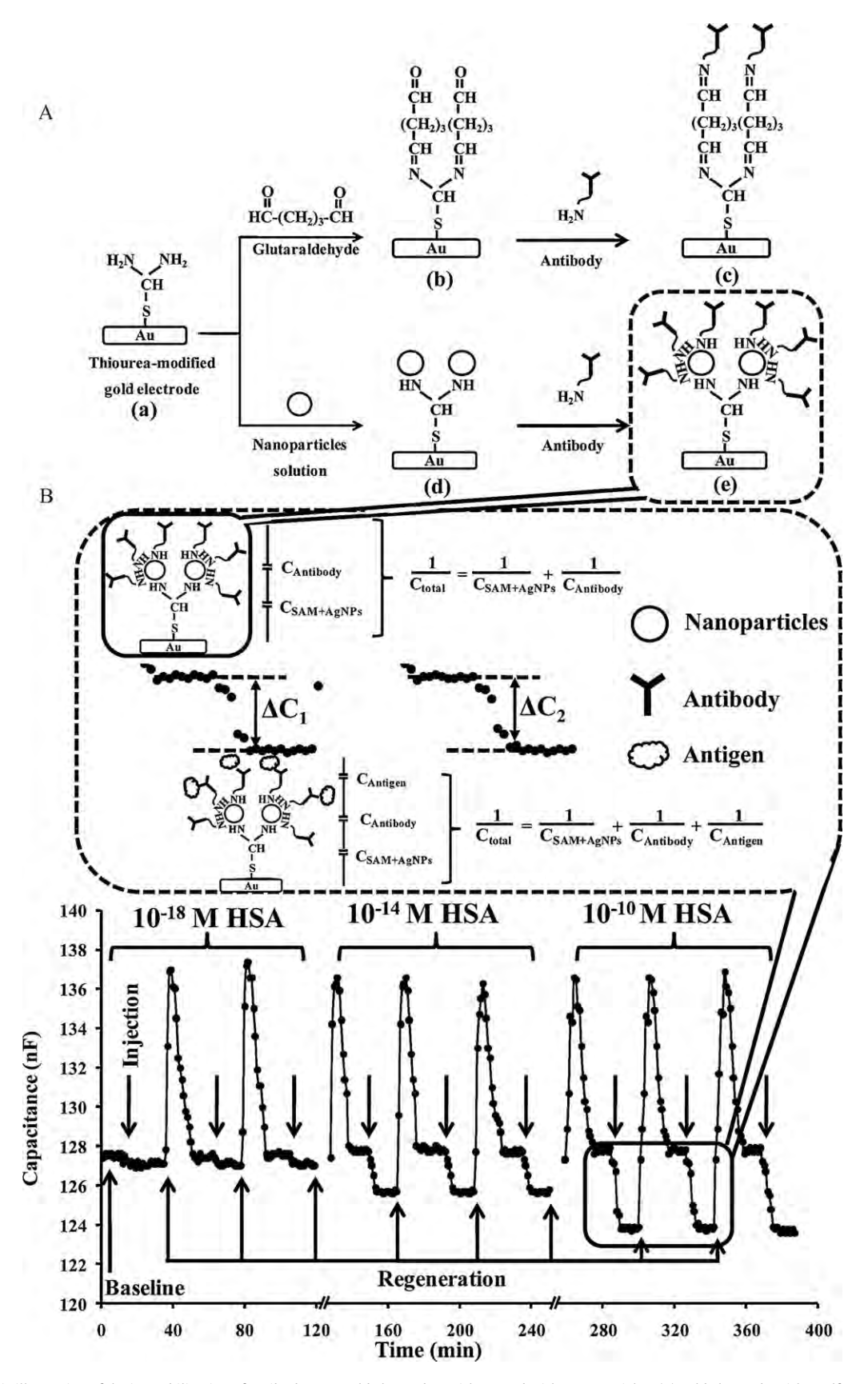


Fig. 1. (A) Schematic illustration of the immobilization of antibody onto gold electrodes, without and with nanoparticles: (a) gold electrode with a self-assembled monolayer (SAM) of thiourea, (b) glutaraldehyde-SAM, (c) antibody-glutaraldehyde-SAM, (d) Nanoparticles-SAM and (e) antibody-nanoparticles-SAM. (B) Example of capacitance responses of the anti-HSA modified electrode with respect to time. Carrier buffer was passed through the system to obtain a baseline of capacitance, contributed by $C_{SAM+AgNPs}$, the capacitance of the self-assembled monolayer and silver nanoparticles and $C_{Antibody}$, the capacitance of the immobilized antibody. When HSA was injected, binding occurred. This is represented by the addition of another capacitor in series ($C_{Antigen}$) causing the capacitance to decrease (ΔC_1). The antigen was removed from the binding by using regeneration solution followed by carrier buffer with the signal returned to the baseline before a new analysis can be performed to obtain a new response (ΔC_2).

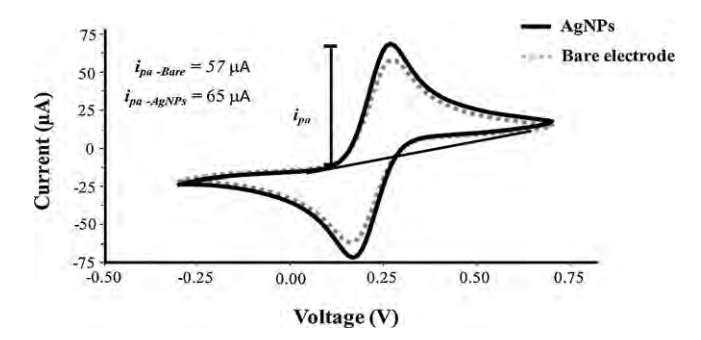


Fig. 2. Example of cyclic voltammograms for the determination of anodic peak current (i_{pa}) carried out in 5 mM potassium ferricyanide solution with a scan rate of $100\,\mathrm{mV}\,\mathrm{s}^{-1}$ vs. Ag/AgCl reference electrode, the voltage range was -0.3 to $0.7\,\mathrm{V}$.

immobilized antibody on the electrode. The total capacitance is given by the relationship for capacitors connected in series [24]. This caused the capacitance to decrease in proportion to the concentration of the analyte. The change in capacitance (ΔC) due to the binding was obtained by subtracting the capacitance after the binding from the capacitance before the binding. The surface of the electrode was then regenerated with a regeneration solution to remove the analytes from the immobilized antibody (Fig. 1B) so a new analytical cycle could be performed.

2.6. Optimization of the amount of nanoparticles for immobilization

Nanoparticles were added onto the modified electrode by adsorption on the self-assembled monolayer of thiourea (Fig. 1A(d)). Antibody was also simply adsorbed on the surface of nanoparticles [25] (Fig. 1A(e)). The use of nanoparticles can help increase the amount of immobilized antibody since the antibody can freely adsorb on the particles surface. In contrast when there were no nanoparticles the antibody can only be immobilized via the limited amine groups on the thiourea monolayer (Fig. 1A(c)). Different amounts of nanoparticles per unit volume were prepared by centrifuging 2, 4, 6, 8 and 10 mL of the prepared nanoparticles solution at 13,000 rpm for 30 min (Centrifuge 5415R Eppendorf, Germany). The supernatant was removed leaving the bottom 2 mL. The centrifuge nanoparticles were then redistributed in this 2 mL of solution by agitation for about 1 min (Vortex-2 genie, USA). The final solutions contained 1, 2, 3, 4 and 5 times the original number of nanoparticles.

2.7. Peak current

To determine the appropriate amount of nanoparticles adsorbed onto the electrode, redox peak currents were studied by voltammetry. The idea being that the increase in the effective surface area (compare to bare gold) due to the adsorption of AgNPs on SAM of thiourea would provide a larger area for the exchange of electrons, hence a higher redox peak current. Cyclic voltammetry was carried out in 5 mM potassium ferricyanide solution (K₃[Fe(CN)₆]) with a scan rate of 100 mV s⁻¹ versus Ag/AgCl reference electrode, the voltage range was -0.3 to $0.7\,\text{V}$. Since a redox reaction of Fe(CN)₆⁴⁻/Fe(CN)₆³⁻ is reversible, the oxidation peak (anodic peak current) and reduction peak (cathodic peak current) are equivalent. Therefore, for simplicity, only the anodic peak current (i_{pa}) was considered (Fig. 2). The anodic peak current of the surface modified with AgNPs ($i_{pa-AgNPs}$) was compared to the anodic peak current of a bare gold electrode ($i_{pa-Bare}$) by Eq. (3).

Peak current(%) =
$$\frac{(i_{pa-AgNPs}) \times 100}{i_{pa-Bare}}$$
 (3)

2.8. Determination of HSA in urine sample

Urine samples were obtained from Songklanagarind Hospital, Hat Yai, Thailand and analyzed by the flow capacitive immunosensor system using electrodes modified with AgNPs. The results were compared with those obtained by the hospital using an immunoturbidimetric assay [26,27].

3. Results and discussion

3.1. Synthesis of nanoparticles

AgNPs and AuNPs were characterized using a transmission electron microscope (TEM; JEM-2010, JEOL) operated in a high vacuum at 160 kV. From the TEM images (Fig. 3), AgNPs and AuNPs had an average size of 10 ± 2 nm (n=150) and 8 ± 2 nm (n=135), respectively. From these sizes and assuming complete conversion of the 0.25 mM solution the number of nanoparticles can be calculated via the mass to be 4.8×10^{15} (AgNPs) and 9.5×10^{15} (AuNPs) nanoparticles per liter or 8.0 nmol (AgNPs) and 15.7 nmol (AuNPs) per liter. The optical absorption properties of Ag and Au nanoparticles were identified using a UV–vis spectrophotometer (Specord S 100, Analytikjana, Germany) at an optical wavelength of 200-700 nm. The spectra of Ag and Au nanoparticles showed absorption peaks at 390 and 516 nm (Fig. 3), respectively.

3.2. Immobilization of antibody

Electrochemical characteristics of the modified electrode were investigated by the redox reaction of potassium ferricyanide solution $(K_3[Fe(CN)_6])$. For the voltammograms of the electrodes modified without nanoparticles, the oxidation and reduction peaks decreased for every step of the modification, i.e. thiourea, cross-linking with glutaraldehyde, presence of antibody and the disappearance of these peaks when the surface was finally blocked with 1-dodecanethiol (Fig. 4A).

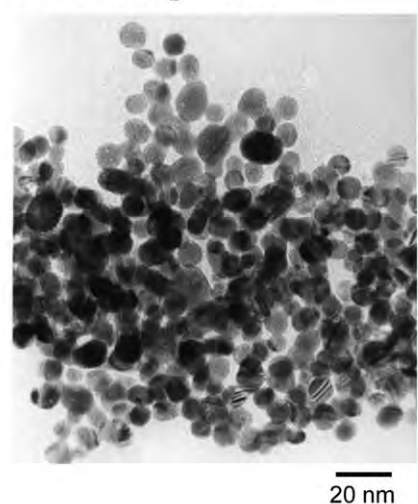
For the electrode coated with AgNPs, when the electrode surface was modified with thiourea the redox peaks decreased. However, after AgNP adsorption the redox reactions increased to indicate that the deposited AgNPs helped to increase the electron exchange. After antibody immobilization, the redox peaks decreased again and finally when treating with 1-dodecanethiol to block the pinholes on the electrode surface, the redox peaks disappeared to demonstrate that the surface was totally insulated (Fig. 4B).

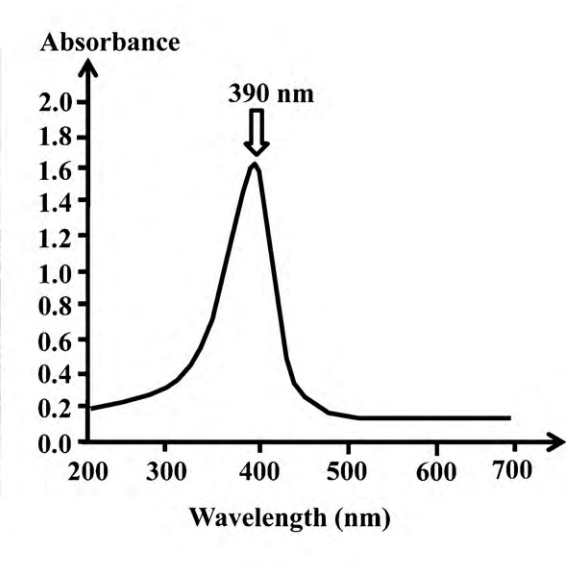
3.3. Optimization of the amount of nanoparticles for immobilization

3.3.1. Anodic peak current

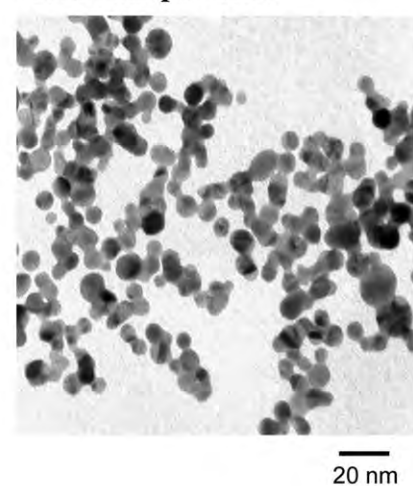
The anodic peak current of the electrodes modified with various amounts of AgNPs were investigated by comparison to a bare gold electrode. The purpose was to obtain the condition that can provide the largest surface area. An optimal amount of AgNPs would provide the highest percentage of the peak current and should be more than 100% compared to the bare gold surface. The results in Table 1 show that anodic peak current increased with the amount of AgNPs up to 48 pmol (in 2 mL) then decreased. At 16 and 32 pmol of nanoparticles the anodic peak currents were lower than those of a bare gold electrode (<100%) indicating that the electron transfer is lower than that of bare gold, i.e., it has a smaller surface area. When the amount of nanoparticles was higher than 48 pmol the anodic peak current decreased because when the density of nanoparticles is too high the particles cluster together and hence decrease the surface area. This behavior is confirmed by the SEM images in Fig. 5. When there was no nanoparticles on the SAM layer (Fig. 5a) the surface of the electrode was relatively smooth. Fig. 5b-d shows

A Silver nanoparticles





B Gold nanoparticles



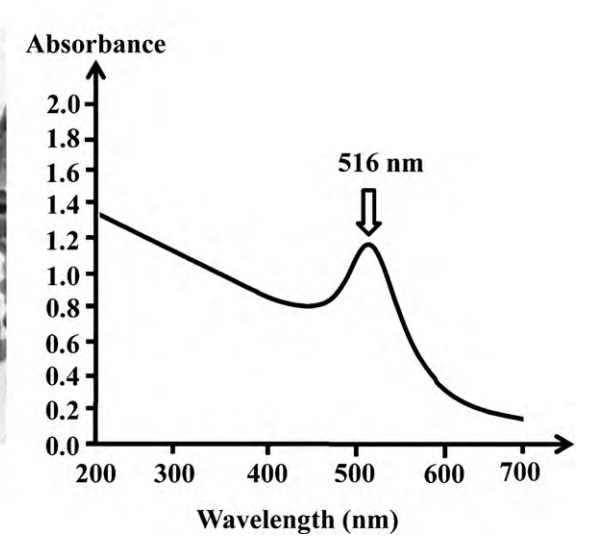


Fig. 3. TEM images and UV spectrum (A) silver nanoparticles and (B) gold nanoparticles.

the surfaces that were prepared with 16, 48 and 80 pmol (in 2 mL) of nanoparticles. Each of the observed nodules consisted of several nanoparticles adsorbed on SAM of thiourea in close vicinity. At 16 pmol (Fig. 5b) a lot of free spaces could be observed and this agreed well with the low value of anodic peak current in Table 1. The other two quantities provided lesser free spaces, however, large clusters could be seen at 80 pmol (Fig. 5d). This leveled out the curvature structure where individual nanoparticles were adsorbed on the surface. That is, nanoparticles at 48 pmol provided the highest enhancement of the surface area for the immobilized antibody.

3.3.2. Immobilization yield

Immobilization yields of the antibody (anti-HSA) on the electrodes modified with various concentrations of AgNPs were tested for 2 electrodes and 3 replications per electrode (Table 1). The electrodes prepared with 48 pmol of nanoparticles provided the highest immobilized yield $88.2-88.6\%\,(3.5\times10^{13}$ molecules, calculated using a molecular weight of $150\,\mathrm{kDa}$ for an IgG [28,29]). This agreed well with the larger surface area as indicated by the higher anodic peak current. However, in one of our previous work under the same immobilization conditions similar immobilization yield

Table 1Effect of the amount of AgNPs on anodic peak currents (compared to a bare gold electrode) and immobilization yield of anti-HSA and performance of the capacitive system with various amounts of AgNPs (y is the capacitance change in nF cm⁻² and x is the concentration in M).

Amount of AgNPs in 2 mL (pmol)	Anodic peak current (%)a	Immobilization yield (%)b	Linear equation	Linear range (M)	LOD (M)
0	-	$37.8 \pm 0.5, 38.0 \pm 0.7$	$y = (1.75 \pm 0.08) \log(x) + (35.8 \pm 0.4)$	10^{-16} to 10^{-10}	10^{-16}
16	83 ± 7	$62.0 \pm 0.2, 61.8 \pm 0.2$	$y = (1.96 \pm 0.08) \log(x) + (41.5 \pm 0.6)$	10^{-18} to 10^{-10}	10^{-18}
32	93 ± 4	$67.8 \pm 0.4, 67.5 \pm 0.2$	$y = (2.37 \pm 0.13) \log(x) + (47.2 \pm 0.8)$	10^{-18} to 10^{-10}	10^{-18}
48	120 ± 5	$88.6 \pm 0.2, 88.2 \pm 0.1$	$y = (3.64 \pm 0.10) \log(x) + (69.7 \pm 0.6)$	10^{-18} to 10^{-10}	10^{-18}
64	108 ± 5	75.6 ± 0.3 , 75.9 ± 0.1	$y = (2.54 \pm 0.09) \log(x) + (49.0 \pm 0.6)$	10^{-18} to 10^{-10}	10^{-18}
80	109 ± 9	$68.0 \pm 0.6, 68.3 \pm 0.2$	$y = (1.83 \pm 0.07) \log(x) + (36.9 \pm 0.5)$	10^{-18} to 10^{-10}	10^{-18}

^a 3 electrodes.

^b 2 electrodes, 3 replications per electrode.

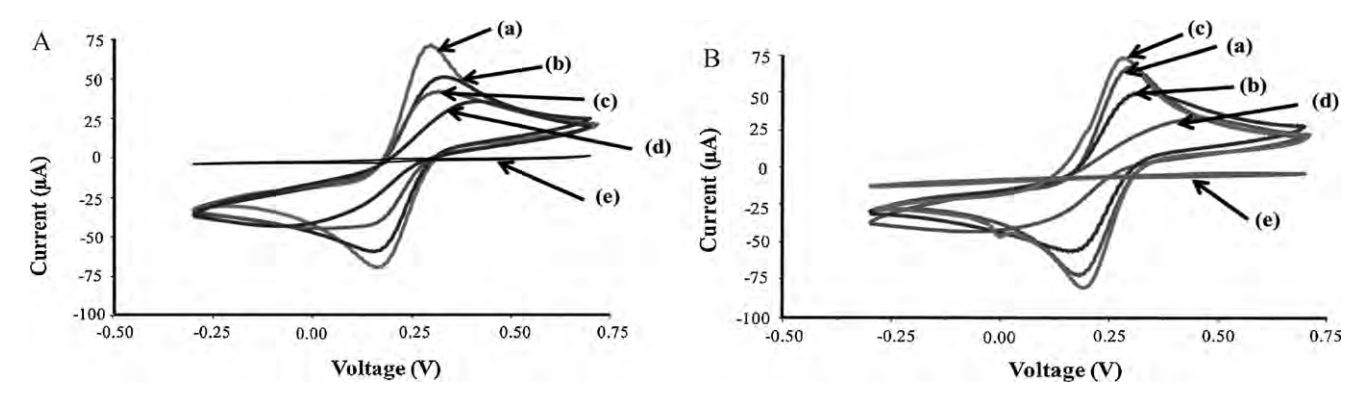


Fig. 4. Cyclic voltammograms of modified electrode obtained in 5 mM potassium ferricyanide solution, (A) without nanoparticles; (a) bare gold, (b) thiourea covered gold, (c) glutaraldehyde cross-link with thiourea self-assembles monolayer, and (e) after 1-dodecanethiol treatment. (B) With AgNPs; (a) bare gold, (b) thiourea covered gold, (c) 48 pmol AgNPs via thiourea self-assembles monolayer, (d) anti-HSA modified on AgNPs-thiourea self-assemble monolayer, and (e) after 1-dodecanethiol treatment.

could be obtained for anti-alpha fetoprotein (anti-AFP) without the nanoparticle layer [17], i.e., $88.5\pm0.8\%$ (7.6×10^{13} molecules). This was probably due to the difference in size of these two antibodies, anti-HSA was about twice the size of anti-AFP, $150\,\mathrm{kDa}$ and $70\,\mathrm{kDa}$ (DakoCytomation, Denmark), respectively. The low immobilization yield of anti-HSA on bare gold electrode ($\sim38\%$) was probably due to the steric interference between the immobilized proteins [30]. With the silver nanoparticles, the larger surface area together with the curvature structure of the indi-

vidual nanoparticles on the surface probably helped to reduce the steric hindrance resulting in a much higher immobilization yield than the bare gold surface. The immobilization yield of anti-MCLR and anti-Pen G were also investigated. For anti-MCLR the yield of 40% (6.4 \times 10^{11} molecule) was obtained for the electrode without nanoparticles and increased to 96% (1.5 \times 10^{12} molecule) with 48 pmol AgNPs. A similar increase was also observed for anti-Pen G, from 41% (8.2 \times 10^{12} molecule) to 93% (1.9 \times 10^{13} molecule).

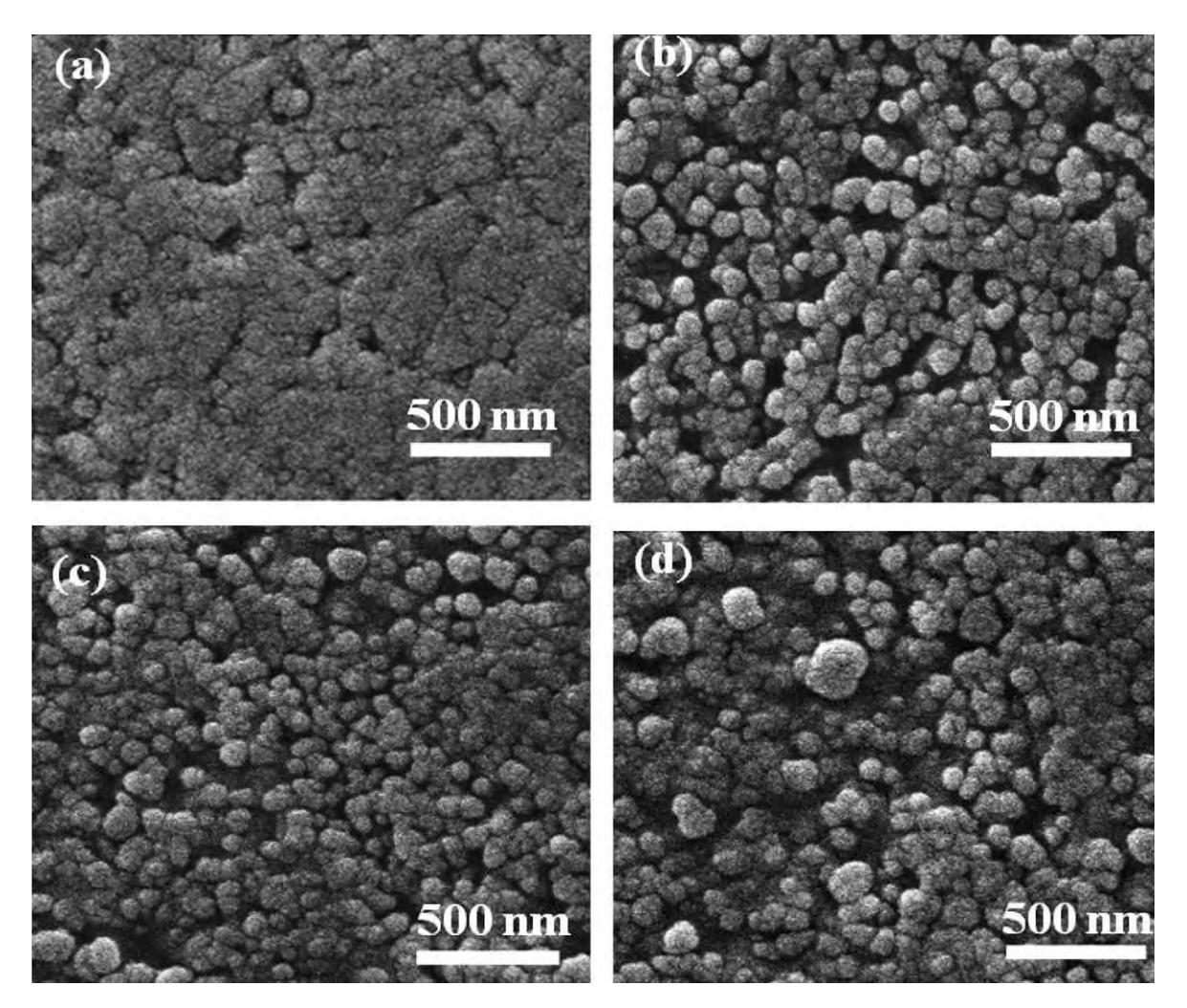


Fig. 5. SEM images of electrode surfaces modified with SAM of thiourea and, (a) without AgNPs, (b) 16 pmol (in 2.0 mL) AgNPs, (c) 48 nmol AgNPs, (d) 80 pmol AgNPs.

3.3.3. *Capacitive measurement*

Performances of the electrodes modified with various amounts of AgNPs were tested using the anti-HSA and HSA binding pair. HSA between 1.0×10^{-16} and 1.0×10^{-8} M were investigated. The operation conditions were, carrier buffer 10 mM Tris–HCl pH 7.00, sample volume 200 μ L [31], flow rate 50 μ L min⁻¹ [14,31] and regeneration solution HCl pH 2.50 [18].

The binding between the injected antigen and the immobilized antibody causes the total capacitance to decrease. This capacitance change was measured by comparing the signal before and after antigen—antibody binding (ΔC). The analysis time was about 15–20 min. The antigen was then removed from its binding with antibody by using the regeneration solution (Fig. 1B). A calibration curve is plotted between the capacitance change (per unit area of bare electrode surface) and the logarithm of the analyte concentration, the sensitivity is the slope of the linear portion of the curve (Fig. 6A). The limit of detection (LOD) is taken as the concentration of the analyte at which the extrapolated linear portion of the calibration curve intercepts the baseline a horizontal line corresponding to a zero change in response over several ten fold changes of concentration change [32] (Fig. 6A).

The linear range and the limits of detection of the various electrodes are summarized in Table 1. Electrodes modified with nanoparticles gave a wider linear range $(1.0\times10^{-18}$ to $1.0\times10^{-10}\,\mathrm{M})$ than without nanoparticles $(1.0\times10^{-16}$ to $1.0\times10^{-10}\,\mathrm{M})$. The sensitivity (slope of the calibration curve) increased with the amount of AgNPs up to 48 pmol and then decreased. The results corresponded well with the anodic peak currents and immobilization yield which provided the maxima at to 48 pmol of AgNPs. The detection limit of the electrodes with nanoparticles was also better than the one without nanoparticles by two orders of magnitude $(1.0\times10^{-18}\,\mathrm{M}$ compared to $1.0\times10^{-16}\,\mathrm{M})$.

The detection limit of 1.0×10^{-18} M is extremely low. Since the sample volume employed in the test was only 200 µL it means that only about 120 molecules of HSA passed through the detection surface. This might seem not to be possible for an electrode to detect such a small number of molecules. Therefore, the performance of the system was further tested by repeatedly injecting $200\,\mu L,~1.0\times 10^{-18}\,M$ of HSA into the continuous flow of carrier buffer at 20 min intervals without regenerating the surface. The idea being that if for some reasons the change of capacitance was due to some artifacts in the HSA solution and not due to the binding of HSA and the immobilized anti-HSA, the response should return to the original baseline after each sample volume has passed the electrode surface. Fig. 6B shows the results of this experiment. At the first injection the capacitance decreased by about 0.28 nF, the same value as the capacitance change obtained in the experiment when the sample was passed through the electrode followed by the regeneration solution (Fig. 1B). However, for the injections that followed, the capacitance decreased less and less. This was probably because the immobilized antibodies on the electrode surface that are free to bind to HSA in the passing solution became less and less. Between the seventh and tenth injections no further change in the response was observed. One possibility would be that the immobilized antibodies were saturated with HSA. However, when a higher concentration of HSA was injected (200 μ L, 1.0 \times 10⁻¹⁷ M) the capacitance decreased again (\sim 0.43 nF). The explanation for this is that the stable signal after the sixth injection of the previous concentration probably occurred because the equilibrium of the formation of antigen-antibody complex had been reached. When a higher concentration was introduced however more binding can occur. It was also observed that the capacitance change was less than the signal of 200 μ L, 1.0×10^{-17} M with subsequent regeneration performed earlier (~0.50 nF). This was because some of the immobilized antibodies on the electrode surface were already bound to HSA by the previous ten injections of 1.0×10^{-18} M, therefore the ability of the modified surface to bind with the passing HSA become less. For the remaining injections, a similar behavior to the previous concentrations was observed, i.e., the response became less and less and no change was observed after three injections (Fig. 6B). Further injections of 1.0×10^{-16} M for 9 times, were also carried out. A similar pattern of the responses was observed, with the first injection providing the highest change. The signal then became smaller and reached a stable equilibrium response only after two injections. That is, at higher concentration the equilibrium was reached faster. Increasing the concentration to 1.0×10^{-15} M did not give any signal change. Then, all the HSA molecules that were bound to the immobilized anti-HSA on the electrode surface were removed using the regeneration solution.

Fig. 6C shows the signal before the regeneration at about 110.6 nF. After the regeneration the signal returned to 113.8 nF. Then 200 μL of HSA solution between 1.0×10^{-18} and 1.0×10^{-10} M were injected with subsequent regeneration. The obtained capacitance changes were proportional to the concentration (Fig. 6C). The sizes of the change were similar to those obtained earlier (Fig. 1B). These results confirmed that the obtained capacitance changes were not artifacts or due to a baseline shift and the proposed system could really detect down to 120 molecules per sample. From the results in Fig. 6B it can also be stipulated that if a larger sample volume was employed an even lower limit of detection could be obtained.

3.4. Determination of HSA in urine sample

When testing real samples, matrix interference generally occurs. The effect can be reduced by diluting the sample. In this case the analyte would also decrease. However, if the analysis system has a very low detection limit the analyte could still be detected. From some of our previous work a dilution factor between 10^4 and 10^6 times was generally required to eliminate the interference from other substances in the sample matrix [18,19]. Therefore, a 10^6 times dilution was applied. Since a normal urine albumin excretion is $<20~\mu g\,m L^{-1}$ or $3.0\times 10^{-7}\,M$ [33–35] if this was diluted 10^6 times it would be $3.0\times 10^{-13}\,M$. Therefore, a calibration curve was prepared between 1.0×10^{-14} and $1.0\times 10^{-12}\,M$. This would cover between $0.67~\mu g\,m L^{-1}$ and $67~\mu g\,m L^{-1}$. If a sample had a higher albumin level, the capacitance response would be beyond the calibration curve, but the sample can be further diluted and tested again.

Seven urine samples were diluted 10⁶ times with carrier buffer and tested by the capacitive immunosensor. The response of each sample was used to determine the HSA concentration from the calibration curve of a standard solution (1.0×10^{-14} to 1.0×10^{-12} M) and multiplied by the dilution factor. The results of the capacitive immunosensor and the results from the hospital (immunoturbidimetric assay) were compared by the regression line method and Wilcoxon signed rank test [36]. For the regression line method, the regression equation of the concentration of HSA obtained from the capacitive immunosensor system (y), and the immunoturbidimetric assay (x) is $y = (1.002 \pm 0.006)x + (0.2 \pm 0.2)$ (Table 2). The slope and the interception did not differ significantly (P > 0.05) from the ideal value of 1 and 0, respectively. Therefore, there is no evidence to suggest that there is any systematic difference between the results of the methods. The Wilcoxon signed rank test was also applied and indicated that there is no evidence for systematic differences between the results obtained from the two methods (P>0.05). That is, the concentrations determined by the capacitive immunosensor system are in good agreement with the immunoturbidimetric assay.

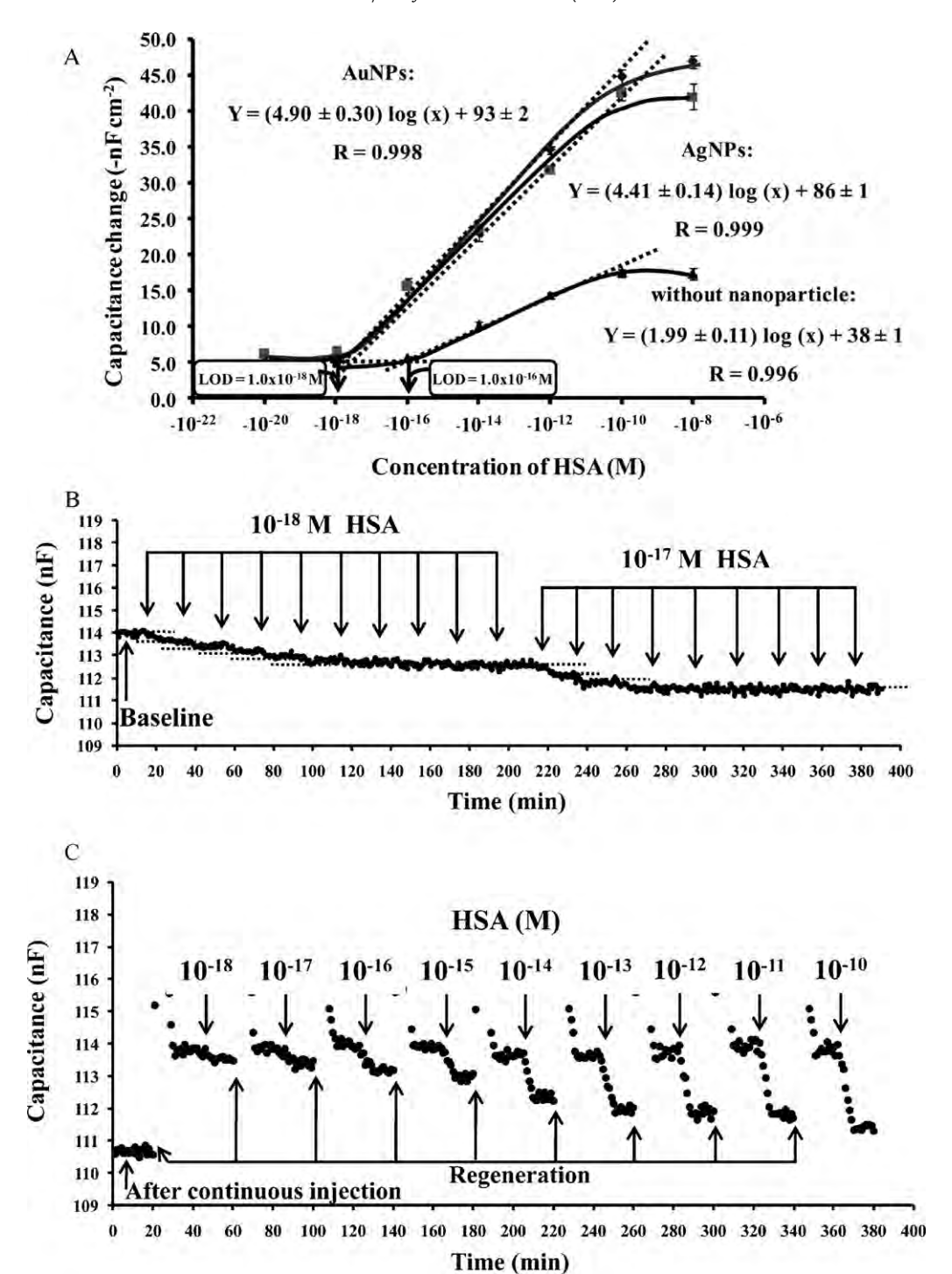


Fig. 6. (A) Comparison of responses of anti-HSA modified with three times the original concentration of AuNPs, AgNPs and without nanoparticles. (B) Capacitance response of the anti-HSA modified electrode with AgNPs, carrier buffer was passed through the system to obtain a baseline of capacitance, $200 \,\mu$ L of 10^{-18} and 10^{-17} M HSA were repeatedly injected 10 and 9 times, respectively, at 20 min intervals. (C) Capacitance responses of anti-HSA after repeated injection of HSA after the bound HSA molecules had been removed by the regeneration solution, various concentrations of HSA were then injected with subsequent regeneration.

3.5. Performance of gold and silver nanoparticles

To compare the performance of the electrodes modified with AgNPs to the one using AuNPs, the two electrodes were modified with nanoparticles of approximately the same size (AgNPs = 10 ± 2 nm and AuNPs = 8 ± 2 nm) both at three times the originally prepared concentration of nanoparticles. This is the optimum concentration for both silver and gold nanoparticles since it provided the highest surface area as

indicated by the highest percentage peak current, $120\pm5\%$ and $117\pm2\%$ for AgNPs and AuNPs, respectively. The binding reaction between anti-HSA and HSA was tested (Fig. 6A). Both electrodes provided the same linear range, 1.0×10^{-18} to 1.0×10^{-10} M and the same detection limit of 1.0×10^{-18} M with nearly the same sensitivity $(4.90\pm0.30-nF\,cm^{-2}\,(\log M)^{-1}$ and $4.41\pm0.14-nF\,cm^{-2}\,(\log M)^{-1}$ for gold and silver nanoparticles). These results showed both nanoparticles could provide the same high sensitivity and low detection limit.

Table 2Results of HSA concentration in urine samples analyzed by the capacitive immunosensor, modified with 48 pmol AgNPs, and immunoturbidimetric assay (IT).

Sample	Capacitive immunosensor $(\times 10^{-8} \text{ M})^a$	Immunoturbidimetric assay ($\times 10^{-8}$ M)
1	14.9 ± 0.6	15.3
2	84.2 ± 0.7	84.4
3	11.2 ± 0.3	11.2
4	17.2 ± 0.2	17.9
5	5.7 ± 0.1	5.7
6	8.5 ± 0.1	8.5
7	60.8 ± 0.5	60.5
Regression equation	$y^{b} = (1.002 \pm 0.006)x^{c} + (0.2 \pm 0.2)$	
R	0.999	

- ^a 3 replications.
- $^{\rm b}\,$ y is the concentration obtained by the capacitive immunosensor ($\times 10^{-8}\,{\rm M}$).
- ^c x is the concentration from the immunoturbidimetric assay ($\times 10^{-8}$ M).

3.6. Effect of the size of analytes

Capacitive immunosensors with incorporated AgNPs were investigated for their performances with different sizes of analytes, i.e. HSA $(68,000 \,\mathrm{g}\,\mathrm{mol}^{-1})$, MCLR $(995.17 \,\mathrm{g}\,\mathrm{mol}^{-1})$ and Pen G (365.37 g mol $^{-1}$). Detection of the three antibody-antigen pairs employed the same flow rate (50 µL min⁻¹) and sample volume $(200 \, \mu L)$. The different operation conditions were carrier buffer and regeneration solution, detection of MCLR used 15 mM Tris-HCl pH 7.20 and HCl pH 2.50 [14] and for Pen G 10 mM Tris-HCl pH 7.40 and 50 mM of glycine-HCl pH 2.50 [19] were used as carrier buffer and regeneration solution, respectively. Table 3 shows the linear range, detection limit and sensitivity of the three immunosensors. The electrodes modified with AgNPs provided a higher sensitivity than without AgNPs for all three analytes. AgNPs enhanced the sensitivity by about 2.2, 2.8 and 2.7 times for HSA, MCLR and Pen G, respectively. The detection limit was also lowered by two orders of magnitude for HSA (macromolecule) and one order of magnitude for MCLR and Pen G (small molecules). The detection limit of the macromolecule was lower than for those of smaller molecules due to its size since macromolecule antigens when bound to the surface adds more thickness than the smaller molecules and this can cause a larger capacitance change. Following this line of reasoning MCLR should have a lower detection limit than Pen G. However, this was not the case, i.e., the system to detect Pen G had a lower detection limit. This is probably because the amount of immobilized anti-MCLR was lower than for the anti-Pen G. The number of immobilized anti-MCLR, calculated from the employed volume and concentration, and the obtained immobilization yield using a molecular weight of 150 kDa for IgG1, was 1.5×10^{12} molecules while it was 1.8×10^{13} molecules for anti-Pen G, The lower amount

Table 3 Performance of the capacitive immunosensor for antigen antibody interactions, the electrodes were modified without and with the optimum of AgNPs compared to some previous work (10^{-15} M = femtomolar (fM); 10^{-18} M = attomolar (aM)).

Analytes	Parameters		
	Linear range (M)	LOD (M)	Sensitivity $(-nF cm^{-2} (log M)^{-1})$
Human serum albumin ((MW = 68,000 g mo	l ⁻¹)	
Without AgNPs	10^{-16} to 10^{-10}	1.0×10^{-16}	2.0 ± 0.1
With 48 pmol AgNPs	10^{-18} to 10^{-10}	1.0×10^{-18}	4.4 ± 0.1
Microcystin-LR (MW = 9	95.17 g mol ⁻¹)		
Without AgNPs	10^{-13} to 10^{-9}	1.0×10^{-13}	4.1 ± 0.2
With 48 pmol AgNPs	10^{-14} to 10^{-9}	1.0×10^{-14}	11.5 ± 0.5
Penicillin G (MW = 356.3	$37 \mathrm{g}\mathrm{mol}^{-1}$		
Without AgNPs	10^{-14} to 10^{-8}	1.0×10^{-14}	2.2 ± 0.3
With 48 pmol AgNPs	10^{-15} to 10^{-9}	7.0×10^{-16}	6.0 ± 0.3

of the immobilized antibodies resulted in less binding, hence, the lower capacitance change.

Comparing the results of this work with nanoparticles, to our previous work, without nanoparticles, using the same concentration of antibody for the immobilized process the detection limit of HSA $(1.0 \times 10^{-18} \,\mathrm{M})$ and Pen G $(7.0 \times 10^{-16} \,\mathrm{M})$ of this work were lower by about 3 and 1 orders of magnitudes, respectively [18,19]. For the detection of MCLR, in the previous work the electrode was modified with AgNPs. Although the optimal amount of AgNPs in this work did not improve the detection limit it did increase the sensitivity (slope of the calibration plot). Using the optimum amount of AgNPs (48 pmol) the sensitivity, when compared to that without using AgNPs, was higher by 2.8 times whereas only 1.7 times $(6.2:3.6-nFcm^{-2}(log M)^{-1})$ was obtained in the previous work [14]. When compared with results from other workers [37,38], the detection limit of HSA in this work was very much lower, i.e., about 10 orders of magnitude, the detection limit of MCLR was lowered by 1–3 orders of magnitude [39,40] and the detection limit of Pen G was lowered by 7–8 orders of magnitude [41,42].

The detection limits of MCLR and Pen G $(1.0\times10^{-14}\,\mathrm{M}$ and $7.0\times10^{-16}\,\mathrm{M})$ are more than sufficient for real samples analysis. Since the provisional guidelines of the World Health Organization for MCLR in drinking water is $1~\mu\mathrm{g}\,\mathrm{L}^{-1}~(1.0\times10^{-9}\,\mathrm{M})~[43,44]$ and the maximum residue limit (MRL) for benzylpenicillin in milk is $4~\mathrm{ppb}\,(1.2\times10^{-8}\,\mathrm{M})~[45]$. That is, real samples can be simply diluted more than 10,000 times before analysis to reduce any matrix effect.

4. Conclusions

The results from this research showed that there is an optimal amount of nanoparticles that can be used to increase the surface area for electrode modification. This has helped to increase the amount of immobilized antibodies and, hence, the performance of the immunosensor. Higher responses were initially observed with increasing amounts (concentration) of nanoparticles. However, there was a particular quantity at which the signals were highest but declined at higher amount of nanoparticles. This was because when the number of nanoparticles was too high, they clustered together, and produced a decrease of the surface area. Electrodes modified with nanoparticles provide better sensitivity and detection limits than without nanoparticles for both large and small molecules. Both AuNPs and AgNPs produced the same efficiencies. Thus, AgNPs that can be prepared with lower cost could be effectively applied. The high sensitivity and extremely low detection limit demonstrated that the system could easily determine the analytes at very low concentrations. The effect of any matrix components could be easily eliminated by simply diluting the sample. This system would be useful for the detection of toxins and residues of small molecule which is quite difficult to analyze with a label-free immunosensor.

Acknowledgements

The authors are grateful for the grant from the Thailand Research Fund (BRG5280014). Financial support from the Center of Excellence for Innovation in Chemistry (PERCH-CIC) Office of the Higher Education Commission; the National Research University Project of Thailand, Office of the Higher Education Commission; Trace Analysis and Biosensor Research Center; and Graduate School, Prince of Songkla University, Hat Yai, Thailand are all gratefully acknowledged. The authors thank Dr Brian Hodgson, Prince of Songkla University, Hat Yai, Songkhla, Thailand for assistance with the English.

References

- [1] C. Berggren, B. Bjarnason, G. Johansson, Electroanalysis 13 (2001) 173.
- [2] C. Berggren, G. Johansson, Analytical Chemistry 69 (1997) 3651.
- [3] C. Berggren, B. Bjarnason, G. Johansson, Biosensors and Bioelectronics 13 (1998)
- [4] M. Hedström, I.Y. Galaev, B. Mattiasson, Biosensors and Bioelectronics 21 (2005) 41.
- [5] D. Jiang, J. Tang, B. Liu, P. Yang, X. Shen, J. Kong, Biosensors and Bioelectronics 18 (2003) 1183.
- [6] M. Labib, M. Hedström, M. Amin, B. Mattiasson, Analytica Chimica Acta 634 (2009) 255.
- [7] W. Limbut, P. Thavarungkul, P. Kanatharana, B. Wongkittisuksa, P. Asawatreratanakul, C. Limsakul, Electrochimica Acta 55 (2010) 3268.
- [8] K. Zór, R. Ortiz, E. Saatci, R. Bardsley, T. Parr, E. Csöregi, M. Nistor, Bioelectrochemistry 76 (2009) 93.
- [9] J.S. Daniels, N. Pourmand, Electroanalysis 19 (2007) 1239.
- [10] I. Bontidean, J. Ahlqvist, A. Mulchandani, W. Chen, W. Bae, R.K. Mehra, A. Mortari, E. Csöregi, Biosensors and Bioelectronics 18 (2003) 547.
- [11] J. Li, Z. Wu, H. Wang, G. Shen, R. Yu, Sensors and Actuators B: Chemical 110 (2005) 327.
- [12] Z.-S. Wu, J.-S. Li, M.-H. Luo, G.-L. Shen, R.-Q. Yu, Analytica Chimica Acta 528 (2005) 235.
- [13] G.-J. Yang, J.-L. Huang, W.-J. Meng, M. Shen, X.-A. Jiao, Analytica Chimica Acta 647 (2009) 159.
- [14] S. Loyprasert, P. Thavarungkul, P. Asawatreratanakul, B. Wongkittisuksa, C. Limsakul, P. Kanatharana, Biosensors and Bioelectronics 24 (2008) 78.
- [15] W. Wu, P. Yi, P. He, T. Jing, K. Liao, K. Yang, H. Wang, Analytica Chimica Acta 673 (2010) 126.
- [16] M. Muniz-Miranda, M. Innocenti, Applied Surface Science 226 (2004) 125.
- [17] W. Limbut, P. Kanatharana, B. Mattiasson, P. Asawatreratanakul, P. Thavarungkul, Biosensors and Bioelectronics 22 (2006) 233.
- [18] K. Teeparuksapun, P. Kanatharana, W. Limbut, C. Thammakhet, P. Asawatreratanakul, B. Mattiasson, B. Wongkittisuksa, C. Limsakul, P. Thavarungkul, Electroanalysis 21 (2009) 1066.
- [19] P. Thavarungkul, S. Dawan, P. Kanatharana, P. Asawatreratanakul, Biosensors and Bioelectronics 23 (2007) 688.
- [20] R. Yuan, Y. Zhuo, Y. Chai, Y. Zhang, A. Sun, Science in China Series B: Chemistry 50 (2007) 97.
- [21] G. Krystal, Analytical Biochemistry 167 (1987) 86.
- [22] G. Krystal, C. Macdonald, B. Munt, S. Ashwell, Analytical Biochemistry 148 (1985) 451.

- [23] B. Wongkittisuksa, C. Limsakul, P. Kanatharana, W. Limbut, P. Asawatreratanakul, S. Dawan, S. Loyprasert, P. Thavarungkul, Biosensors and Bioelectronics 26 (2011) 2466.
- [24] A. Gebbert, M. Alvarez-Icaza, W. Stoecklein, R.D. Schmid, Analytical Chemistry 64 (1992) 997.
- [25] C.M. Niemeyer, Angewandte Chemie International Edition 40 (2001) 4128.
- [26] J.H. Contois, C.J. Lammi-Keefe, S. Vogel, J.R. McNamara, P.W.F. Wilson, T. Massov, E.J. Schaefer, Clinica Chimica Acta 253 (1996) 21.
- [27] B. Mali, D. Armbruster, E. Serediak, T. Ottenbreit, Clinical Biochemistry 42 (2009) 1568.
- [28] R.G. Heideman, R.P.H. Kooyman, J. Greve, Biosensors and Bioelectronics 9 (1994) 33.
- [29] G. Li, K. Stewart, B. Conlan, A. Gilbert, P. Roeth, H. Nair, Vox Sanguinis 83 (2002) 332.
- [30] N.H. Beyer, M.Z. Hansen, C. Schou, P. Højrup, N.H.H. Heegaard, Journal of Separation Science 32 (2009) 1592.
- [31] W. Limbut, P. Kanatharana, B. Mattiasson, P. Asawatreratanakul, P. Thavarungkul, Analytica Chimica Acta 561 (2006) 55.
- [32] R.P. Buck, E. Lindner, Pure and Applied Chemistry 66 (1994) 2527.
- [33] N. Chaturvedi, S. Bandinelli, R. Mangili, G. Penno, R.E. Rottiers, J.H. Fuller, Kidney International 60 (2001) 219.
- [34] C. Cobeñas, F. Spizzirri, Pediatric Nephrology 18 (2003) 309.
- [35] W. Hofmann, W.G. Guder, Clinical Chemistry and Laboratory Medicine 27 (2009) 589.
- [36] J.N. Miller, J.C. Miller, Statistics and Chemometrics for Analytical Chemistry, fourth ed., Peason Education Limited, England, 2000.
- [37] G. Sakai, T. Saiki, T. Uda, N. Miura, N. Yamazoe, Sensors and Actuators B: Chemical 24 (1995) 134.
- [38] S.P. Sakti, P. Hauptmann, B. Zimmermann, F. Bühling, S. Ansorge, Sensors and Actuators B: Chemical 78 (2001) 257.
- [39] P. Lindner, R. Molz, E. Yacoub-George, H. Wolf, Analytica Chimica Acta 636 (2009) 218.
- [40] F. Zhang, S.H. Yang, T.Y. Kang, G.S. Cha, H. Nam, M.E. Meyerhoff, Biosensors and Bioelectronics 22 (2007) 1419.
- [41] G. Cacciatore, M. Petz, S. Rachid, R. Hakenbeck, A.A. Bergwerff, Analytica Chimica Acta 520 (2004) 105.
- [42] E. Gustavsson, J. Degelaen, P. Bjurling, A. Sternesjo, Journal of Agricultural and Food Chemistry 52 (2004) 2791.
- [43] N. Graham, Urban Water 1 (1999) 183.
- [44] WHO, Guidelines for Drinking-Water Quality Second Edition Recommendations – Addendum, 1998.
- [45] Commission-Regulation, Off. J. Eur. Commun. L60 (1999) 16.

ELSEVIER

Contents lists available at ScienceDirect

Biosensors and Bioelectronics

journal homepage: www.elsevier.com/locate/bios



Ultra trace analysis of small molecule by label-free impedimetric immunosensor using multilayer modified electrode

Kochaporn Chullasat^{a,b,c}, Proespichaya Kanatharana^{a,b,c}, Warakorn Limbut^{a,b,d}, Apon Numnuam^{a,b,c}, Panote Thavarungkul^{a,b,e,*}

- ^a Trace Analysis and Biosensor Research Center, Prince of Songkla University, Hat Yai, Songkhla 90112, Thailand
- b Center of Excellence for Innovation in Chemistry, Faculty of Science, Prince of Songkla University, Hat Yai, Songkhla 90112, Thailand
- ^c Department of Chemistry, Faculty of Science, Prince of Songkla University, Hat Yai, Songkhla 90112, Thailand
- ^d Department of Applied Science, Faculty of Science, Prince of Songkla University, Hat Yai, Songkhla 90112, Thailand
- e Department of Physics, Faculty of Science, Prince of Songkla University, Hat Yai, Songkhla 90112, Thailand

ARTICLE INFO

Article history: Received 10 February 2011 Received in revised form 3 May 2011 Accepted 16 May 2011 Available online 23 May 2011

Keywords: Label-free Trace analysis Small molecule Chloramphenicol Impedance biosensor Sensitivity enhancement

ABSTRACT

A multilayer electrode modified with a self-assembled thiourea monolayer (SATUM) followed by gold nanoparticles (AuNPs), mercaptosuccinic acid (MSA) and antibody was investigated for the detection of ultra trace amount of a small molecule (chloramphenicol) in an impedimetric system. The formation of the antibody-antigen complex at the electrode surface caused the impedance to increase. Under optimum conditions three modified electrodes were compared the SATUM/AuNPs/MSA electrode provided a wide linear range $(0.50-10)\times 10^{-16}$ M, and a very low determination limit of 1.0×10^{-16} M. This determination limit was much lower than the SATUM/AuNPs electrode, 1.0×10^{-15} M, and SATUM electrode, 1.0×10^{-14} M. The modified electrode provided good selectivity for chloramphenicol detection and can be reused up to 45 times with a relative standard deviation of lower than 4%. When applied to determine chloramphenicol in shrimp samples, the results agreed well with those obtained by the high-performance liquid chromatography coupled with a photo diode array detector (P>0.05). The developed system can be applied to detect other small molecules using appropriate affinity binding pairs.

© 2011 Elsevier B.V. All rights reserved.

1. Introduction

Impedimetric immunosensor is a sensitive technique for real-time, label-free detection of antigen–antibody binding. The principle is based on the change in interfacial property (resistance and/or capacitance) between the electrode surface and solution when an antibody attached to an electrode surface reacts with an antigen to form a complex (Lisdat and Schäfer, 2008; Thavarungkul et al., 2007). Real-time non-faradaic impedimetric systems have been reported, for example, for the detection of interferon-γ, a relatively large molecule (15.5 kDa), at the attomolar level (Bart et al., 2005; Dijksma et al., 2001). For a smaller molecule, such as penicillin-G (MW 334 g mol⁻¹), the limit of detection is higher, at the femtomolar level (Thavarungkul et al., 2007). In some applications, such as for detecting toxic residues in food, the limit is sometimes recommended as the minimum required performance limit (MRPL) of the analytical method (Commission Decision of 13

E-mail address: panote.t@psu.ac.th (P. Thavarungkul).

March, 2003). In the case of toxins it is obviously better to be able to detect them at the lowest possible level. Therefore, a system that can provide a higher analysis response with a lower limit of detection would provide many advantages.

One way to enhance the response of a label-free immunosensor is to increase the amount of an immobilized antibody on the electrode so that a larger immunological complex can occur, and therefore produce a larger signal. Recently such an enhancement was investigated by immobilizing antibody on an electrode surface incorporating with gold (Wang et al., 2004a) or silver nanoparticles (Loyprasert et al., 2008) to increase the surface area for attachment of the immobilized antibody and which led to a higher signal. Multilayer gold nanoparticles (AuNPs) networks have also been employed to allow for further increases of the electrode surface area (Wang et al., 2004b) and these may be useful for detection of small molecule analytes.

In this work we have proposed a slightly different strategy for producing the "multilayer". Instead of using a multilayer of AuNPs, only one layer of nanoparticles (on a self-assembled thiourea monolayer) was employed. Then a layer of mercaptosuccinic acid (MSA), a thiol compound, was formed on the nanoparticles layer. This MSA has two free functional carboxylic groups (Lewis, 1992) that are used to immobilize the antibody. The electrode

^{*} Corresponding author at: Department of Physics, Faculty of Science, Prince of Songkla University, Hat Yai, Songkhla 90112, Thailand. Tel.: +66 74 288753; fax: +66 74 558849.

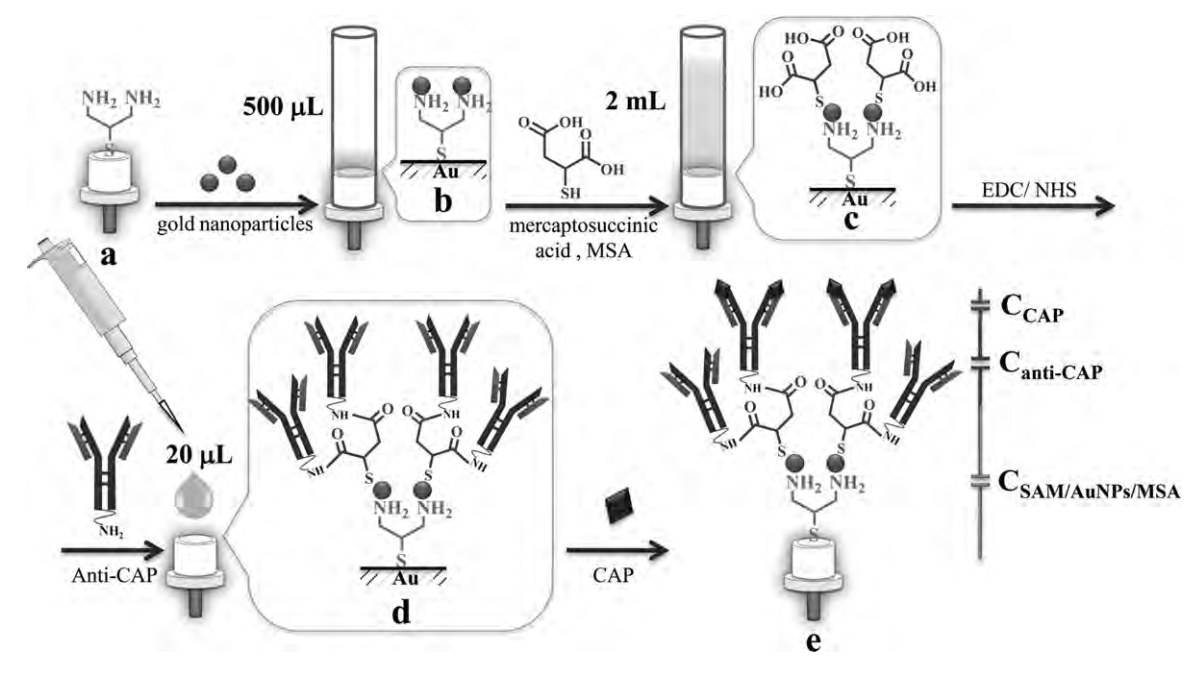


Fig. 1. Schematic illustration of the modified electrode: the cleaned gold electrode with a self-assembled thiourea monolayer (SATUM) (a), a small tube containing the gold nanoparticles solution was fitted on the electrode, gold nanoparticles was adsorbed on the electrode via SATUM (SATUM/AuNPs) (b), mercaptosuccinic acid adsorbed on the AuNPs layer (SATUM/AuNPs/MSA) and activated with EDC/NHS to immobilize the antibody (anti-CAP) (d). The layers on the modified gold electrode surface are represented by capacitors in series (e) where $C_{\text{SATUM}/AuNPs/MSA}$ is the capacitance related to the SATUM/AuNPs/MSA layer, $C_{\text{anti-CAP}}$ is the capacitance related to the chloramphenicol antibody layer and C_{CAP} is the capacitance related to the binding between CAP and immobilized antibody on the modified electrode.

modification steps were optimized to obtain the maximum amount of immobilized antibody. Chloramphenicol (CAP) was chosen as a model analyte because it is a synthetic antibiotic with a low molecular weight (MW 323.13 g mol⁻¹) that is widely used as an anti-microbial agent (Zhang et al., 2008). Also there is need to detect very small residual amounts of CAP in food samples to ensure there will be no possible dangers to human health. The proposed system was then applied to analyze CAP (analyte) in shrimp samples.

2. Materials and methods

2.1. Chemical and materials

Monoclonal anti-CAP was obtained from US biological (Massachusetts, USA). CAP, thiourea and chloroauric acid trihydrate (HAuCl₄·3H₂O) were obtained from Sigma (St. Louis, USA). 3-Mercaptosuccinic acid was obtained from Fluka Chemie (Buchs, Switzerland) and 1-dodecanethiol from Aldrich (Milwaukee, USA). All other chemicals were of analytical grade. Buffers were prepared with water treated with a reverse osmosis-deionized system, filtered through a nylon membrane filter (pore size $0.2\,\mu m$) (Albet, Spain) with subsequent degassing before use.

2.2. Gold nanoparticles (AuNPs) preparation

AuNPs were prepared followed the method described by Wang et al. (2004a) with a slight modification. In brief, a 600 mL mixture of 0.10 mM chloroauric acid trihydrate and 0.15 mM tri-sodium citrate were vigorously stirred in a dark glass bottle while adding 6.0 mL of 50 mM sodium borohydride. The mixture was left under vigorous stirring for 18 h at room temperature and stored at 4 °C.

2.3. Modified electrode preparation

Gold electrodes (diameter 3.0 mm, 99.99% purity) were first polished (Gripo[®] 2V, Metkon Instrument Ltd., Turkey) using alumina slurries (5, 1 and 0.3 μm, respectively). They were washed with

distilled water and ethanol, followed by electrochemical etching in $0.5\,\mathrm{M}\,\mathrm{H}_2\mathrm{SO}_4$ by cyclic voltammetry at a scan rate of $100\,\mathrm{mV}\,\mathrm{s}^{-1}$ from 0.10 V to 1.50 V vs a Ag/AgCl electrode and washed with distilled water. Finally they were dried with pure nitrogen gas. Surface modifications were performed by immersing the electrode in 250 mM thiourea solution (in 0.10 mM $H_2SO_4)$ at room temperature for $24\,h$ (Limbut et al., 2006) during which time a self-assembled thiourea monolayer (SATUM) was formed (Fig. 1a). A small tube containing a solution of AuNPs was fitted on the top of the electrode and left to stand at 4°C. During this time the AuNPs in the solution were adsorbed onto the SATUM via the -NH2 group (Fig. 1b). The volume (amount) of the AuNPs and incubation time were studied to obtain the conditions that provided the largest surface area. MSA was then adsorbed onto the AuNPs via the -SH moieties at room temperature by filling the tube on top of the electrode with 2.0 mL of MSA solution (Fig. 1c). At this time the concentration of MSA and the incubation time were investigated to obtain the conditions that yielded the maximum amount of the adsorbed MSA. The modified surface was then activated with 500 μ L of EDC/NHS (EDC 1% (v/v), NHS 2.5% (v/v) in 50 mM phosphate buffer pH 5.00 with 50 mM KCl) for 5 h. After that $20 \,\mu\text{L}$ of anti-CAP ($50 \,\mu\text{g}\,\text{mL}^{-1}$ in $10 \,\text{mM}$ phosphate buffer pH 7.00) was dropped onto the modified electrode and left for the binding reaction to occur overnight at 4°C (Fig. 1d). The electrode was then immersed in 0.1 M ethanolamine pH 8.00 for 7 min to block any unreacted aldehyde groups on the surface. Finally, the remaining pinholes on the modified electrode were blocked by 10 mM 1-dodecanethiol. This is now the SATUM/AuNPs/MSA modified electrode.

For the SATUM modified electrode, after the SAM was formed the surface was treated with 5% (v/v) glutaraldehyde in 10 mM phosphate buffer pH 7.00 at room temperature for 20 min, this step was to activate the aldehyde groups. Then $20\,\mu\text{L}$ of $50\,\mu\text{g}\,\text{mL}^{-1}$ anti-CAP was dropped onto the surface and left overnight at $4\,^{\circ}\text{C}$. The electrode was immersed in 0.1M ethanolamine pH 8.00 for 7 min to block any unreacted aldehyde groups on the surface. Finally, the modified electrode was blocked by 10 mM 1-dodecanethiol.

Table 1Tested and optimum conditions of the modified electrode and the flow injection system. Three replicates were tested for each studied value.

Parameter	Studied value	Optimum
Electrode modification		
AuNPs		
Volume (µL)	200, 300, 400, 500, 600, 700 and 800	500
Incubation time (h)	2, 3, 4, 5, 6 and 8	4
MSA		
Concentration (mM)	50, 75 and 100	75
Incubation time (h)	3, 6, 9, 12 and 18	9
Flow injection system		
Regeneration solution		
Type	0.1 M MgCl ₂ , HCl pH 2.50, 25 mM glycine–HCl pH 2.50, 25 mM NaOH and 50 mM NaOH	NaOH
Concentration (mM)	10, 25, 50, 75 and 100	50
Carrier buffer	Phosphate buffer saline	
Concentration (mM)	5, 10 and 15	10
pН	6.80, 7.00 and 7.20	7.00
Flow rate and sample volume		
Flow rate (µLmin ⁻¹)	50, 100 and 150	100
Sample volume (µL)	400, 450 and 500	450

For the SATUM/AuNPs modified electrode, after the formation of SAM and adsorption of the AuNPs, 20 μL of anti–CAP was placed on the modified electrode, left overnight at $4\,^{\circ}\text{C}$ and then blocked by 10 mM 1-dodecanethiol.

During immobilization, the degree of insulation of the different layers was investigated by cyclic voltammetry performed in a batch cell containing 5 mM K_3 [Fe(CN)₆] and 0.1 M KCl. The modified gold electrode was used as the working electrode (WE) together with a Ag/AgCl reference electrode (RE) and a platinum rod auxiliary electrode (AE). The amount of the immobilized antibody on the electrode was also measured using the silver binding method (Krystal, 1987). Briefly, the protein sample solution was treated with glutaraldehyde and then exposed to ammonical silver. After 15 min the absorbance of the solution was measured at 420 nm and the amount of protein was calculated from the calibration equation.

2.4. Optimization of electrode modification

The optimum volume and incubation time of the AuNPs for the modification of the electrode (Table 1) were studied in term of surface coverage obtained from a cyclic voltammogram performed in $0.1\,\mathrm{M\,H_2SO_4}$, using three electrodes for each test. The percentage of the surface coverage was evaluated from the area of the reduction peak of electroadsorption of oxygen atom on the AuNPs modified electrode compared with a bare gold electrode (Limbut et al., 2006; Xiang et al., 2001) (Fig. 2) by Eq. (1).

$$Surface coverage(\%) = \frac{Q_{SATUM/AuNPs}}{Q_{BGE}} \times 100$$
 (1)

where $Q_{SATUM/AuNPs}$ and Q_{BGE} are the amount of electric charge exchanged during the electroadsorption of oxygen (C cm⁻²) on the electrode modified with AuNPs and on a bare gold electrode, respectively.

For the modified MSA layer, the optimum volume and incubation time were considered through its insulating property. The adsorption of the MSA layer was studied by a cyclic voltammograms performed in 5 mM $K_3[Fe(CN)_6]$ containing 0.1 M KCl. The average peak height (P) was calculated from the anodic (i_{pa}) and the cathodic (i_{pc}) peak height (Fig. 2 inset) by Eq. (2). Then the differential peak height was evaluated by Eq. (3).

Average peak height,
$$P = \frac{i_{pa} + i_{pc}}{2}$$
 (2)

Differential peak height(%) =
$$\frac{P_{\text{SATUM/AuNPs/MSA}} - P_{\text{SATUM/AuNPs}}}{P_{\text{SATUM/AuNPs}}} \times 100 \tag{3}$$

where $P_{\rm SATUM/AuNPs/MSA}$ is the average peak height of the MSA modified electrode and $P_{\rm SATUM/AuNPs}$ is the average peak height of the AuNPs modified electrode.

The concentration and incubation time of MSA (Table 1) were optimized together. Three electrodes were tested for each value.

2.5. Impedimetric measurement

CAP was determined using a flow injection impedimetric immunosensor system. The measurements were carried out using an Autolab PGSTAT30 electrochemical impedance analyzer and a potentionstat/galvanostat (Metrohm Autolab, The Netherlands) connected to a computer. The modified electrode was used as the WE together with a custom-made Ag/AgCl RE and a Pt wire auxiliary electrode (99.95% purity diameter 1.5 mm, Alfa Aesar, USA). The volume of the flow cell was 10 µL. The Eco

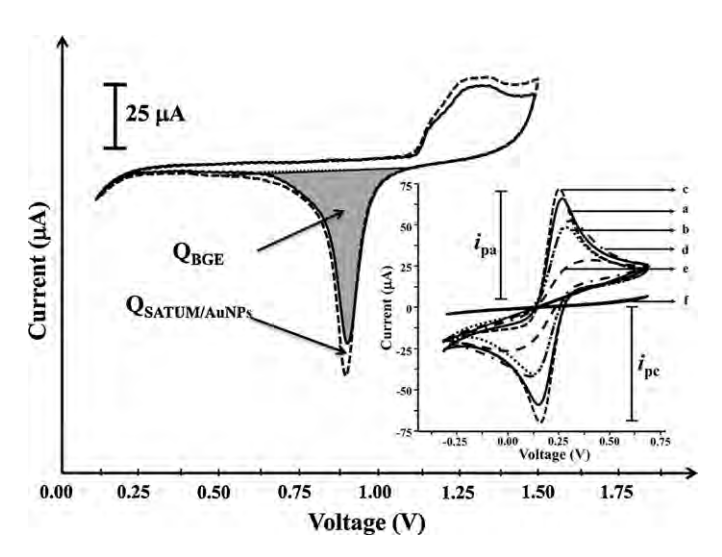


Fig. 2. Example of a cyclic voltammograms of bare gold electrode (BGE) (solid line) compared with the electrode modified with AuNPs via a self-assembled monolayer (500 μL, 4h incubation time) (dash line) performed in 0.1 M H₂SO₄ solution at a scan rate of 100 mV s⁻¹ vs an Ag/AgCl reference electrode. The voltage range was 0.10–1.50V. Inset, cyclic voltammograms of the immobilization steps of anti-CAP modified electrode (under optimum condition of the modification steps) obtained with 5 mM K₃[Fe(CN)₆] in 0.1 M KCl solution at a scan rate of $100 \, \text{mV} \, \text{s}^{-1}$ vs a Ag/AgCl reference electrode. The voltage range was $-0.30 \, \text{to} \, 0.70 \, \text{V}$. (a) Bare gold electrode, (b) self-assembled thiourea monolayer (SATUM), (c) SATUM/AuNPs, (d) SATUM/AuNPs/MSA, (e) anti-CAP immobilized on the multilayer of SATUM/AuNPs/MSA and (f) after treatment with 1-dodecanethiol. The anodic peak height (i_{De}) are also shown.

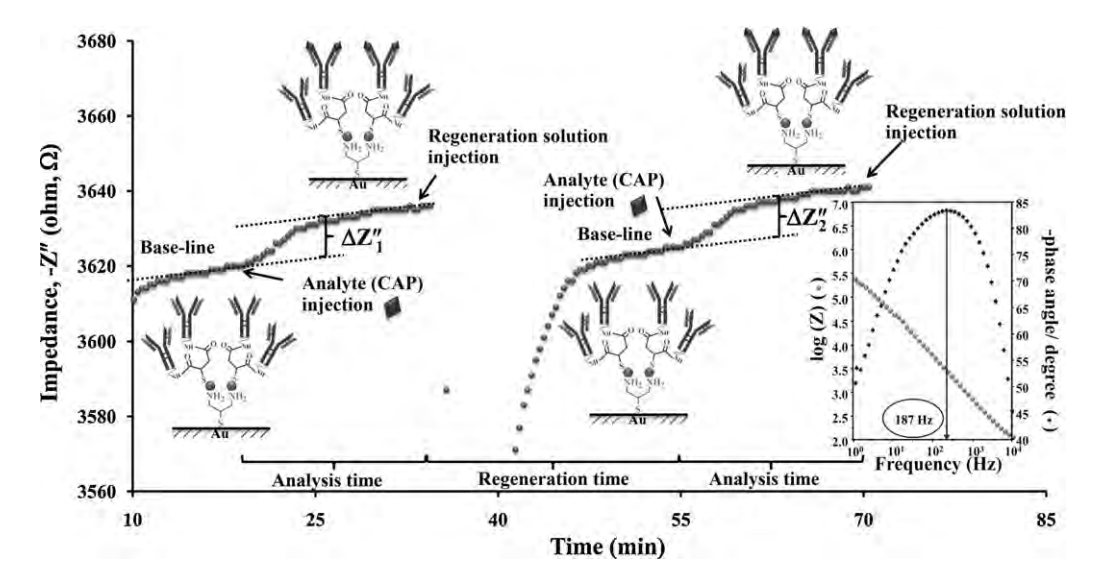


Fig. 3. Impedance response of the modified electrode monitor at a single frequency. The base-line signal of the carrier buffer was first recorded. After solution containing CAP was injected, the immunocomplex of antigen, CAP, and antibody, anti-CAP, caused the impedance to increase (ΔZ_1^n) . Regeneration solution was then injected to remove CAP from the immobilized anti-CAP. When the signal base-line was recovered a new analysis cycle was applied (ΔZ_2^n) . The time used to monitor CAP-anti-CAP binding is the analysis time. The time used, after the injection of regeneration solution, to remove the bound antigen followed by continuous flow of buffer to bring back to the base-line is the regeneration time. Inset: the optimum frequency was determined from a Bode plot in the region where the system show nearly ideal capacitor behavior, i.e., the plot of logarithm of impedance against logarithm of frequency is a straight line with a slope of -1 and the phase angle closest to -90° .

Chemie software, Frequency Response Analyzer (FRA 4.9.005), was used to monitor the impedance by applying an AC amplitude of $\pm 10\,\text{mV}$ with a DC potential of $0.00\,\text{mV}$ (vs Ag/AgCl reference electrode). The CAP-anti-CAP interaction was monitored via the change of the imaginary part of the impedance (Z'') as a function of time at a single frequency. The optimum frequency was determined from a Bode plot (Fig. 3 inset) (Bart et al., 2005; Thavarungkul et al., 2007). The carrier buffer was first passed though the system and the Z'' base-line was recorded (Fig. 3). When the CAP was injected, it bound to the immobilized anti-CAP on the modified electrode. This was like adding another capacitor in series (Fig. 1e) and this led to the increase of impedance ($\Delta Z''$) which corresponded with the concentration of CAP (Fig. 4 inset).

2.6. Optimization of the flow injection impedimetric immunosensor

The modified electrode can be reused by removing the antigen from the immobilized antibody using a regeneration solution. Type and concentration of regeneration solutions were studied. These were followed by concentration and pH of the carrier buffer, flow rate and sample volume, respectively (Table 1). Each of these parameters was investigated by analyzing the same concentration of CAP, $1.0\times 10^{-15}\,\mathrm{M}.$ Initial conditions of the flow injection impedimetric immunosensor were: carrier buffer 10 mM phosphate buffer saline [2.7 mM KCl and 137 mM NaCl pH 7.40 (Maupas et al., 1997)], regeneration solution HCl pH 2.50, flow rate 50 $\mu\mathrm{L}\,\mathrm{min}^{-1}$ and sample volume 400 $\mu\mathrm{L}.$ The optimal conditions

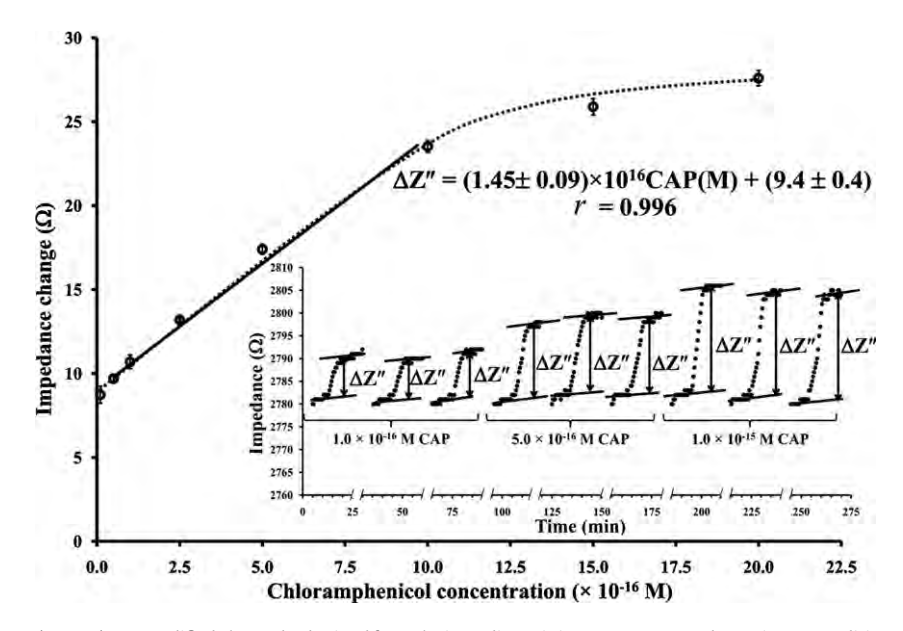


Fig. 4. A calibration plot of SATUM/AuNPs/MSA modified electrode obtained from the impedimetric immunosensor under optimum conditions: 10 mM PBS pH 7.00 containing 2.7 mM KCl and 137 mM NaCl, flow rate $100 \,\mu$ L min⁻¹, sample volume $450 \,\mu$ L and $50 \,m$ M NaOH as regeneration solution. Inset shows example of the impedance changes ($\Delta Z''$) caused by the binding of analyte (CAP)-immobilized anti-CAP interaction.

were selected by achieving a balance between a high response and a short analysis time.

2.7. Real sample analysis

Six shrimp samples were collected from six markets in Hat Yai, Songkhla, Thailand. The effect of the matrix was first studied by comparing the impedimetric immunosensor responses obtained from standard and spiked samples. Standard CAP solutions (CAP in carrier buffer) were analyzed at 5.0×10^{-17} , 1.0×10^{-16} , 2.5×10^{-16} , 5.0×10^{-16} and 1.0×10^{-15} M. Spiked samples were prepared by spiking 20 µL of the standard CAP at concentrations of 2.5×10^{-10} , 5.0×10^{-10} , 12.5×10^{-10} , 2.5×10^{-9} and 5.0×10^{-9} M in 2.0 g of blended shrimp. Then 10.0 mL of carrier buffer was added and homogenized by an ultrasonic homogenizer (Biologics, Inc., USA) for 15 min. The mixture was centrifuge at 10,000 rpm for 15 min. 200 µL of the supernatant was then transferred to a desalt column (Bio-Rad Laboratories, USA). The desalted spiked sample was diluted 10,000 times by the carrier buffer. The final concentrations of the analyte were 5.0×10^{-17} , 1.0×10^{-16} , 2.5×10^{-16} , 5.0×10^{-16} and 1.0×10^{-15} M. A blank sample was also analyzed with each sample. Responses were plotted against the known concentration of CAP. The slope of the standard CAP and the spiked samples were evaluated by two-way ANOVA calculated by R software (R Development Core Team, 2006) to test whether the slopes of the two plots differ significantly. If there is no difference, this indicates that the matrix has no effect on the response of the sys-

For real sample analysis 2.0 g of blended shrimp sample was mixed with 10.0 mL of carrier buffer, homogenized, centrifuged, desalted and diluted as described above before being analyzed.

2.8. Comparison between the impedimetric immunosensor and a HPLC-DAD method

The six shrimp samples were extracted with 20 mL of ethyl acetate and defatted with 10 mL n-hexane (Xia et al., 2007; Zhang et al., 2008). They were analyzed with the impedimetric immunosensor under optimum conditions and the high performance liquid chromatography combined with a diode array detector (HPLC-DAD) (Agilent Series 1100, USA). For the HPLC-DAD technique, the analysis was operated on an Alltima HP C18 column, 150 mm \times 4.6 mm, 3 μ m (Alltech, USA). The conditions were 0.4 mL min $^{-1}$ of mobile phase (80:20, acetonitrile:water) and a 20 μ L sample volume and a wavelength of 278 nm (Hong et al., 2002). Results from the two techniques were compared by the Wilcoxon signed rank test.

3. Results and discussion

3.1. Gold nanoparticles

The sizes of the nanoparticles were measured from TEM images (JEM-2010, JEOL, Japan, operating at $80\,\mathrm{kV}$). The average diameter was $2.7\pm0.4\,\mathrm{nm}$ (n=311). Assuming that the gold solution (0.10 mM) was completely converted to AuNPs, the amount of the gold nanoparticles could be calculated from the concentration and the diameter via the mass to be 9.9×10^{16} particles per liter.

3.2. Electrochemical characteristics of anti-CAP modified electrode

The electrochemical characteristics of the modified electrode were investigated after each immobilization step by voltammetry. The increase or decrease of the redox peaks helped to determine whether each immobilization step was successful. The bare

gold electrode clearly showed the signals of the redox couple $[Fe(CN)_6]^{4-}/[Fe(CN)_6]^{3-}$ (Fig. 2 inset a). The redox peaks decreased when the SATUM was formed on the gold electrode surface (Fig. 2 inset b). This is because the SATUM impeded the electron transfer of the system. The redox peaks then increased when AuNPs were deposited on SATUM (Fig. 2 inset c) due to the increase of electron transfer through the AuNPs. When the electrode was modified with MSA followed by anti-CAP, the redox peaks reduced after each step due to the added insulation by these materials (Fig. 2 inset d and e). Finally, after treatment with 1-dodecanethiol the redox peaks disappeared (Fig. 2 inset f), to indicate total insulation.

For modification of the electrode with AuNPs the volume (amount) of AuNPs (with 8 h incubation time) was tested between 200 and 800 μL . The percentage of surface coverage increased with the volume of AuNPs from 200 μL to 500 μL , then decreased (Table 1, Supplementary data Table S-1). It is possible that when the number of the AuNPs becomes too high gold nanoparticles cluster together, thus, reducing the surface area due to the curvature of individual particles. The effect of the incubation time was then studied using 500 μL of AuNPs (Table 1). The percentage of surface coverage increased with incubation time from 2 to 4 h and became stable (Table 1, Supplementary data Table S-1). Therefore, 500 μL and a 4 h incubation time were used as the optimum conditions for modification by AuNPs.

When MSA was adsorbed on the AuNPs layer, the insulation caused electron transfer to decrease. The purpose was to obtain the condition that can provide the most adsorbed MSA indicated by the insulation of the surface. By increasing the concentration and incubation time of MSA more MSA was adsorbed, the surface became more insulated and the percentage of the differential peak height became more negative. Between the three tested concentrations (Table 1, Supplementary data Table S-2), 75 and 100 mM provided similar insulation property, much better than with 50 mM. For the incubation time the insulation property increase from 3 to 9 h after which (9–18 h) the percentage of the differential peak height did not differ significantly (*P* > 0.05). Therefore, 75 mM of MSA with a 9 h incubation time was chosen to modify the electrode since it used lesser reagent and provided similar characteristic to 100 mM MSA.

3.3. Operating frequency

The optimal frequency was tested for each modified electrode before use (Fig. 3 inset). For the 54 electrodes tested, an average of 189 ± 44 Hz was obtained. The optimum frequency was then set for the real-time detection of the interaction of CAP with the anti-CAP.

3.4. Optimization of the flow impedimetric immunosensor system

The parameters that affected the responses of the flow injection impedimetric immunosensor system were optimized. When an optimal condition was obtained for one parameter it was used in the optimization of the next parameter following the sequence described in this following section.

3.4.1. Type and concentration of regeneration solution

The ability of the regeneration solution was evaluated in terms of the percentage of residual activity determined from the impedance changed when the anti-CAP bound to CAP (400 μ L, 1.0×10^{-15} M) before ($\Delta Z_1''$) and after ($\Delta Z_2''$) regeneration (Fig. 3) using Eq. (4).

Residual activity(%) =
$$\frac{\Delta Z_2'' \times 100}{\Delta Z_1''}$$
 (4)

Three types of regeneration solution were studied, high ionic strength, low pH and high pH (Table 1, Supplementary data Table

S-3), using three replicates for each of the solutions. NaOH, the high pH, provided the highest residual activities with a short regeneration time. This is because at high pH both CAP (p K_a 5.5) and anti-CAP (pI 7.00–8.00) are deprotonated and the net negative charge causes the repulsion between the affinity binding pair. The effect of the concentration of NaOH was then studied. The highest residual activity was obtained at 50 mM with a relatively short regeneration time (18–22 min). Therefore, 50 mM of NaOH was used as the regeneration solution.

3.4.2. Concentration and pH of carrier buffer

Phosphate buffer saline, often used for impedance immunosensors (Maupas et al., 1997; Thavarungkul et al., 2007), was employed as the carrier buffer. The influences of the concentration and pH were optimized together (Table 1). The highest impedance change was provided by 10 mM phosphate buffer saline pH 7.00 (27.3 \pm 0.6 Ω). This was probably because one of the binding forces of the affinity binding is electrostatic (Cunningham, 1998) which depends on the charges on the antibody and antigen. At pH 7.00 CAP (p K_a 5.5) was deprotonated and is negatively charged while anti-CAP had a positive charge (pI 7.00–8.00) which helped with the binding (Li et al., 2006). It is possible that at this pH the different charges on each side of the affinity pair enabled maximum binding compared to other pH.

3.4.3. Flow rate and sample volume

The flow rate and sample volume were studied together (Table 1). A low flow rate and a high sample volume provided a high response due to the longer contact time between the affinity binding pair and the large amount of analyte (Supplementary data Table S-4). In this study $100~\mu L\, min^{-1}$ and $450~\mu L$ were chosen because these conditions provided a high response $(23.3\pm0.6~\Omega)$ with a relatively short analysis time.

The determinations of the optimal conditions are summarized in Table 1.

3.5. Linear range and determination limit

Performance of the electrodes modified with SATUM, SATUM/AuNPs and SATUM/AuNPs/MSA were studied under optimum conditions (Table 1), using three replications for each concentration. Fig. 4 shows the calibration plot of the SATUM/AuNPs/MSA modified electrode. It provided a wide linear range of $(0.50-10)\times10^{-16}\,\mathrm{M}.$ For the SATUM/AuNPs modified electrode, a linear range of $(1.0-10)\times10^{-15}\,\mathrm{M}$ was obtained with the linear regression equation $\Delta Z''_{\mathrm{SATUM/AuNPs}}(\Omega) = (1.05\pm0.08)\times10^{15}\mathrm{CAP(M)} + (11.2\pm0.4), \ r = 0.995.$ The SATUM modified electrode gave a linear range of $(1.0-10)\times10^{-14}\,\mathrm{M}$ with $\Delta Z''_{\mathrm{SATUM/AuNPs}}(\Omega) = (0.62\pm0.04)\times10^{14}\mathrm{CAP(M)} + (8.8\pm0.2), \ r = 0.997.$

Besides the lower detectable linear concentration range, the determination limit of the SATUM/AuNPs/MSA modified electrode was also better than the electrode modified with SATUM/AuNPs and SATUM. For residue analysis the result can be reported as determinable if it is greater than or equal to the determination limit. This value can be calculated from three times the maximum blank signal (Vogelgesang and Hädrich, 1998). Using the SATUM/AuNPs/MSA modified electrode the maximum of the blank signal (carrier buffer) was $3.6\,\Omega$ (average = $3.2\pm0.2\,\Omega$, n = 20), three times the blank signal corresponded to a very low determination limit of $1.0\times10^{-16}\,\mathrm{M}$. A higher determination limit was obtained for the SATUM/AuNPs and SATUM electrode, i.e., $1.0\times10^{-15}\,\mathrm{M}$ (maximum blank signal = $4.1\,\Omega$, average = $3.7\pm0.2\,\Omega$, n = 20) and $4.7\times10^{-14}\,\mathrm{M}$ (maximum blank signal = $3.9\,\Omega$, average = $3.2\pm0.4\,\Omega$, n = 20), respectively.

The reason for the better performance of the SATUM/AuNPs/MSA was probably due to the larger amount of immobilized antibody. The use of MSA with two functional groups that can bind to the antibody and at the same time acted as a spacer to increase the distance between the immobilized antibody and the AuNPs surface can reduce the steric hindrance (Weimer et al., 2000) and this led to a higher immobilization yield and hence a higher response. These results were confirmed by determining the amount of immobilized antibody on the modified electrode by the silver binding method (Krystal, 1987). The immobilization yield of 91.2 \pm 0.4% was obtained for SATUM/AuNPs/MSA electrode while only 62 \pm 1% and 41 \pm 1% were attained by the SATUM/AuNPs and SATUM electrode, respectively (Supplementary data Table S-5).

It is generally expected that for label-free measurements impedance changes will be most pronounced if the target is substantially larger than the probe or has significantly different properties (Berggren et al., 2001; Daniels and Pourmand, 2007). However, the proposed impedimetric immunosensor can provide very good response for a small CAP molecule. Therefore, the molecular weight might not be the only factor affecting the response (Berggren and Johansson, 1997; Jiang et al., 2003). It has been suggested that "Mechanisms by which the affinity interaction changes the measured interface impedance are still poorly understood. There is need for both experimental and theoretical work in this regard." (Daniels and Pourmand, 2007).

3.6. Reproducibility

The reproducibility of the responses of two SATUM/AuNPs/MSA electrodes was evaluated at optimum conditions, by repeatedly injecting the same concentration of standard CAP (1.0×10^{-15} M). The regeneration solution was used to remove CAP analyte from the immobilized anti-CAP after each analysis. For the first electrode the average percentage residual activity of the first 45 cycles of regeneration (3 days) was 97 ± 3 (%R.S.D. = 3). After that the residual activity decreased rapidly. For another modified electrode, the average percentage residual activity of the first 47 regeneration cycles (3 days) was 100 ± 4 (%R.S.D. = 4). The loss of activity may be due to either the loss of antibody from the modified surface or reduction of the antibody activity. Cyclic voltammetry was used to test this hypothesis. A cyclic voltammogram of the electrode after the loss of activity appeared to be as flat as for the electrode blocked with 1-dodecanethiol to indicate that the modified electrode layer remained intact. The decrease of the percentage of residual activity was therefore probably due to the loss of activity of the immobilized antibody.

The reproducibility of the different electrodes modified with SATUM/AuNPs/MSA and anti-CAP were tested by comparing the sensitivity (slope) of the calibration plot of the electrodes prepared in the same batch. The linear regression equation, between 5.0×10^{-17} and 1.0×10^{-15} M, of the six modified electrodes were $\Delta Z_1''(\Omega) = (1.14 \pm 0.09) \times 10^{16} \text{CAP(M)} + (14.2 \pm 0.5)$, $\Delta Z_2''(\Omega) = (1.28 \pm 0.06) \times 10^{16} \text{CAP(M)} + (10.5 \pm 0.3)$, $\Delta Z_3''(\Omega) = (1.20 \pm 0.08) \times 10^{16} \text{CAP(M)} + (12.4 \pm 0.4)$, $\Delta Z_4''(\Omega) = (1.17 \pm 0.10) \times 10^{16} \text{CAP(M)} + (12.6 \pm 0.5)$, $\Delta Z_5''(\Omega) = (1.26 \pm 0.11) \times 10^{16} \text{CAP(M)} + (10.4 \pm 0.6)$ and $\Delta Z_6''(\Omega) = (1.22 \pm 0.09) \times 10^{16} \text{CAP(M)} + (9.5 \pm 0.5)$ with r in the range of 0.990–0.997.

The sensitivities of the calibration plot therefore did not differ significantly among each electrode (P > 0.05) to indicate that the performance of the different electrodes can be reproduced.

3.7. Selectivity

The immunosensor was tested for its selectivity to CAP at a concentration of 1.0×10^{-15} M and the average response was

Table 2 Comparison of CAP concentrations in spiked shrimp samples obtained from the label-free immunosensor and HPLC-DAD technique $(1.00 \text{ ppm} = 3.09 \times 10^{-6} \text{ M}) (n = 3)$.

Sample no.	Spiked concent	trations (ppm)						
	1.00		1.50		2.00		2.50	
	HPLC	Immunosensor	HPLC	Immunosensor	HPLC	Immunosensor	HPLC	Immunosensor
1	0.97 ± 0.01	1.03 ± 0.06	1.49 ± 0.01	1.49 ± 0.11	2.00 ± 0.02	2.10 ± 0.06	2.52 ± 0.05	2.49 ± 0.16
2	0.96 ± 0.02	1.00 ± 0.12	1.53 ± 0.04	1.46 ± 0.06	2.01 ± 0.02	2.10 ± 0.16	2.49 ± 0.03	2.59 ± 0.12
3	0.98 ± 0.03	0.92 ± 0.06	1.53 ± 0.03	1.59 ± 0.12	2.03 ± 0.02	1.99 ± 0.14	2.48 ± 0.05	2.48 ± 0.18
4	0.95 ± 0.02	1.04 ± 0.05	1.52 ± 0.02	1.46 ± 0.15	2.04 ± 0.01	2.04 ± 0.15	2.49 ± 0.02	2.53 ± 0.08
5	0.94 ± 0.02	1.03 ± 0.06	1.57 ± 0.03	1.52 ± 0.11	2.06 ± 0.05	2.04 ± 0.06	2.47 ± 0.06	2.51 ± 0.16
6	1.02 ± 0.01	1.16 ± 0.06	1.48 ± 0.01	1.44 ± 0.11	2.05 ± 0.03	2.04 ± 0.06	2.53 ± 0.01	2.57 ± 0.06

 $27.3\pm1.2\,\Omega$ (n=3). Antibiotics with similar structure to CAP, i.e., florfenicol, thiamphenicol and chloramphenicol base, and those that are frequency tested in shrimp, i.e., oxolinic acid and tetracycline were tested at the same concentration as for CAP and at a 100 and 10,000 times higher concentration. All of these antibiotics provide very low impedance changes $(4.4\pm1.3\,\Omega)$ for all concentrations that are much lower than the response at the determination limit (10.8 Ω). The responses from these antibiotics also did not change with concentration. Hence, this system showed very good selectivity for CAP.

3.8. Matrix interference

Preliminary tests indicated that spiked shrimp sample when diluted about 10,000 times provided a signal similar to the signal of the standard solution, i.e., there was no matrix interference at this dilution. The six shrimp samples, each spiked with 2.5×10^{-10} , 5.0×10^{-10} , 12.5×10^{-10} , 2.5×10^{-9} and 5.0×10^{-9} M of CAP were then tested for the matrix effect after the simple extraction and 10,000 times dilution (the concentrations were 5.0×10^{-17} , 1.0×10^{-16} , 2.5×10^{-16} , 5.0×10^{-16} and 1.0×10^{-15} M, see Section 2.7). The standard and the spiked sample calibration equations were obtained between 5.0×10^{-17} and 1.0×10^{-15} M. The slopes of the standard and spiked samples were compared by two-way ANOVA. For all six samples, there were no significant differences (P > 0.05) between the two slopes, to indicate that the matrix has no effect on the responses of the system (Eurachem, 1998). Therefore, all samples, with a 10,000 times dilution, can be directly analyzed using the standard calibration plot.

3.9. Real sample analysis

The six samples were analyzed by the label-free impedimetric immunosensor under optimum conditions with a 10,000 times dilution. The response was used to determine the concentration of CAP in the shrimp sample from the standard calibration plot $(0.50-10)\times 10^{-16}\,\mathrm{M}$ and multiplied by the dilution factor. For all samples, the concentration of chloramphenicol was not determinable because the obtained signals were much lower than the determination limit.

Although chloramphenicol could not be determined in any of the samples, the proposed impedimetric system using the SATUM/AuNPs/MSA modified electrode would be more than sufficient for quantitative analysis of CAP in shrimp at an ultra-trace level. Since the determination limit of the system is $1.0\times 10^{-16}\,\mathrm{M}$ and taking into consideration the simple extraction procedure and dilution before analysis (see Section 2.7) this corresponded to a determination limit of $1.6\times 10^{-3}\,\mu\mathrm{g}$ of CAP per kilogram of shrimp (1.6 ppt). This is still much lower than the MRPL for the analytical method used for the determination of chloramphenicol set by the European Communities, i.e., $0.3\,\mu\mathrm{g}\,\mathrm{kg}^{-1}$ (Commission Decision of 13 March, 2003).

Comparing to other reports on conventional method for CAP detection in shrimp, i.e., ELISA (Shen and Jiang, 2005), HPLC–UV (Sridl and Cichna-Markl, 2007) and LC–MS-MS (Tittlemier et al., 2007; Zhang et al., 2008), the proposed system provided the lower determination limit and only a simple sample preparation is required, without the use of solvent. As for other biosensors, they are mostly based on indirect assay, i.e., inhibition (Ferguson et al., 2005) or competitive assay (Park and Kim, 2006) which required several steps and have a higher determination limit than this work. Although the reusability of the electrode for this proposed method was less than the competitive method of Yuan et al. (2008) the analysis is much simpler.

3.10. Recovery

To validate the method, recovery was studied from shrimp samples (2.0 g) spiked with 20 μ L of 5.0 \times 10⁻¹⁰, 12.5 \times 10⁻¹⁰, 2.5 \times 10⁻⁹ and 5.0 \times 10⁻⁹ M CAP. These corresponded to 1.6, 4.0, 8.1 and 16.2 ppt of CAP in the shrimp samples. The samples were then extracted with 10 mL of carrier buffer, centrifuged, desalted diluted 10,000 times and tested by the impedimetric immunosensor. The percentage of recovery of CAP (analyte) was calculated by Eq. (5).

Recovery(%) =
$$\frac{(C_1 - C_2) \times 100}{C_3}$$
 (5)

where C_1 is the determined concentration of the spiked CAP sample, C_2 is the concentration of the real sample and C_3 is the concentration of the spiked CAP (Eurachem, 1998).

The recoveries of CAP in the shrimp sample were in the range of 87–116% with a relative standard deviation of between 1 and 14% (Supplementary data Table S-6). These values were acceptable. Since for 1 ppb level $(3.1\times10^{-9}\,\text{M})$ the recovery is acceptable if it was in the range 40–120% with \leq 30% R.S.D. (Taverniers et al., 2004). Therefore, the range of recoveries and %R.S.D. obtained by the proposed method are acceptable since the tested concentrations were in the ppt range. These results showed that the developed label-free injection impedimetric immunosensor is suitable for small molecule (analyte, CAP) determination in real sample (shrimp).

3.11. Comparison with HPLC-DAD

To further validate the system, concentrations from spiked samples obtained from the immunosensor were compared with those from HPLC-DAD analysis. A preliminary study with HPLC-DAD indicated that it could determine CAP in the range of 1.00–2.50 ppm. The extractant that had been defatted from each of the six shrimp samples was spiked with four concentrations within this range and analyzed. These same samples were then diluted 10,000 times and analyzed using the impedimetric immunosensor. CAP was not found by both methods in unspiked samples (Table 2). The

recoveries from the impedimetric immunosensor and HPLC-DAD were in the range of 99 ± 2 to $103\pm1\%$ and 95 ± 1 to $105\pm1\%$, respectively. These are within the acceptable range for the ppm level, i.e., 80-110% for recovery at this level (Thévenot et al., 2001). Comparison between the two analysis techniques by the Wilcoxon signed rank test indicated that there was no evidence for any systematic difference between the results obtained from the two methods (P > 0.05).

4. Conclusions

The multilayer SATUM/AuNPs/MSA modified electrode is well-suited for the detection of ultra trace levels of small molecules. CAP, a small molecule is determinable at very low concentration of 1.0×10^{-16} M, 1.6 ppt. The sample preparation step is simple and does not require any solvent extraction and preconcentration steps. One preparation of the electrode can be reused up to 45 analysis cycles and this helps to reduce the cost of analysis. Other antigen–antibody couples can easily be applied by modifying the electrode with different antibodies. The good performance of the developed system implied that it would be very useful for the detection of toxin, and small molecules, present at ultra trace concentrations.

Acknowledgements

The authors are grateful for the grant from the Thailand Research Fund (BRG5280014). Support by the Center of Excellence for Innovation in Chemistry (PERCH-CIC), Office of the Higher Education Commission; the National Research University Project of Thailand, Office of the Higher Education Commission; the Trace Analysis and Biosensor Research Center (TAB-RC), and Graduate School and Faculty of Science, Prince of Songkla University, Hat Yai, Thailand are also gratefully acknowledged. The authors thank Dr. Brian Hodgson, Prince of Songkla University, Hat Yai, Thailand for assistance with the English.

Appendix A. Supplementary data

Supplementary data associated with this article can be found, in the online version, at doi:10.1016/j.bios.2011.05.029.

References

Publication, NY.

Bart, M., Stigter, E.C.A., Stapert, H.R., de Jong, G.J., van Bennekom, W.P., 2005. Biosens. Bioelectron. 21 (1), 49–59.

Berggren, C., Bjarnason, B., Johansson, G., 2001. Electroanalysis 13 (3), 173–180.

Berggren, C., Johansson, G., 1997. Anal. Chem. 69 (18), 3651–3657. Commission Decision of 13 March, 2003. Off. J. Eur. Commun. L71 (15.3.2003), 17–18. Cunningham, A.J., 1998. Introduction to Bioanalytical Sensor. Wiley-Interscience

Daniels, J., Pourmand, S.N., 2007. Electroanalysis 19 (12), 1239-1257.

Dijksma, M., Kamp, B., Hoogvliet, J.C., van Bennekom, W.P., 2001. Anal. Chem. 73 (5), 901–907.

Eurachem, W.G., 1998. EURACHEM Guide.

Ferguson, J., Baxter, A., Young, P., Kennedy, G., Elliott, C., Weigel, S., Gatermann, R., Ashwin, H., Stead, S., Sharman, M., 2005. Anal. Chim. Acta 529, 109–113.

Hong, L., Horni, A., Hesse, M., Altorfer, H., 2002. Chromatographia 55 (1), 13–18. Jiang, D., Tang, J., Liu, B., Yang, P., Kong, J., 2003. Anal. Chem. 75 (17), 4578–4584.

Krystal, G., 1987. Anal. Biochem. 167, 86-96.

Lewis, R.J., 1992. Condensed Chemical Dictionary. 12ed. Van Nostrand Reinhold is an International Thomson Publishing company, NY.

Li, X., Yuan, R., Chai, Y., Zhang, L., Zhuo, Y., Zhang, Y., 2006. J. Biotechnol. 123 (3), 356–366.

Limbut, W., Kanatharana, P., Mattiasson, B., Asawatreratanakul, P., Thavarungkul, P., 2006. Biosens. Bioelectron. 22 (2), 233–240.

Lisdat, F., Schäfer, D., 2008. Anal. Bioanal. Chem. 391 (5), 1555-1567.

Loyprasert, S., Thavarungkul, P., Asawatreratanakul, P., Wongkittisuksa, B., Limsakul, C., Kanatharana, P., 2008. Biosens. Bioelectron. 24 (1), 78–86.

Maupas, H., Soldatkin, A.P., Martelet, C., Jaffrezic-Renault, N., Mandrand, B., 1997. J. Electroanal. Chem. 421 (1–2), 165–171.

Park, I.-S., Kim, N., 2006. Anal. Chim. Acta 578 (1), 19-24.

R Development Core Team, 2006. Vienna, Austria.

Shen, H.-Y., Jiang, H.-L., 2005. Anal. Chim. Acta 535 (1-2), 33-41.

Sridl, R., Cichna-Markl, M., 2007. J. Sol-Gel Sci. Technol. 41, 175–183.

Taverniers, I., De Loose, M., Van Bockstaele, E., 2004. Trends Anal. Chem. 23 (8), 535–552.

Thavarungkul, P., Dawan, S., Kanatharana, P., Asawatreratanakul, P., 2007. Biosens. Bioelectron. 23 (5), 688–694.

Thévenot, D.R., Toth, K., Durst, R.A., Wilson, G.S., 2001. Biosens. Bioelectron. 16 (1–2), 121–131.

Tittlemier, S.A., Van De Riet, J., Burns, G., Potter, R., Murphy, C., Rourke, W., Pearsne, H., Dufresne, G., 2007. Food Addit. Contam. 24 (1), 14–20.

Vogelgesang, J., Hädrich, J., 1998. Accred. Qual. Assur. 3 (6), 242-255.

Wang, M., Wang, L., Wang, G., Ji, X., Bai, Y., Li, T., Gong, S., Li, J., 2004a. Biosens. Bioelectron. 19 (6), 575–582.

Wang, M., Wang, L., Yuan, H., Ji, X., Sun, C., Ma, L., Bai, Y., Li, T., Li, J., 2004b. Electroanalysis 16 (9), 757-764.

Weimer, B.C., Walsh, M.K., Wang, X., 2000. J. Biochem. Biophys. Methods 45 (2), 211–219.

Xia, X., Li, X., Zhang, S., Ding, S., Jiang, H., Shen, J., 2007. Anal. Chim. Acta 586 (1–2), 394–398.

Xiang, J., Wu, B.-L., Chen, S.-L., 2001. J. Electroanal. Chem. 517 (1-2), 95-100.

Yuan, J., Oliver, R., Aguilar, M.-I., Wu, Y., 2008. Anal. Chem. 80 (21), 8329-8333

Zhang, S., Liu, Z., Guo, X., Cheng, L., Wang, Z., Shen, J., 2008. J. Chromatogr. B 875 (2), 399–404

FISEVIER

Contents lists available at SciVerse ScienceDirect

Electrochimica Acta

journal homepage: www.elsevier.com/locate/electacta



Characterization and application of self-assembled layer by layer gold nanoparticles for highly sensitive label-free capacitive immunosensing

Saluma Samanman a,b,c, Proespichaya Kanatharana a,b,c, Punnee Asawatreratanakul a,b,d, Panote Thavarungkul a,b,e,*

- ^a Trace Analysis and Biosensor Research Center, Prince of Songkla University, Hat-Yai, Songkhla, 90112, Thailand
- ^b Center for Innovation in Chemistry, Faculty of Science, Prince of Songkla University, Hat-Yai, Songkhla, 90112, Thailand
- ^c Department of Chemistry, Faculty of Science, Prince of Songkla University, Hat-Yai, Songkhla, 90112, Thailand
- d Department of Biochemistry, Faculty of Science, Prince of Songkla University, Hat-Yai, Songkhla, 90112, Thailand
- e Department of Physics, Faculty of Science, Prince of Songkla University, Hat-Yai, Songkhla, 90112, Thailand

ARTICLE INFO

Article history: Received 20 April 2012 Received in revised form 29 June 2012 Accepted 2 July 2012 Available online 16 July 2012

Keywords: Layer-by-layer Gold nanoparticles Capacitive immunosensor Deposition direction Highly sensitive

ABSTRACT

A highly sensitive label-free capacitive immunosensor was developed based on layer by layer (LBL) selfassembled gold nanoparticles (AuNPs) using thiourea (TU) as a cross-linker on a poly-tyramine (Pty) modified gold electrode. One to five layers at various concentrations of AuNPs were tested. The LBL AuNPs increased the surface area of the electrode, enabling more antibodies to be immobilized and resulted in an increase of the sensitivity. Testing for human serum albumin (HSA) by anti-human serum albumin (anti-HSA) was used as a model. It is shown that there is an optimal concentration and number of AuNPs layer that can effectively enhance the sensitivity of a label-free capacitive immunosensor system. The electrode with two layers of 71 nmol l^{-1} AuNPs provided the highest sensitivity, compared to 24 nmol l^{-1} and $236\,\mathrm{nmol}\,l^{-1}$ AuNPs. It is also shown for the first time the interfacial properties of each layer through the investigated surface coverage, impedance spectroscopy electrochemical values, and surface morphology. The high sensitivity was related to the surface coverage (%) and hence the immobilization yield (%). In addition, it is presented for the first time the effect of the direction of AuNPs deposition. The face-down deposition direction of the electrode into AuNPs solution, provided a better sensitivity, lower detection limit $(10^{-19} \text{ mol } l^{-1})$ and a wider linear range $(1.0 \times 10^{-19} \text{ to } 1.0 \times 10^{-10} \text{ mol } l^{-1})$ than the face-up, into the AuNPs, deposition direction. When this electrode was used to determine the amount of albumin in urine samples, the results agreed well with those obtained by the conventional clinical methods (P > 0.05) and provided good recovery (%). This method could be applied for the sensitive detection of other analytes using other affinity binding pairs.

© 2012 Elsevier Ltd. All rights reserved.

1. Introduction

Label-free immunosensor combines a specific interaction between antigen and antibody that rely on the direct detection of the change in physical properties during the formation of the immune complex. These changes can be measured by a number of transducers such as mass sensitive [1], optical [2,3] and electrochemical [4,5] detectors. Among these techniques electrochemical detections generally offer a low cost, highly sensitive and highly efficient method [6–8]. One of these methods that has attracted recent interest due to its high sensitivity, simple

E-mail address: panote.t@psu.ac.th (P. Thavarungkul).

instrumentation, rapid analysis and low cost is the potential step capacitive technique [3,9–14]. It can directly detect the binding between antigen and antibody [12,15-17]. The principle of this capacitive immunosensor is based on measuring the capacitance change caused by the change of dielectric properties when the immobilized antibody and the antigen in the sample is formed on the electrode surface, causing the capacitance to decrease [9]. This technique has been applied to detect many analytes such as disease markers [3,17,18], residual toxin [12,15,19], total bacteria [20] and viruses [13]. Although the technique can provide a sensitive detection it still requires further modification for trace level analysis where low detection limits and high sensitivity are needed. One way to increase the signal is to increase the sensing elements by increasing the effective surface area of the electrode using nanoparticles. Gold nanoparticles (AuNPs) are often used because they provide a large surface to-volume-ratio, have strong adsorption ability for protein and good biocompatibility. AuNPs have been

^{*} Corresponding author at: Department of Physics, Faculty of Science, Prince of Songkla University, Hat-Yai, Songkhla, 90112, Thailand. Tel.: +66 74 288753; fax: +66 74 558849.

used to increase the amount of the sensing element [15,21]. Using AuNPs with the capacitive transducer has provided very low detection limits in the order of nanograms or even femtograms per milliliter [10,15].

To further increase the amount of the sensing element additional layers of AuNPs can be used. This so called layer by layer (LBL) technique is a versatile and powerful strategy that has frequently been employed [11,22-28]. This technique can increase the amount of AuNPs attached to the electrode surface resulting in a larger electrode surface area [28,29] and enables more of the sensing elements to be immobilized. It can be fabricated via an electrostatic interaction [27,30,31] or via a molecular linker such as a dithiol [26,28] and cystamine [32]. In this work thiourea (TU), a low cost and less toxic compound compared to other cross linkers, was used as the cross linker. The aim of this work was to develop a highly sensitive label-free capacitive immunosensor based on layer by layer self-assembled AuNPs using TU as a cross linker on a poly-tyramine (Pty) modified gold electrode. Anti-human serum albumin (anti-HSA) and human serum albumin (HSA) were used as a model of the immunosensing due to its clinical importance. HSA is widely measured in daily clinical examination in order to evaluate liver function, severity of disease or hypermetabolic states [33,34]. This work also investigated the electrochemical properties and the morphology of the electrode with different layers and different concentration of AuNPs using cyclic voltammetry (CV), electrochemical impedance spectroscopy (EIS) and scanning electron microscopy (SEM) techniques. The direction of deposition of the AuNPs was also tested, i.e., with the electrode face-up and face-down into the AuNPs solution. Finally, the performance of the capacitive immunosensor system such as its linear range, limit of detection and real sample analysis were studied.

2. Experimental

2.1. Materials

Polyclonal anti-human serum albumin and human serum albumin were obtained from Dako (Glostrup, Denmark), chlorauric acid (HAuCl₄) solution and 1-dodecanethiol ethanolic acid were from Aldrich (Miwaukee, USA), sodium borohydride (NaBH₄) was from Fluka Chemie AG (Buchs, Switzerland), trisodium citrate from Univar (Auckland, New Zealand), tyramine and thiourea were from Sigma–Aldrich (Steinheim, Germany). All other chemicals were of analytical grade. All buffers were prepared with deionized water treated with a reverse osmosis–deionizing system. Before use, buffers were filtered through a nylon membrane filter (Albet, Spain, pore size $0.20\,\mu\text{m}$) with subsequent degassing.

2.2. Gold nanoparticles (AuNPs) synthesis

AuNPs were synthesized followed the procedure reported by Loyprasert et al. [15]. Briefly, $500\,\mathrm{ml}$ of a $2.5\,\mathrm{mmol\,l^{-1}}$ chloroauric acid trihydrate solution and $3.75\,\mathrm{mmol\,l^{-1}}$ tri-sodium citrate solution was prepared in a dark glass bottle. Five milliliter of $1.25\,\mathrm{mol\,l^{-1}}$ sodium borohydride was rapidly added into the gold solution under continuous stirring. The solution was stirred overnight. The prepared AuNPs were then stored at $4\,^\circ\mathrm{C}$ for further use.

The particle size of the AuNPs was measured from transmission electron microscope images (TEM, JEM-2010, JEOL). The TEM was operated in a high vacuum mode with a voltage of 200 kV.

2.3. Fabrication of the electrode with layers of gold nanoparticles

A gold electrode (diameter = 3.0 mm, 99.99% purity) was polished by hand using alumina slurries with particle diameters of

5.0, 1.0 and 0.3 μ m, respectively. The electrode was then cleaned by rinsing with distilled water and electrochemically etched by cyclic voltammetry in 0.5 mol l⁻¹ H₂SO₄ using a potential from 0.0 to 1.5 V versus a Ag/AgCl reference electrode with a scan rate of 0.1 V s⁻¹ for 25 scans (Microautolab type III, Methrohm Autolab B.V., Netherland). The electrode was then dried using pure nitrogen gas. Pty was then electropolymerized onto the gold electrode from a 50 mmol l⁻¹ tyramine monomer solution, dissolved in a mixed solution of ethanol and phosphate buffer (2.0 mmol l⁻¹) pH 7.00 (volume ratio of 3:1), using the potential from 0.0 to 0.8 V versus a Ag/AgCl reference electrode with a scan rate of 0.05 V s⁻¹ for 10 scans [15].

The Pty modified electrode was then immersed in 1.0 ml of colloidal AuNPs for 4h at 4°C, then removed and rinsed with water. This will be referred to as the first layer of AuNPs (AuNPs₁). The AuNPs₁/Pty modified electrode was then immersed in 2.0 ml of 250 mmol l⁻¹ TU, the cross linker, for 24 h at room temperature. This step will be referred to as the TU₁ step. These two steps were repeated to obtain a multilayered electrode (AuNPs_n/ TU_{n-1}) where *n* is the number of layers (n = 1-5). The electrode with different numbers of layers and different concentrations of AuNPs were studied for the conditions that provided the largest surface area, good electron transfer (see Section 2.5), the largest immobilization yield (see Section 2.6) and the highest detection sensitivity by the capacitive system (see Sections 2.7-2.8). The electrodes with different layers of colloidal particles were immobilized with 20 µL of $500 \,\mu g \, ml^{-1}$ anti-HSA and left overnight at $4 \,^{\circ}$ C. Finally, the electrode was immersed in $10 \text{ mmol } l^{-1}$ 1-dodecanethiol ethanolic acid solution for 20 min to block the remaining pinholes (Scheme 1).

2.4. Effect of AuNPs deposition direction

The deposition of the AuNPs layer was carried out through two arrangements of the electrode. The "face-up" method where a small tube containing 1.0 ml of the solution of AuNPs was fitted on top of the electrode and left to stand for 4 h at $4\,^{\circ}$ C. For the "face-down" method the electrode was immersed in 1.0 ml of the solution of AuNPs (in a 5 ml beaker) for 4 h at $4\,^{\circ}$ C. The electrode with the number of layers of AuNPs that provided the highest sensitivity (see Section 3.3.2) was employed in this study.

2.5. Surface characterization

2.5.1. Surface coverage

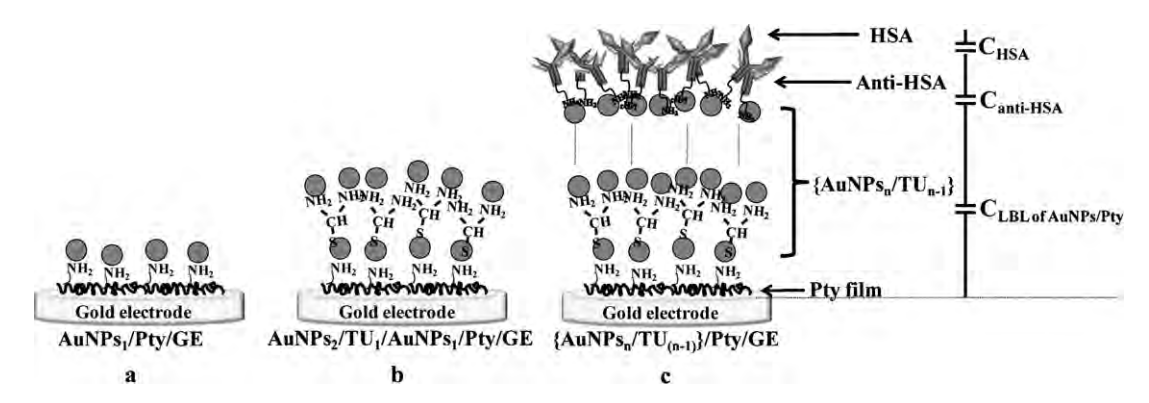
The surface coverage of the electrode with different layers of AuNPs was determined by cyclic voltammetry in $0.10\,\mathrm{mol\,l^{-1}}$ H_2SO_4 using a potential from 0.1 to $1.2\,\mathrm{V}$ with a scan rate of $100\,\mathrm{mV\,s^{-1}}$ versus an Ag/AgCl reference electrode. The surface coverage was evaluated from the area of the reduction peak of the gold oxide on the different layers of AuNPs modified electrode compared with a bare gold electrode [21,35,36] by Eq. (1)

Surface coverage (%) =
$$\frac{Q_{(AuNPs)_n}}{Q_{BGE}} \times 100$$
 (1)

where $Q_{(AuNPs)_n}$ and Q_{BGE} are the amount of the surface gold oxide formed on the electrode modified with AuNPs_n and on a bare gold electrode, respectively.

2.5.2. Scanning electron microscopy

The surface morphology of the electrodes with different layers of AuNPs was observed by scanning electron microscopy (SEM, JSM-5800, JEOL, Japan) operated at an accelerating voltage of 20 kV. The SEM samples were prepared by placing the modified gold electrode on the carbon tape.



Scheme 1. Illustration of the fabrication of the multilayered gold nanoparticles electrode: the cleaned gold electrode (GE) with a poly-tyramine film (Pty), gold nanoparticles (AuNPs) was adsorbed on the electrode via the amine-group of Pty and this was called the AuNPs₁ layer (a), thiourea (TU) was adsorbed on the AuNPs₁ layer followed by the AuNPs and this is AuNPs₂ layer (b). The two steps of AuNPs and TU adsorption were continued to obtain the multilayered AuNPs electrode (n = 5) and the antibody was immobilized on the AuNPs (anti-HSA) to bind with the antigen (HSA) (c). The layers on the modified gold electrode surface are represented by capacitors in series where $C_{\text{LBL of AuNPs/Pty}}$ is the capacitance related to the LBL of AuNPs/Pty layer, $C_{\text{anti-HSA}}$ is the capacitance related to the binding between antigen and immobilized antibody on the modified electrode.

2.5.3. Electrochemical impedance spectroscopy

The electrochemical cell consisted of a working electrode (with the different layers of AuNPs), a platinum wire auxiliary electrode, and an Ag/AgCl reference electrode. Electrochemical impedance spectroscopy was performed with the Autolab PGSTAT30 electrochemical impedance analyzer and potentiostat/galvanostat (Methrohm Autolab B.V., The Netherlands) in 10 mmol l⁻¹ PBS containing $10 \text{ mmol } l^{-1} [Fe(CN)_6]^{3-}/[Fe(CN)_6]^{4-} (1:1) \text{ mixture at a}$ bias potential of 0.20 V. A small alternative voltage of 5 mV was applied with a frequency between 0.1 Hz and 10 kHz. The measured impedance spectra were fitted to an equivalent circuit model using the Autolab and the Frequency Response Analysis system software, FRA (version 4.9.004) [37]. The resistance of the electron transfer between the solution and the electrode surface (R_{et}), the resistance of the solution (R_s) , the constant phase element (CPE) and the Warburg element (Z_W) were obtained from their Nyquist plot.

2.6. Immobilization yield

Using a silver binding protein method [38], the immobilization yield of the anti-HSA was determined as the difference between the amount of the anti-HSA in the solution prepared before the immobilization and the solution collected from the electrode surface after the immobilization. Five-microliter of the anti-HSA solution was first diluted to 50 μl with distilled water containing 0.2% of sodium dodecyl sulfate (SDS) and 0.4% of Tween 20. Then 950 μl of distilled water and 20 μl of 2.5% glutaraldehyde were added to each sample and mixed with 200 μl of ammoniacal silver. After 20 min the reaction was stopped by adding 40 μl of 30 mg ml $^{-1}$ sodium thiosulfate solution. Absorbance was measured at 420 nm and this was used to calculate the concentration from the calibration curve of the standard antibody.

2.7. Capacitance measurement

The experimental set-up of the flow injection capacitive immunosensor system is shown in Fig. 1(a). The modified gold electrode (working electrode), stainless steel tube (auxiliary electrode) and a custom made Ag/AgCl (reference electrode) were placed in a custom-made measuring flow cell ($10\,\mu$ l) and they were connected to a potentiostat (Model EA161, EDAQ, New South Wales, Australia). The capacitance was determined from the obtained current response when a potential step of $50\,\mathrm{mV}$ (pulse width

6.4 ms) was applied to the working electrode. The system can be represented by a simple RC circuit model and the current–time response can be expressed by Eq. (2) [9].

$$i(t) = \frac{u}{R_{\rm S}} \exp\left(\frac{-t}{R_{\rm S}C_{\rm total}}\right) \tag{2}$$

where i(t) is the current in the circuit as a function of time, u is the applied pulse potential, $R_{\rm S}$ is the dynamic resistance of the recognition layer, t is the time elapsed after the potential step is applied, and $C_{\rm total}$ is the total capacitance measured at the working electrode/solution interface. Eq. (3) is obtained by taking the logarithm of Eq. (2).

$$\ln(t) = \ln\left(\frac{u}{R_{\rm S}}\right) - \frac{t}{R_{\rm S}C_{\rm total}} \tag{3}$$

From the linear least-square fitting of $\ln i(t)$ versus t, $R_{\rm s}$ and $C_{\rm total}$ was calculated from the intercept and slope of the linear regression equation, respectively. During the continuous flow of the running buffer, a baseline capacitance was obtained. When HSA was injected into the flow system it bound to the immobilized anti-HSA on the working electrode, and the $C_{\rm total}$ decreased as described by Eq. (4) [9]

$$\frac{1}{C_{\text{total}}} = \frac{1}{C_{\text{LBL of AuNPs/Pty}}} + \frac{1}{C_{\text{anti-HSA}}} + \frac{1}{C_{\text{HSA}}}$$
 (4)

where $C_{\rm total}$ is the total capacitance measured at the working electrode/solution interface, $C_{\rm LBL~of~AuNPs/Pty}$ is the capacitance of the modified electrode layer, $C_{\rm anti-HSA}$ is the capacitance of the anti-HSA layer, and $C_{\rm HSA}$ is the capacitance of the HSA layer. $C_{\rm total}$ was measured every minute and the results were later plotted as a function of time. The capacitance change (ΔC) could be determined (Fig. 1(b)) as

$$\Delta C = C_{\text{before binding with HSA}} - C_{\text{after binding with HSA}}$$
 (5)

The regeneration solution, 300 μ l of HCl pH 2.50 [39], was then injected to break the binding interaction of the immobilized anti-HSA and HSA. The capacitance then returned to its original baseline, ready for a new analysis cycles (Fig. 1(b)).

2.8. Determination of the sensitivity

The calibration plot of the capacitance change (per unit area of the bare electrode surface) with the logarithm of the HSA concentration was first studied by injecting different concentrations of standard HSA with a subsequent regeneration step to remove the HSA (Fig. 1). The tested concentrations were 1.0×10^{-16}

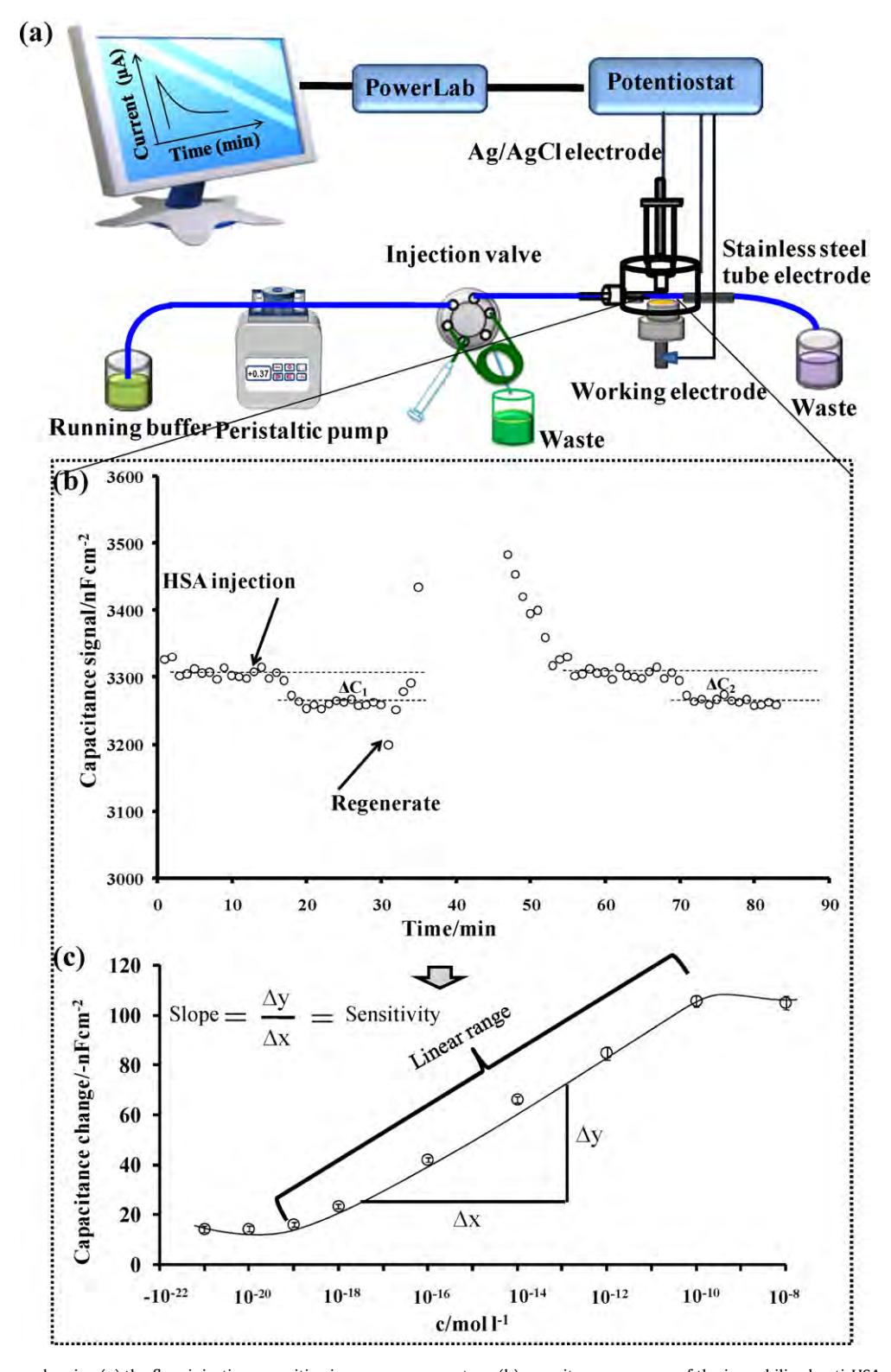


Fig. 1. Schematic diagram showing (a) the flow injection capacitive immunosensor system, (b) capacitance response of the immobilized anti-HSA multilayered electrode as a function of time. The baseline signal of the carrier buffer was first recorded. After HSA was injected, the binding between HSA and immobilized anti-HSA caused the capacitance to decrease (ΔC_1). The regeneration solution was then injected to remove HSA from the immobilized anti-HSA. When the signal baseline was recovered a new analysis cycle was applied. (c) The obtained capacitance changes ($-nFcm^{-2}$) (ΔC) were then plotted versus the logarithm of the HSA concentration and the sensitivity was obtained as the slope of the linear equation.

to $1.0 \times 10^{-10} \, \text{mol} \, l^{-1}$ that represented the linear range of the HSA detection (obtained from the preliminary study). Each concentration of standard HSA was done in three replicates. The measurements were carried out using the following operation

conditions: regeneration solution HCl pH 2.50, $10\,\mathrm{mmol\,l^{-1}}$ Tris–HCl buffer pH 7.00 as the running buffer, sample volume $300\,\mu l$ and flow rate $50\,\mu l\,\mathrm{min^{-1}}$ [19]. The performance of the capacitive immunosensor system was determined by the

sensitivity, which is the slope of the calibration plot. A higher sensitivity reflects a more efficient system.

2.9. Determination of HSA in a real sample

Urine samples were obtained from Songklanagarind Hospital, Hat Yai, Thailand. The samples were analyzed by the flow capacitive immunosensor system using the electrode with optimal deposition direction of AuNPs (see Section 3.3.3). The results of the samples were compared with those obtained by the Hospital, an immunoturbidimetric assay. In brief, the urine sample was added into the buffer followed by anti-albumin to start the reaction. The antigen–antibody complexes agglutinated and the turbidity was measured [40,41].

3. Results and discussion

3.1. AuNPs synthesis

Fig. 2 shows a TEM image of the prepared AuNPs, the size distribution was 7 ± 2 nm (n = 200) (inset). From this size and assuming complete conversion of the 2.5 mmol l⁻¹ chloroauric acid solution the number of nanoparticles (assuming solid spheres) was calculated via the mass (197 g mol⁻¹), volume (1 nanoparticle = $4\pi r^3/3$) and density (19.3 g ml⁻¹) to be 1.42×10^{17} nanoparticles per liter or 236 nmol l⁻¹. Other concentrations of AuNPs were prepared by diluting the synthesized AuNPs with deionized water.

3.2. Characterization of the electrode consisting of different layers of gold nanoparticles

3.2.1. Surface coverage (%)

From a preliminary study the surface coverage (%) of 1 layer of AuNPs was determined for various concentrations of the prepared AuNPs solution (9, 24, 47, 71, 95, 118 and 236 nmol l⁻¹), the 71 nmol l⁻¹ of AuNPs or 0.75 mmol l⁻¹ of the original chloroauric acid solution, provided the highest surface coverage. However, other reports have used the 0.25 mmol l⁻¹ and 2.5 mmol l⁻¹ of chloroauric acid solution for the preparation of AuNPs for the immobilization of a biorecognition element [10,15]. Therefore, these three concentrations (0.25, 0.75 and 2.5 mmol l⁻¹) chloroauric acid solution were chosen for a more detailed study. The amount of AuNPs of these three concentrations is 24 nmol l⁻¹, 71 nmol l⁻¹ and 236 nmol l⁻¹, respectively. The surface coverage of the electrode with different layers of AuNPs was determined from the cyclic

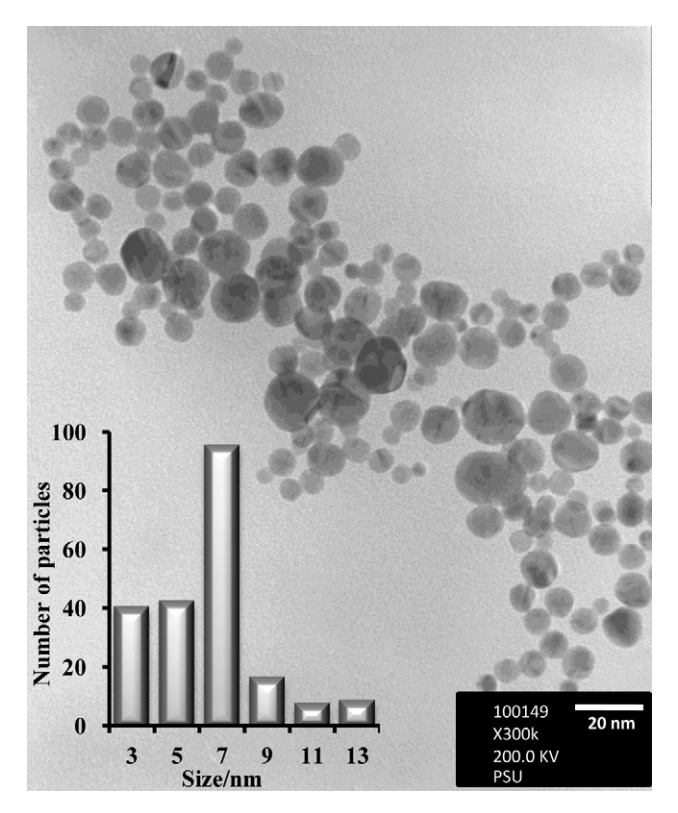
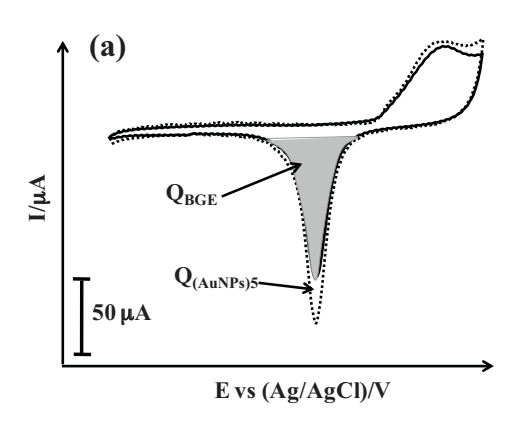


Fig. 2. An example of a TEM image of gold nanoparticles. The histogram in the inset shows the characteristic particle size distribution. The mean diameter is 7 ± 2 nm (n = 200)

voltammograms (Fig. 3(a)). The effective surface area increased with the number of AuNPs layer up to two layers (AuNPs₂) then decreased (Fig. 3(b)). The decrease of the surface area (n>2) is possibly because more and more particles were adsorbed on the surface and they came into contact with each other. Therefore, the total surface area from the curvature surface of separated individual nanoparticles decreased. These results corresponded well to the report by Zhang and Srinivasan that when the number of layers increased the aggregation of the particles became more and more pronounced [27].

Comparing the amount of the three AuNPs concentrations, the $71 \text{ nmol } l^{-1}$ of AuNPs provided the highest surface coverage. At a lower concentration a lower surface area was caused by a lower



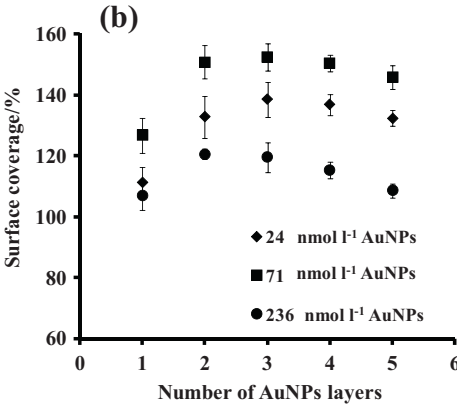


Fig. 3. Example of (a) cyclic voltammograms of a bare gold electrode (solid line) compared with the electrode modified with AuNPs₅ (dash line) performed in 0.1 mol l^{-1} H₂SO₄ solution at a scan rate of 100 mV s⁻¹ versus with a Ag/AgCl reference electrode. The voltage range was 0.10–1.50 V, $Q_{(AuNPs)_5}$ and Q_{BGE} are the amount of electric charge exchanged during the oxygen electroadsorption on the electrode modified with AuNPs₅ and on a bare gold electrode, respectively, (b) the surface coverage (%) versus the number of AuNPs layers with different concentrations of gold nanoparticles.

amount of AuNPs and at a higher concentration a lower surface area was probably caused by too many nanoparticles were adsorbed, leading to a reduction of the total surface area as described above. The results are in line with the study made by Dawan et al. on Ag nanoparticles [10].

3.2.2. Surface morphology

The surface morphology of different layer of AuNPs was investigated using scanning electron microscopy. Fig. 4(a) and (b) shows an example of the SEM images of the bare gold electrode and Pty modified gold electrode, respectively. The Pty surface provided a rougher surface than the bare gold electrode. Examples of the SEM images of the surfaces after deposition of AuNPs_n/ TU_{n-1} are shown in Fig. 4(c)-(k). When AuNPs were assembled onto the Pty surface via the binding of the -NH₂ group to AuNPs, the distribution of AuNPs of this first layer were rather scattered (AuNPs₁) (Fig. 4(c)). When it was exposed to the TU solution, a tightly organized packed layer was formed (Fig. 4(d)). Denser AuNPs were obtained after the formation of the second layer of AuNPs (AuNPs₂) (on TU₁ layer) (Fig. 4(e)). This denser layer of AuNPs provided a larger surface area. Electrodes with more than two layers of AuNPs showed large clusters (Fig. 4(g), (i) and (k)) clearly indicated the closely packed particles. For the other two concentrations of AuNPs ($24\,\mathrm{nmol}\,l^{-1}$ and 236 nmol l^{-1}), the SEM images of the different layers showed a similar trend, i.e., large clusters of the closely packed colloidal particles were observed after two layers of AuNPs. In the case of the higher concentration of AuNPs (236 nmol l⁻¹) larger clusters were observed. These closely packed particles leveled out the curvature of the individual nanoparticles adsorbed on the surface, hence, less surface area.

3.2.3. Electrochemical impedance spectroscopy characterization

The fitting in terms of the magnitude and phase of impedance were compared between the simulation based on the theoretical circuit model and experimental results obtained on the modified electrode. The equivalent circuit model with a double layer capacitor ($C_{\rm cll}$) did not provide a good fitting to the experimental data (Fig. 5(a)). An improved fitting was by using a constant phase element (CPE) in place of $C_{\rm cll}$ (Fig. 5(b)). A CPE generates the impedance that can be expressed by $Z_{\rm CPE}(\omega) = Z_0(j\omega)^{-n}$ where 0 < n < 1, j is the imaginary number, Z_0 is a constant, and ω the angular frequency [8]. From all the fittings, the obtained n values were between 0.84 and 0.93 demonstrated a deviation from an ideal capacitor (n = 1). The obtained errors of the n value originated from the difference between the simulated and the experimental results were only 0.3–0.8%, indicating the good fitting. Hence, the equivalent circuit model with the CPE was used throughout the study.

Fig. 6(a) shows the impedance spectrum of the bare gold electrode with a very small semicircle, i.e., a very low electron transfer resistance, and a linear part that indicated a diffusion limiting process. An example of the impedance spectra of the electrode with different modification layers of 71 nmol l-1 AuNPs is shown in Fig. 6(b). Fig. 6(c) is the zoom in the impedance spectra (within the rectangle of Fig. 6(b)) from the TU₂ layer to the AuNPs₅ layer. The EIS values were obtained by fitting the impedance data of one electrode, with three scans, using the Randles' equivalent circuit for bare gold electrode (Fig. 6(a) inset), the equivalent circuit of Fig. 6(b) (inset) for the Pty layer and the equivalent circuit of Fig. 6(c) (inset) for TU₁ to AuNPs₅ layer. The R_{et} values of these surfaces are shown in Fig. 6(d). The bare gold electrode gave a very low $R_{\rm et}$ because of the good electron transfer. The Pty film modified gold electrode formed a non-conducting layer on the surface and this acted as the electron transfer barrier, thus, the large increase of the $R_{\rm et}$. When AuNPs were attached to the Pty films (AuNPs₁), the R_{et} decreased, implying that the AuNPs play a similar role to a conducting layer, which makes it easier for the electron transfer to take place. The $R_{\rm et}$

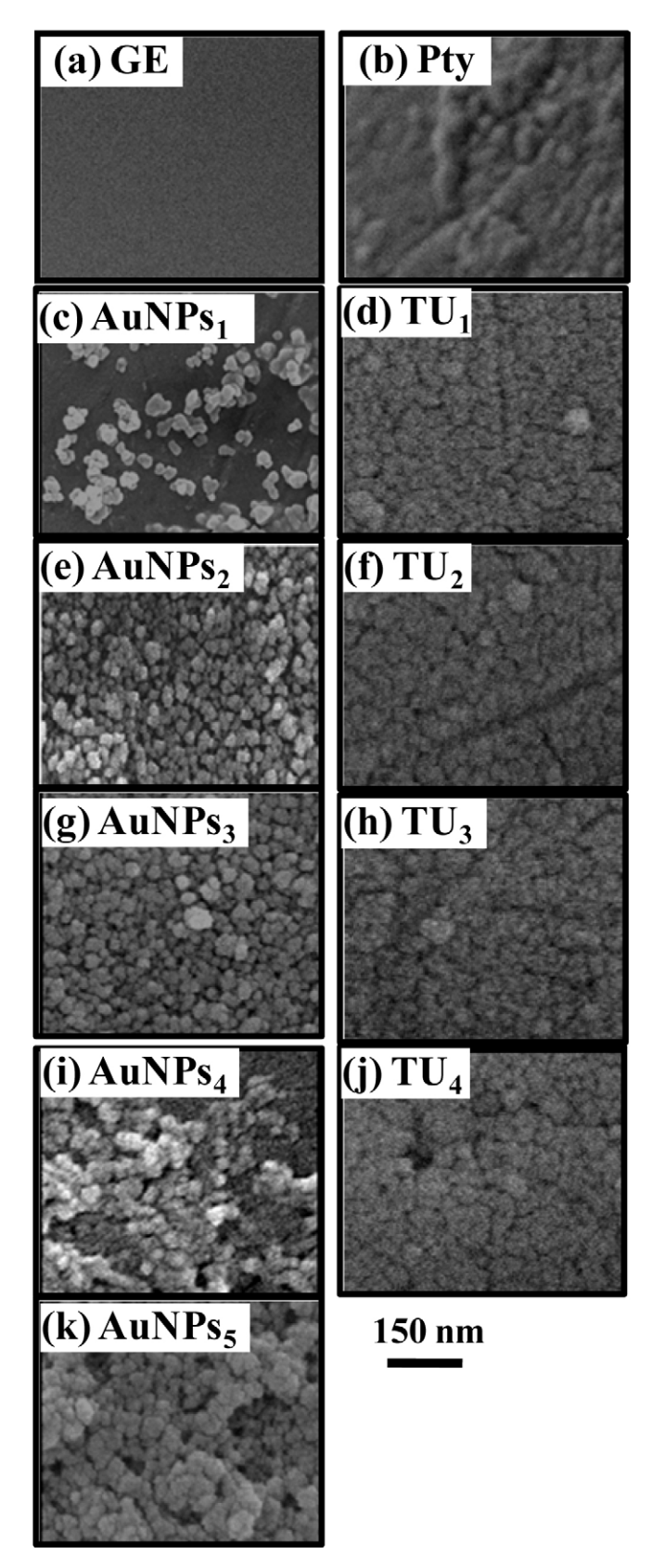


Fig. 4. An example of the SEM images of electrode surfaces modified with 71 nmol l⁻¹ of AuNPs and thiourea on a Pty modified gold electrode (a) the bare gold electrode, (b) Pty, (c) AuNPs₁, (d) TU₁, (e) AuNPs₂, (f) TU₂, (g) AuNPs₃, (h) TU₃, (i) AuNPs₄, (j) TU₄ and (k) AuNPs₅.

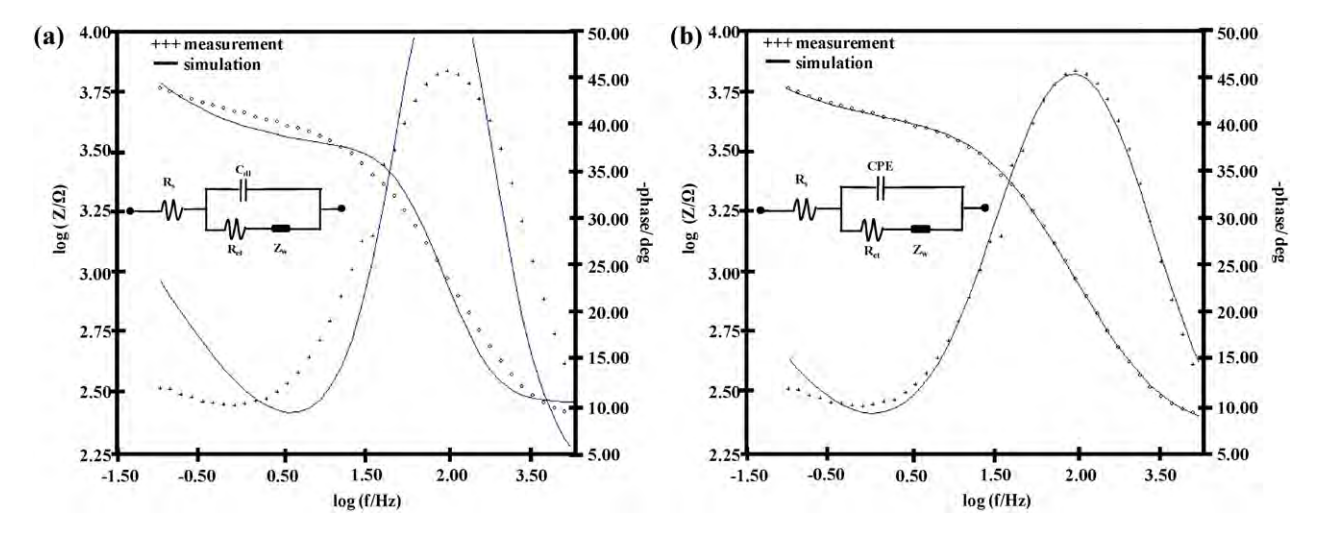


Fig. 5. An example of the fittings in terms of the magnitude and phase of impedance, compared between the simulation based on the equivalent circuit model (inset) of the electrochemical interface and the measured values from the modified electrode: $R_{\rm et}$, the resistance of the electron transfer; $R_{\rm s}$, the resistance of the solution; $C_{\rm dl}$, the double layer capacitance; CPE, the constant phase element and $Z_{\rm W}$, Warburg element. The different between (a) and (b) is the capacitance component. From the fitting, the obtained n value was 0.84 demonstrated a deviation from an ideal capacitor (n = 1). The obtained error of the n value originated from the difference between the simulated and the experimental result at (b) was only 0.8%.

value increased again after the TU layer was formed on the AuNPs₁ because of the tightly packed TU₁ insulated surface. The diameter of the semicircle decreased again after the introduction of AuNPs₂ on the TU₁ surface because the redox reaction of the redox probe occurred far more rapidly on the AuNPs₂ surface than the insulating TU₁ surface, resulting in a decrease of the $R_{\rm et}$ values. These behaviors were repeated with an additional layer, i.e., the $R_{\rm et}$ increased when the surface was terminated with the TU and decreased when the surface was terminated with the metal nanoparticles. However, after the second layer the $R_{\rm et}$ values showed little change. These results corresponded very well to the results of the surface coverage (%) (Fig. 3(b)).

For the R_s value, the resistance of the solution, there should be no change with the modified surface. The results in Fig. 6(e) confirmed this, i.e., the R_s values were not significantly difference.

Fig. 6(f) shows that the capacitance, CPE, decreased from the bare gold electrode to the Pty surface. This is due to the insulating nature of the Pty. The increase in the thickness by an insulated layer can be described as an addition of a capacitor in series, hence the total capacitance decreased. After the AuNPs₁ layer was assembled on to the Pty surface the CPE increases because the AuNPs provided a good electron transfer layer [9,42,43]. The interface can then be considered to be an array of capacitors in parallel [43], hence the total capacitance increased. When the TU was formed on the AuNPs₁ layer another insulated layer was formed and again the CPE value decreased. That is, the CPE increased when the surface was terminated with the conducting metal nanoparticles and decreased when the surface was terminated with the insulated TU. The CPE value increased with the number of AuNPs layers up to two layers (AuNPs₂) then decreased. The highest capacitance at the second AuNPs layer correlated well to its highest surface area ($C \propto \text{area}$).

3.3. Capacitive immunosensor system

3.3.1. Electrochemical characterization of immobilization

Cyclic voltammetry was used to test the immobilization step by evaluating the electron transfer kinetics of $[Fe(CN)_6]^{4-/3-}$ on the modified electrode in the electrolyte solution. Fig. 7 is an example of the electrode with two layers of 71 nmol l^{-1} AuNPs. The voltammogram of a clean gold electrode presented large oxidation and reduction peaks (Fig. 7(a) inset), which decreased when the Pty

Table 1Effect of the number of layers of AuNPs on the sensitivities (slope of the calibration plot) and the immobilization yield of anti-HSA with different concentrations of AuNPs using the face-up deposition direction method.

The number of layers of AuNPs	Sensitivities $(-nF cm^{-2} log(mol l^{-1})^{-1})$		
	24 nmol l ⁻¹	71 nmol l ⁻¹	236 nmol l ⁻¹
1	3.51 ± 0.14	5.64 ± 0.23	2.87 ± 0.12
2	5.05 ± 0.15	7.08 ± 0.26	4.77 ± 0.21
3	5.12 ± 0.26	6.79 ± 0.18	3.39 ± 0.16
4	4.04 ± 0.21	5.82 ± 0.18	2.64 ± 0.10
5	2.60 ± 0.25	4.83 ± 0.20	1.95 ± 0.12

Immobilization yield (%)a

	$24\mathrm{nmol}l^{-1}$	71 nmol l ⁻¹	236 nmol l ⁻¹
1	$72.1\pm0.9,73.3\pm0.4$	$81.3\pm0.6,80.9\pm0.6$	$64.7 \pm 0.5, 64.0 \pm 0.2$
2	$84.3 \pm 0.7, 85.0 \pm 0.6$	89.7 ± 0.5 , 90.2 ± 0.5	$79.1\pm0.1,79.9\pm0.7$
3	$80.0 \pm 0.6, 81.4 \pm 0.3$	85.2 ± 0.4 , 85.4 ± 0.6	$66.0\pm0.6,65.4\pm1.1$
4	$76.4 \pm 0.4, 76.8 \pm 0.6$	$83.9 \pm 0.4, 82.1 \pm 0.1$	$58.7 \pm 0.3, 58.1 \pm 0.4$
5	$62.8\pm0.2,64.7\pm0.5$	$79.8\pm0.7, 79.1\pm0.9$	$55.5\pm0.6,54.5\pm0.9$

^a 2 electrodes.

film was added, hence, the ability to transfer electrons was reduced (Fig. 7(b)). The redox peaks increased when the first layer of AuNPs was assembled to the Pty surface due to the better transfer of the electrons of the metal nanoparticles (Fig. 7(c)) then decreased when the first layer of TU was formed (Fig. 7(d)). The increase of the redox peaks was observed again after adding the second layers of AuNPs (Fig. 7(e)), much higher than after the first layer. This corresponded well with the lower $R_{\rm et}$ in Fig. 7(d). The redox peaks then decreased when the anti-HSA was immobilized (Fig. 7(f)). For the last step using the 1-dodecanethiol ethanolic solution the redox peaks completely disappeared (Fig. 7(g)) indicating total insulation which is the necessary condition for the non-Faradaic detection of the employed capacitive system [14].

3.3.2. Effect of the number of layers of gold nanoparticles

The performance of the label-free capacitive immunosensor system was determined from the sensitivity, which is the slope of the linear calibration plot between 1×10^{-16} and 1×10^{-10} mol l^{-1} . The electrode with two layers provided the highest sensitivities (Table 1). The decreased in the sensitivity is related to the surface coverage. The electrode with one layer of AuNPs provided a

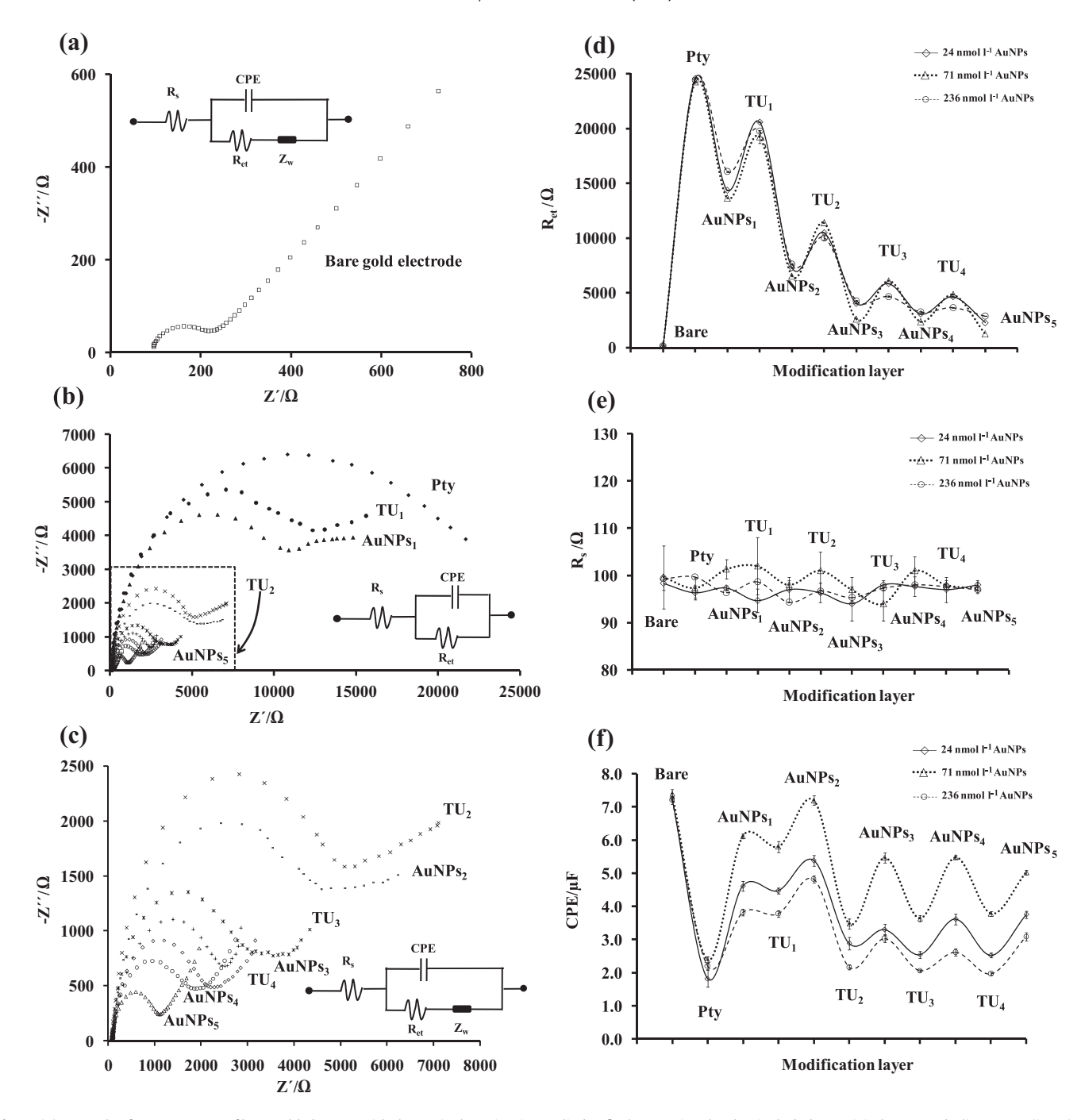


Fig. 6. (a) Example of an EIS spectra of bare gold electron with the equivalent circuits applied to fit the Nyquist plot that included a semicircle part and a linear part (inset), (b) the EIS spectra of the different layer of 71 nmol I^{-1} AuNPs with the equivalent circuits applied to fit the Nyquist plot that has only the semicircle part (Pty), R_s , the resistance of the solution; Z_W , the Warburg impedance; R_{et} , the resistance of the electron transfer between the solution and the electrode surface; CPE, the capacitance of the double layer, (c) EIS spectra of TU_2 to $AuNP_5$ (zoom out from inset Fig. 5(b)) obtained in the $10 \text{ mmol } I^{-1}$ Fe(CN) $_6^{3-/4-}$ solution containing 0.1 mol I^{-1} KCI. EIS values of the electrode with different layers and different concentrations of AuNPs, (d) R_{et} values, (e) R_s values and (f) CPE values of one electrode with three scans (n=3).

lower sensitivity than the two layers because of the reduced surface area due to the presence of fewer nanoparticles, hence, less antibody was immobilized. The electrodes with more than two layers also provided a lower sensitivity because of a lower surface area, however, in this case it was caused by too many nanoparticles became closely packed and, hence, there was a reduced surface enhancement caused by the reduction of the curvature from individual particles. The smaller surface area also increased the steric hindrance of immobilized anti-HSA [30]. To confirm the above reasoning, immobilization yields of the anti-HSA on the electrode with different layers of AuNPs in the face-up arrangement of the

electrode were tested for 2 electrodes and 3 replications per electrode. The electrode with two layers bound the largest amount of antibody and this corresponded to the highest sensitivity (Table 1). For the electrode with different concentrations of AuNPs, the highest immobilization yield was provided by the 71 nmol l⁻¹ AuNPs followed by 24 nmol l⁻¹ AuNPs and 236 nmol l⁻¹ AuNPs. This is also related to the surface coverage. It can be concluded that a larger surface area enabled a larger amount of sensing element to be immobilized. From the results the electrode with two layers [AuNPs]₂ was chosen for further testing the effect of the direction of deposition of the AuNPs.

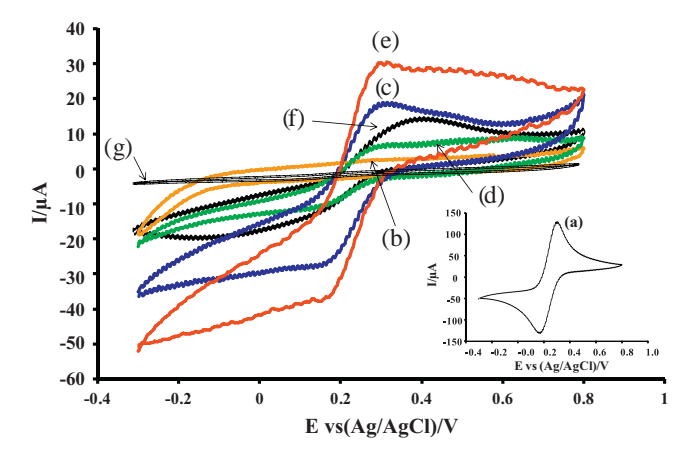


Fig. 7. Cyclic voltammograms of a 71 nmol l^{-1} AuNPs modified electrode obtained in 10 mmol l^{-1} Fe(CN)₆ $^{4-/3-}$ solution, (a) bare gold, (b) Pty electropolymerized gold electrode, (c) AuNPs₁ layer adsorbed on the —NH₂ group of Pty, (d) TU₁, (e) AuNPs₂ layer, (f) anti-HSA modified on AuNPs₂/(TU/AuNPs)₁/Pty modified gold electrode, and (g) after 1-dodecanethiol treatment.

3.3.3. Effect of the deposition direction of the AuNPs

The electrode with two layers of AuNPs was then tested to obtain the best direction for deposition of the colloidal nanoparticles. An example of the comparison of the response of immobilized anti-HSA with two layers of 71 nmol l⁻¹ AuNPs through the two arrangements of the electrode is shown in Fig. 8. The facedown arrangement provided a higher sensitivity than the face-up arrangement of the electrode. From the SEM images (Fig. 8 inset) the face-down arrangement provided a smaller size clusters than the face-up arrangement of the electrode. As indicated earlier (Section 3.2.2) smaller clusters of the AuNPs resulted in a larger total surface area from the curvature of separated individual particles, i.e., larger area for antibody immobilization, hence, the better responses.

Table 2 summarizes the performance of the capacitive immunosensor system with various concentrations of the two layered AuNPs. With the face-down arrangement of the electrode, all concentrations of AuNPs provided a better immobilization yield and sensitivity, a wider linear range and lower detection limit than the face-up arrangement. Between the three concentrations of AuNPs, the 71 nmol l^{-1} AuNPs provided the highest sensitivity, 1.2 times higher than for the 24 nmol l^{-1} and 1.3 times higher than the 236 nmol l^{-1} . The reasons were as described earlier in Section 3.3.2.

3.4. Determination of HSA in real samples

Six urine samples were obtained from Songklanagarind Hospital, Hat Yai, Thailand. When testing with real samples matrix

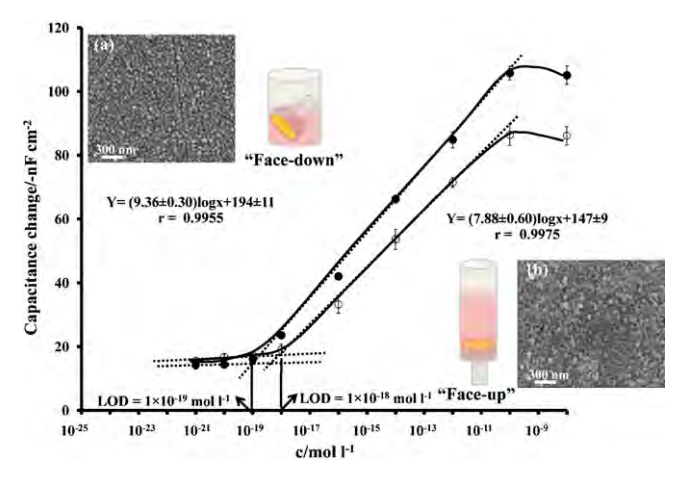


Fig. 8. Comparison of the responses of the anti-HSA modified electrode made with two layers of 71 nmol l $^{-1}$ AuNPs on the electrode in either the "face-down" (\bullet) and "face-up" (\bigcirc). The SEM images and figures inset were presented after the AuNPs $_2$ was deposited on the electrode in either the "face-down" (a) and "face-up" (b). The limit of detection (LOD) was determined by following IUPAC recommendation 1994 where the limit of detection is taken as the concentration of an analyte at the point of intersection of the extrapolated linear range and final low concentration level segments of the calibration plot [51].

Table 3Results of determination of the HSA concentration in urine samples analyzed by the capacitive immunosensor, using an electrode with two layers of 71 nmol l^{-1} AuNPs and the face-down deposition direction compared to an immunoturbidimetric assay used by the hospital analysis [40,41].

Urine samples	Capacitive immunosensor $(mg l^{-1})^a$	Immunoturbidimetric assay (mg l ⁻¹)
1	38.4 ± 1.1	38.5
2	27.7 ± 0.5	27.1
3	6.9 ± 2.4	7.2
4	42.0 ± 2.4	42.6
5	7.1 ± 0.4	6.9
6	9.7 ± 1.2	9.6

^a 3 replications.

interference generally occurs. One way to reduce the effect of the matrix is by dilution, however, the amount of analyte would also be reduced. Since the detection limit of this system is very low this should not be a problem. From some of our previous work a dilution factor of between 10^6 and 10^7 times was generally required to eliminate interference from other substances in the sample matrix [10,39]. Therefore, a 10^6 times dilution was applied. Since normal urine albumin excretion is $<\!20\,\mu\mathrm{g}\,\mathrm{ml}^{-1}$ or $3.0\times10^{-7}\,\mathrm{mol}\,l^{-1}$ (molecular weight of HSA=68,000 g mol $^{-1}$) [36,39] after a 10^6 times dilution, the concentration would be $3.0\times10^{-13}\,\mathrm{mol}\,l^{-1}$. Therefore, a calibration curve was prepared between 1.0×10^{-13} and $1.0\times10^{-12}\,\mathrm{mol}\,l^{-1}$. The diluted urine samples were injected

Table 2Effect of the direction of AuNPs deposition on the performance of the capacitive immunosensor system with various concentration of AuNPs by immobilization of anti-HSA through AuNPs₂ on a Pty modified gold electrode (y is the capacitance change in -nF cm⁻² and x is the concentration of HSA in log mol l⁻¹).

AuNPs concentration (nmol l ⁻¹)	Deposition direction	Sensitivities $(-nFcm^{-2} log(mol l^{-1})^{-1})$	Immobilization yield (%)	Linear range (mol l ⁻¹)	Limit of detection (mol l ⁻¹)
24	Face-down	7.69 ± 0.19	92.7 ± 0.1, 91.6 ± 0.1	10 ⁻¹⁹ to 10 ⁻¹⁰	10-19
	Face-up	5.07 ± 0.15	$84.1 \pm 0.2, 86.6 \pm 0.4$	10^{-18} to 10^{-10}	10^{-18}
71 ^a	Face-down-1	9.36 ± 0.30	$96.3 \pm 0.2, 96.2 \pm 0.3$	10^{-19} to 10^{-10}	10^{-19}
	Face-down-2	9.78 ± 0.30	_	10^{-19} to 10^{-10}	10^{-19}
	Face-up-1	7.88 ± 0.60	$93.2 \pm 0.1, 91.3 \pm 0.1$	10^{-18} to 10^{-10}	10^{-18}
	Face-up-2	7.52 ± 0.30	-	10^{-18} to 10^{-10}	10^{-18}
236	Face-down	7.23 ± 0.24	$89.7 \pm 0.5, 90.2 \pm 0.5$	10^{-19} to 10^{-10}	10^{-19}
	Face-up	4.10 ± 0.15	$76.4 \pm 0.4, 73.3 \pm 0.4$	10^{-18} to 10^{-10}	10^{-18}

^a 2 electrodes per deposition direction.

Table 4 Recoveries in spiked urine sample with 10^6 times dilution factor (mean \pm SD, n = 3).

Unfortified sample concentration (C_2) (×10 ⁻⁷ mol l ⁻¹)	Spiked concentration (C_3) $(\times 10^{-7} \text{ mol l}^{-1})$	Determined concentration (C_1) $(\times 10^{-7} \text{ mol l}^{-1})$	Parameters	
			% Recovery	% RSD
1.43 ± 0.18	1.0	2.40 ± 0.05	97 ± 5	6
	3.0	4.50 ± 0.06	102 ± 2	2
	5.0	6.37 ± 0.20	99 ± 4	4
	7.0	8.35 ± 0.26	99 ± 4	4
	9.0	10.58 ± 0.37	102 ± 4	4

Table 5Properties comparison of this current study and other biosensor methods.

Detection methods	Modified electrode	Linear range (mg l ⁻¹)	Detection limit (mg l ⁻¹)	References
DPV	AuNPs-Ab/PVA/SPCE	2.5–200	2.5×10^{-2}	[46]
QCM	Ab/GA/ED/quartz crystal	16.0-128	=	[47]
SPR	CB/PEG/gold	10.0-1.0	4	[48]
EIS	Ab/GA/Si-p/SiO ₂ /Si ₃ N ₄	6.8×10^{-6} to 6.8	6.8×10^{-7}	[49]
Capacitive	Ab/GA/Pty/gold	$1.8 \times 10^{-3} \text{ to } 368 \times 10^{-3}$	1.6×10^{-3}	[50]
Capacitive	Ab/GA/PoPD/gold	$6.8 \times 10^{-7} \text{ to } 6.8 \times 10^{-2}$	5.4×10^{-7}	[39]
Capacitive	Ab/AgNPs/TU/gold	6.8×10^{-11} to 6.8×10^{-3}	6.8×10^{-11}	[10]
Capacitive	Ab/AuNPs/TU/gold	6.8×10^{-11} to 6.8×10^{-3}	6.8×10^{-11}	[10]
Capacitive	Ab/[AuNPs] ₂ /Pty/gold	6.8×10^{-12} to 6.8×10^{-3}	6.8×10^{-12}	This work

DPV: differential pulse voltammetry, Ab: antibody, PVA; polyvinyl alcohol, SPCE: screen-printed carbon electrode, QCM: quartz crystal microbalance, GA: glutaraldehyde, ED: ethylene diamine, SPR: surface plasmon resonance, CB: cibacron blue, PEG: poly ethylene glycon, EIS: electrochemical impedance spectroscopy, Pty: poly tyramine, PoPD: poly-o-phenylenediamine, AgNPs: silver nanoparticles, TU: thiourea, AuNPs: gold nanoparticles.

into the capacitive system. The responses were used to obtain the concentrations from the calibration plot. The results obtained from the capacitive immunosensor and the results from the hospital analysis (Table 3) were compared by the Wilcoxon signed rank test. There is no evidence for systematic differences between the results obtained from the two methods (P>0.05). That is, the concentrations determined by the capacitive immunosensor system are in good agreement to the normal hospital analysis.

To further validate the capacitive immunosensor, a percentage recovery test was studied by spiking different concentrations of standard HSA into urine sample $(1.0\times10^{-7}\ \text{to}\ 9.0\times10^{-7}\ \text{mol}\ l^{-1})$ to obtain the final concentration range after dilution $(10^6\ \text{times})$ between 1.0×10^{-13} and $9.0\times10^{-13}\ \text{mol}\ l^{-1}$. Then the spiked sample was analyzed by the capacitive immunosensor. The percentage of recovery was calculated by Eq. (6).

Recovery (%) =
$$\left[\frac{(C_1 - C_2)}{C_3}\right] \times 100$$
 (6)

where C_1 = concentration determined in fortified (or spiked) sample, C_2 = concentration determined in unfortified sample and C_3 = concentration of fortification [44]. C_2 was calculated based on a standard calibration curve done prior to the test. The signal obtained from the unfortified urine sample after diluted 10^6 times was then used to calculate the concentration of HSA from the standard calibration equation. The obtained concentration was then multiplied by 10^6 . The concentration of HSA in the urine sample was $(1.43 \pm 0.18) \times 10^{-7}$ mol 1^{-1} . Recoveries of the spiked five albumin concentrations were between 97 and 102% with RSD = 2-6% (Table 4). Since the acceptable recovery in an analytical analysis in the $\times 10^{-7}$ mol 1^{-1} level is 80-110% and RSD is 15-22% [45], the recoveries for all spiked concentrations of HSA in the urine sample are acceptable.

In this work selectivity of the system to detect HSA was not tested since it has been shown in a previous work of our group that the anti-HSA provided good selectivity to HSA [39].

Table 5 summarizes the detection limit and the linear range obtained by this work and previously reported methods. In comparison with some other detection methods for albumin,

such as differential pulse voltammetry (DPV) [46], quartz crystal microbalance (QCM) [47], surface plasmon resonance (SPR) [48], electrochemical impedance spectroscopy (EIS) [49] and capacitive [10,39,50], our transducer with the proposed immobilization step provided lower detection limit and wider linear range in the very low concentration area.

4. Conclusions

The sensitivity of a label-free capacitive immunosensor can be improved by the LBL technique due to the increase of the amount of assembled gold nanoparticles that results in an increase of the effective surface area for the immobilized sensing elements. The electrode with two layers of 71 nmol l⁻¹ AuNPs provided the highest sensitivity and this was related to the highest surface coverage (%) and hence the immobilization yield (%). A face-down arrangement of the electrode for the deposited AuNPs provided a better sensitivity, a wider linear range and a lower detection limit $(10^{-19} \text{ mol } l^{-1})$ than the face-up arrangement $(10^{-18} \text{ mol } l^{-1})$ of the electrode because the self-assembled AuNPs were not as closely packed. The electrode with one layer had a lower sensitivity because of a lower surface area. The electrode with more than two layers provided a lower sensitivity because of there was less surface area. This was caused by too many adsorbed AuNPs became very closely packed, reducing the surface area due to the curvature of individual particle. The high sensitivity (9.36 ± 0.30 , $9.78 \pm 0.30 - nF \, cm^{-2} \, log \, mol \, l^{-1})^{-1}$ and extremely low detection limit $(10^{-19} \, \text{mol} \, l^{-1})$ demonstrated that the system could easily determine the analyte at ultra trace level. The effect of any matrix interferences was eliminated by simply diluting the sample. This method was tested for its ability to detect HSA in urine samples. The concentrations determined by the capacitive immunosensor system were in good agreement with the immunoturbidimetric assay used by the hospital (P>0.05). This work also determined the characteristic properties of the AuNPs modified electrodes based on the LBL technique. This information can be useful for other electrochemical technique detection. This method could certainly be applied for the sensitive detection of other analytes using other affinity binding pairs such as in genosensors to detect target DNAs.

Acknowledgements

The authors are grateful for the grant from the Thailand Research Fund (BRG5280014). The Royal Golden Jubilee Ph.D. Program supported by The Thailand Research Fund (3.C.PS/50/B.1); Center of Excellence for Innovation in Chemistry (PERCH-CIC), Office of the Higher Education Commission; The Higher Education Research Promotion and National Research University Project of Thailand, Office of the higher Education Commission (HERP-NRU); Trace Analysis and Biosensor Research Center; and Graduate School, Prince of Songkla University, Hat Yai, Thailand are all gratefully acknowledged. The authors thank Dr. Brian Hodgson, Prince of Songkla University, Hat Yai, Songkhla, Thailand for assistance with the English.

References

24 (2008) 1020.

- [1] Y. Xia, J. Zhang, L. Jiang, Colloids and Surfaces B: Biointerfaces 86 (2011) 81.
- [2] S.C. Hong, H. Chen, J. Lee, H.-K. Park, Y.S. Kim, H.-C. Shin, C.-M. Kim, T.J. Park, S.J. Lee, K. Koh, H.-J. Kim, C.L. Chang, J. Lee, Sensors Actuators B: Chemical 156 (2011) 271.
- [3] S. Suwansa-ard, P. Kanatharana, P. Asawatreratanakul, B. Wongkittisuksa, C. Limsakul, P. Thavarungkul, Biosensors and Bioelectronics 24 (2009) 3436.
- [4] D. Tang, R. Niessner, D. Knopp, Biosensors and Bioelectronics 24 (2009) 2125.
- 2125. [5] S. Wang, Z. Wu, F. Qu, S. Zhang, G. Shen, R. Yu, Biosensors and Bioelectronics
- [6] S.D. Bolis, P.C. Charalambous, C.E. Efstathiou, A.G. Mantzila, C.A. Malamou, M.I. Prodromidis, Sensors Actuators B: Chemical 114 (2006) 47.
- [7] C.-C. Lin, L.-C. Chen, C.-H. Huang, S.-J. Ding, C.-C. Chang, H.-C. Chang, Journal of Electroanalytical Chemistry 619–620 (2008) 39.
- [8] M.I. Prodromidis, Electrochimica Acta 55 (2010) 4227.
- [9] C. Berggren, B. Bjarnason, G. Johansson, Electroanalysis 13 (2001) 173.
- [10] S. Dawan, P. Kanatharana, B. Wongkittisuksa, W. Limbut, A. Numnuam, C. Limsakul, P. Thavarungkul, Analytica Chimica Acta 699 (2011) 232.
- [11] D. Jiang, J. Tang, B. Liu, P. Yang, X. Shen, J. Kong, Biosensors and Bioelectronics 18 (2003) 1183.
- [12] M. Labib, M. Hedström, M. Amin, B. Mattiasson, Analytica Chimica Acta 634 (2009) 255.
- [13] S. Samanman, P. Kanatharana, W. Chotigeat, P. Deachamag, P. Thavarungkul, Journal of Virological Methods 173 (2011) 75.
 [14] B. Wongkittisuksa, C. Limsakul, P. Kanatharana, W. Limbut, P. Asawa-
- [14] B. Wongkittisuksa, C. Limsakul, P. Kanatharana, W. Limbut, P. Asawatreratanakul, S. Dawan, S. Loyprasert, P. Thavarungkul, Biosensors and Bioelectronics 26 (2010) 2466.
- [15] S. Loyprasert, M. Hedstr m. P. Thavarungkul, P. Kanatharana, B. Mattiasson, Biosensors and Bioelectronics 25 (2011) 1977.
- [16] K. Yang, H. Wang, K. Zou, X. Zhang, Nanotechnology 17 (2006) S276.
- [17] W. Limbut, P. Kanatharana, B. Mattiasson, P. Asawatreratanakul, P. Thayarungkul. Analytica Chimica Acta 561 (2006) 55.
- [18] C. Berggren, B. Bjarnason, G. Johansson, Biosensors and Bioelectronics 13 (1998) 1061.

- [19] S. Loyprasert, P. Thavarungkul, P. Asawatreratanakul, B. Wongkittisuksa, C. Limsakul, P. Kanatharana, Biosensors and Bioelectronics 24 (2008) 78.
- [20] R. Wannapob, P. Kanatharana, W. Limbut, A. Numnuam, P. Asawatreratanakul, C. Thammakhet, P. Thavarungkul, Biosensors and Bioelectronics 26 (2010) 357.
- [21] K. Chullasat, P. Kanatharana, W. Limbut, A. Numnuam, P. Thavarungkul, Biosensors and Bioelectronics 26 (2011) 4571.
- [22] R. Chai, R. Yuan, Y. Chai, C. Ou, S. Cao, X. Li, Talanta 74 (2008) 1330.
- [23] J.Y. Chen, Y.C. Chen, Analytical and Bioanalytical Chemistry 399 (2011) 1173.
- [24] X. Lu, F. Zhi, H. Shang, X. Wang, Z. Xue, Electrochimica Acta 55 (2010) 3634.
- [25] L. Qian, Q. Gao, Y. Song, Z. Li, X. Yang, Sensors Actuators B: Chemical 107 (2005) 303.
- [26] L. Su, L. Mao, Talanta 70 (2006) 68.
- [27] F. Zhang, M.P. Srinivasan, Journal of Colloid and Interface Science 319 (2008)
- [28] M. Lu, X.H. Li, B.Z. Yu, H.L. Li, Journal of Colloid and Interface Science 248 (2002) 376
- [29] M. Brust, D. Bethell, C.J. Kiely, D.J. Schiffrin, Langmuir 14 (1998) 5425.
- [30] B. Su, J. Tang, H. Chen, J. Huang, G. Chen, D. Tang, Analytical Methods 2 (2010) 1702.
- [31] H. Zhang, H. Lu, N. Hu, The Journal of Physical Chemistry B 110 (2006) 2171.
- [32] R.K. Shervedani, A. Farahbakhsh, M. Bagherzadeh, Analytica Chimica Acta 587 (2007) 254.
- [33] G. Fanali, A. di Masi, V. Trezza, M. Marino, M. Fasano, P. Ascenzi, Molecular Aspects of Medicine 33 (2012) 209.
- [34] A.M. Johnson, Clinical chemistry and laboratory medicine 37 (2005) 91.
- [35] W. Limbut, P. Kanatharana, B. Mattiasson, P. Asawatreratanakul, P. Thavarungkul, Biosensors and Bioelectronics 22 (2006) 233.
- [36] J. Xiang, B.L. Wu, S.L. Chen, Journal of Electroanalytical Chemistry 517 (2001)
- [37] J.J.M. Coenen, User Manual FRA for Frequency Response Analysis (FRA) for window version 4.9, in: Description of the Instrument: Instrument for Electrochemical Research and Voltammetric Analyses, Eco Chemie B.V., Utrecht, The Netherlands. 2001.
- 38] G. Krystal, Analytical Biochemistry 167 (1987) 86.
- [39] K. Teeparuksapun, P. Kanatharana, W. Limbut, C. Thammakhet, P. Asawatreratanakul, B. Mattiasson, B. Wongkittisuksa, C. Limsakul, P. Thavarungkul, Electroanalysis 21 (2009) 1066.
- [40] J.H. Contois, C.J. Lammi-Keefe, S. Vogel, J.R. McNamara, P.W.F. Wilson, T. Massov, E.J. Schaefer, Clinica Chimica Acta 253 (1996) 21.
- [41] B. Mali, D. Armbruster, E. Serediak, T. Ottenbreit, Clinical Biochemistry 42 (2009) 1568.
- [42] İ. Hafaid, A. Gallouz, W. Mohamed Hassen, A. Abdelghani, Z. Sassi, F. Bessueille, N. Jaffrezic-Renault, Journal of Sensors 2009 (2009).
- [43] S.L. Horswell, I.A. O'Neil, D.J. Schiffrin, Journal of Physical Chemistry B 107 (2003) 4844.
- [44] Eurachem, The Fitness for Purpose of Analytical Methods: A Laboratory Guide to Method Validation and Related Topics, Laboratory of the Government Chemist,
- [45] I. Taverniers, M. De Loose, E. Van Bockstaele, TrAC Trends in Analytical Chemistry 23 (2004) 480.
- [46] K. Ömidfar, A. Dehdast, H. Zarei, B.K. Sourkohi, B. Larijani, Biosensors and Bioelectronics 26 (2011) 4177.
- [47] R. Saber, S. Mutlu, E. Pişkin, Biosensors and Bioelectronics 17 (2002) 727.
- [48] S.-W. Tsai, J.-W. Liaw, F.-Y. Hsu, Y.-Y. Chen, M.-J. Lyu, M.-H. Yeh, Sensors 8 (2008) 6660.
- [49] D. Caballero, E. Martinez, J. Bausells, A. Errachid, J. Samitier, Analytica Chimica Acta 720 (2012) 43.
- [50] Z.S. Wu, J.S. Li, T. Deng, M.H. Luo, G.L. Shen, R.Q. Yu, Analytical Biochemistry 337 (2005) 308.
- [51] R.P. Buck, E. Lindneri, Pure and Applied Chemistry 66 (1994) 2527.